GENOME-WIDE LIVER X RECEPTOR ALPHA BINDING AND CHROMATIN ACCESSIBILITY IN DIFFERENT MACROPHAGE MODELS

Cornelius Fischer B. rer. nat.

A thesis submitted to the Freie Universität Berlin in partial fulfillment of the requirements for the degree of

MASTER OF SCIENCE

in

Molecular and Cell Biology

November 2011

THESIS ADVISERS

Prof. Dr. Hans Lehrach
Vertebrate Genomics, Max Planck Institute for Molecular Genetics Berlin

Prof. Dr. Wolfgang Schuster
Applied Genetics, Freie Universität Berlin

SUPERVISOR

Dr. Sascha Sauer
Nutrigenomics and Gene Regulation Group, Otto-Warburg Laboratories, Max Planck Institute for Molecular Genetics Berlin

TO MY GRANDFATHER, LOTHAR EISSMANN.

Science moves with the spirit of an adventure characterized both
by youthful arrogance and by the belief that the truth,
once found, would be simple as well as pretty.

— James D. Watson

ACKNOWLEDGEMENT

In particular, I would like to thank Dr. Sascha Sauer for giving me the opportunity to work in his lab, allowing me to study in a state of the art environment in the exciting new field of nutrigenomics. I also thank him for enlightening discussions, his constant support and for critical reading of the manuscript.

I would like to thank Prof. Dr. Wolfgang Schuster for taking me on as a student back in 2008, his outstanding work in managing the master's degree program and for advising this thesis.

I also thank Prof. Dr. Hans Lehrach for taking on the task of being my thesis advisor.

My special thanks go to my tutor Radmila Feldmann for her valuable wet lab assistance, full time support and for our long discussions on patterns emerging from high-throughput data. This thesis is mainly based on her work. She has established and performed ChIP-seq and microarray experiments.

I thank Anne Geikowski for joining me with validation experiments. Also I would like to thank Claudia Quedenau and Anja Freiwald for the excellent technical support. Thanks to Stefanie Becker for the assistance in the beginning of our projects. I thank all the other members of the Nutrigenomics and Gene Regulation group for their help and advice.

I am thankful to my grandmother Eva Eissmann for the english proofreading.

Finally, I thank my girlfriend Barbara Stoeger for her patience, Matthias Ebert for the useful Latex hints, Ulrike Hardam for the laptop and Fabian Blattner for the latest mixtapes.

A special thought is devoted to my parents and grandparents for the support during my studies.

Contents

List of Figures

List of Tables

1 Summary

The transcription factor liver X receptor alpha (LXRα), a member of the nuclear receptor family, is a key factor that regulates intracellular cholesterol homeostasis and inhibit inflammatory gene expression. LXR agonists have been considered as promising anti-atherosclerotic drugs, and several natural or synthetic LXR ligands are currently under investigation for pharmaceutical develoment. Macrophages and lipid-loaded macrophage foam cells are an early and persistent component of atherosclerotic lesions and likely play an important role in disease progression. However, LXRα-dependent genome-wide regulation of target genes in human macrophages remained incompletely elucidated. This thesis was addressed to correlate global ChIP-sequencing-derived LXRα cistromes and gene expression profiles to investigate the effects of LXRα activation on direct and putative indirect LXRα target genes. Moreover, the recruitment mechanisms whereby LXRα selects genomic regions and interacts with the chromatin landscape were studied. These analyses were carried out using THP-1 cell-derived differentiated macrophages, and oxidized low density lipoprotein (oxLDL) triggered macrophage-derived foam cells that were exposed to the synthetic LXR agonist T0901317. The results of this thesis revealed that LXRα DNA binding is not restricted to gene promoters but appears predominantly at distal enhancer regions. LXRα cistromes in macrophages and foam cells are largely distinct although a number of genes were commonly occupied. Correlation of LXRα cistromes and gene expression data confirmed known and defined novel direct LXRα target genes. It also revealed that LXRα cooperates with and directly regulates other transcription factors including retinoic acid receptor alpha (RARα) and activator protein 1 (AP-1). To regulate gene expression LXRα binds to DNA in a ligand-dependent way and the majority of functional binding events is targeted to regions of accessible chromatin and transcription factor hotspots. Together, the results of this thesis define a basis for understanding regulatory factor-genome interactions, provide a framework for the effects of LXR activation, and how to develop optimized LXR agonists.

2 Introduction

Heart disease and stroke – cardiovascular disease – are the largest cause of sickness and morbidity and a major cause of death for the citizens of the EU and the Western world (Leal et al. 2006). Cardiovascular disease currently costs the European health system more then 500 million euro each day, and these costs are likely to escalate over the next few years. Atherosclerotic plaque rupture and subsequent luminal thrombus formation are considered the major step in the development of acute cardiovascular events (Carson 2010). Therefore, atherosclerosis has been the subject of an immense amount of basic and applied research.

Atherosclerosis is considered as a multifactorial, multistep disease with various processes that have to act together to initiate and promote atherosclerotic development. Fatty streaks, accumulation of cholesterol-loaded macrophages in the arterial wall, are a hallmark of early atherosclerotic lesions that gradually thickens the arterial wall and may ultimately lead to major blockage of blood flow (Libby 2002). The ligand sensitive transcription factor liver X receptor alpha (LXRα) is involved in signalling pathways that clearly display anti-atherogenic properties by regulating cholesterol homoeostasis, as well as metabolic and inflammatory signal integration. Advances in our knowledge of the molecular mechanisms underlying lipid metabolism and its regulation by transcription factors may have an enormous effect on the prevention and treatment of this major health issue.

2.1 Macrophage foam cells and atherosclerosis

The development of fatty streaks is initiated by endothelial dysfunction, possibly caused by traumatic damage, infectious microorganisms, free radicals caused by cigarette smoking, elevated oxidized low-density lipoprotein cholesterol (oxLDL) or other factors (Ross 1999). Endothelial activation results in expression of adhesion molecules, chemokines and cytokines, leading to adherence of circulating monocytes and subsequent monocyte recruitment into the subendothelial space of the vascular wall. Within the artery wall monocytes differentiate into macrophages and take up oxLDL, which

itself acts as major chemoattractant (Li and Glass 2002). The modification of native lipoproteins is required for the recognition by macrophage scavenger receptors and several lines of evidence suggest that macrophages and endothelial cells promote LDL oxidation in the presence of high LDL levels (Skalen et al. 2002). In macrophages, this process involves myeloperoxidase (MPO), NADPH oxidase and the nitric oxide synthases (iNOS) as means to generate antimicrobial reactive oxygen species. Therefore, macrophages contribute to the amplification of oxidative reactions and promote lesion initiation and progression (Li and Glass 2002). As macrophages convert the imported cholesterol into the ester form, they become filled with cholesteryl ester lipid droplets, resulting in foam cell formation. In response to cholesterol over-loading, macrophages activate different compensatory pathways. Endogenous, cholesterol and lipid biosynthesis is repressed by inhibition of the sterol regulatory element-binding transcription factor 1 (SREBF1) pathway (Yoshikawa et al. 2001). As cells cannot degrade cholesterol, it is exported to extracellular acceptors for transport to the liver for biliary excretion. These acceptors include apolipoproteins apolipoprotein A-I (APOA1), apolipoprotein E (APOE) and high-density lipoprotein (HDL) particles (Beyea et al. 2007). The cellular cholesterol efflux is mediated through ATP-binding cassette transporters ABCG1 and ABCA1 to protect the cells from cholesterol overload (Oram and Heinecke 2005, Wang et al. 2007). In the face of continuous cholesterol uptake homeostatic mechanisms are overwhelmed, leading to enhanced macrophage foam cell formation and further recruitment of monocytes. The transition of fatty streak lesions to more advanced lesions further involves the production of cytokines and other signalling molecules by macrophages and other cells within the arterial wall leading to the migration of smooth muscle cells into the subendothelial space. Smooth muscle cells synthesize collagen, fibrin and proteoglycans leading to the formation of the fibrous cap found in advanced atherosclerotic lesions (Glass and Witztum 2001). Apoptosis and necrosis of macrophage and smooth muscle cells further lead to necrotic cores. Necrotic cores surrounding macrophages secrete matrix metalloproteinases that degrade the collagen of the endothelium causing its rupture and subsequent platelet recruitment that initiates thrombus formation (Lee and Libby 1997). Taken together, lipid metabolism and

immune responses in macrophages play a crucial role in the progression of atherosclerotic plaque development. Insights into the mechanisms underlying the macrophage responses are required to develop novel therapeutic strategies for prevention and treatment of atherosclerosis.

2.2 Liver X receptors

LXRα (NR1H3) (Willy et al. 1995) and LXRβ (NR1H2) (Song et al. 1994) are members of the nuclear receptor transcription factor superfamily. Nuclear receptors are a unique group of transcription factors that all act as sensors for hormonal and metabolic signals. Therefore, ligands such as steroids, thyroid hormones, cholesterol derivatives and fatty acids bind and therefore activate the receptor leading to gene expression regulation of nuclear receptor specific target genes. The largest subfamily NR1 includes LXR, peroxisome proliferator-activated receptor (PPAR), thyroid hormone receptor (TR), retinoic acid receptor (RAR) and RAR-related orphan receptor (ROR) (Germain et al. 2006).

LXRs are master regulators of cholesterol homoeostasis, metabolic and inflammatory pathways and are commonly known as cholesterol sensors (Peet et al. 1998). In macrophage foam cells LXR activation is triggered by oxLDL-derived oxysterols (Janowski et al. 1999). Moreover, synthetic agonists such as T0901317 were developed that activate LXRs. This has made LXRs an established tool to investigate molecular mechanisms of transcriptional regulation. In humans LXRα and LXRβ share almost 80% amino acid identity in their DNA-binding domain and ligand-binding domain. Amongst both LXR isoforms, LXRα is highly expressed in the liver and at lower levels in intestine, adipocytes and macrophages. In contrast, LXRβ is expressed ubiquitously (Zelcer and Tontonoz 2006). The known role of LXR expands with the growing number of studies. Therefore, LXRs are also implicated in de-novo cholesterol synthesis, detoxification of bile acids and lipids, glucose homoeostasis, skin homoeostasis and neurological functions (Viennois et al. 2011).

2.3 Mechanism of LXR target gene regulation

As other nuclear receptors of the NR1 family, LXRs form obligate heterodimers with the retinoic X receptor (RXR). Activation of the heterodimer complex can be induced by ligands for either RXR or LXR (Lu et al. 2001). RXR-LXR heterodimers bind to specific DNA sequences, LXR response elements (LXREs), consisting of two direct repeats of hexanucleotides separated by a spacer of four nucleotides (Repa and Mangelsdorf 1999). Three different mechanisms of transcriptional regulation of target genes have been categorized. First, LXR-RXR heterodimers can actively repress gene expression in the absence of a ligand by the recruitment of co-repressor complexes, including silencing mediator of retinoic acid and thyroid hormone receptor (SMRT), nuclear receptor co-repressor (N-CoR) and histone deacetylases (HDACs) (Hu et al. 2003). Second, in the presence of a ligand, conformation changes of the receptors lead to displacement of co-repressors and the subsequent recruitment of co-activators such as activating signal cointegrator-2 (ASC-2) (Lee et al. 2008), steroid receptor co-activator 1 (SRC-1) (Son and Lee 2010) and histone acetyl transferases (Viennois et al. 2011) leading to target gene transcription. Third, LXR ligand activation can inhibit gene expression by trans-repression as shown for the nuclear factor $\varkappa$B (NF- $\varkappa$B) (Wu et al. 2009).

2.4 LXR in mouse models

LXR dependent signalling pathways clearly display anti-atherogenic properties, both by reducing cholesterol levels and supressing anti-inflammatory genes. In mouse models for atherosclerosis (LDLR$^{-/-}$ and apoE$^{-/-}$) bone marrow transplantation of cells from LXR$\alpha/\beta^{-/-}$ mice lead to significantly greater atherosclerotic lesion development compared to their counterparts that received bone marrow cells from wild-type mice (Tangirala et al. 2002). The central importance for macrophage LXRs in atherosclerosis was further confirmed by the finding that LXR$\alpha/\beta^{-/-}$ mice exhibit increased cholesterol accumulation in arterial wall macrophages even on normal diet. Consistently, activation of LXR by synthetic agonists leads to protection and regression of atherosclerotic lesions (Joseph et al. 2002). Importantly, LXRα was shown to be required for positive

agonist effects in mice (Levin et al. 2005) and macrophage-specific over-expression of LXRα ameliorated atherosclerosis in mice, independent of synthetic agonist treatment (Li et al. 2011).

2.5 LXR-dependent regulation of gene expression

If cellular oxysterols accumulate as a result of elevated concentrations of cholesterol, LXR induces the transcription of genes that protect cells from cholesterol overload. Thus, investigations of LXR-dependent gene expression regulation in macrophages revealed its involvements in cholesterol absorption, transport, and elimination. LXR activation leads to induced expression of ABCA1 (Qiu and Hill 2008), ABGG1 (Lee et al. 2010) and APOE (Bradley et al. 2007) in macrophages mediating cholesterol efflux, which facilitates cholesterol transport to extracellular receptors APOAI and HDL. Moreover, HDL levels are increased by direct LXR induction of phospholipid transfer protein (PLTP) that contributes to HDL formation and therefore accelerates cholesterol transport to the liver (Laffitte et al. 2003). LXR also reduces LDL uptake by inhibiting the LDL receptor pathway through the transcriptional induction of myosin regulatory light chain interacting protein (MYLIP) (Zelcer et al. 2009a). On the other hand, LXR directly up-regulates sterol regulatory element-binding transcription factor 1 (SREBF1) that induces transcription of genes related to lipid biosynthesis (Ferre and Foufelle 2007). Positive regulation of lipid biosynthesis associated genes through LXR-RXR heterodimer binding in macrophages is also described for fatty acid synthase (FASN), fatty acid desatuase (FADS), stearoyl-CoA desaturase (SCD) and elongation of very long chain fatty acids protein 5 (ELOVL5) (Schultz et al. 2000, Repa et al. (2000), Wang et al. 2004, Qin et al. 2009). Interestingly, LXRs and SREBF1 bind to and activate many of the same genes involved in *de novo* fatty acid biosynthesis including FASN (Shibata and Glass 2010). FASN contributes to the synthesis of free fatty acids used for cholesterol esterification of free cholesterol by sterol O-acyltransferases (SOATs) that protect cells from toxic effects of free cholesterols (Repa et al. (2000)). Taken together, LXRs activation and regulation of specific target gens antagonizes the process of cholesterol accumulation by promoting cholesterol efflux resulting in

enhanced reverse cholesterol transport to the liver.

2.6 LXRα as therapeutic targets

As described above, accumulation of cholesterol in macrophages is considered a primary event in the development of atherosclerosis. Thus removal of excess cholesterol from differentiated macrophages and macrophages-derived foam cells is important for prevention and treatment of atherosclerotic cardiovascular diseases. The abundant expression of LXRα in macrophages present in human atherosclerotic lesions (Watanabe et al. 2005) and the observations from targeted LXRα over-expression in mice (Li et al. 2011) support the hypothesis that specific LXRα agonists could have a positive effect against development of atherosclerosis (Zhao and Dahlman-Wright 2010). Despite the positive effects on atherosclerosis in mouse models, targeting LXR for therapeutic purposes in humans must overcome the obstacle of LXR-induced hepatic steatosis in mice (Joseph et al. 2002). Additionally, it is not clear how good the results from mouse studies will be predictive of potentially targeting LXRα pathways in humans for therapy.

In spite of many advances in previous studies in different human cell lines, the complete list of direct target genes for LXR remains elusive. Only a subset of known LXR target genes was elucidated specifically in human macrophage models by single gene approaches. Moreover, LXR binding was mainly shown by reporter assays independent of the endogenous genomic background. Those approaches were also restricted to genes associated with clear LXR-RXR consensus binding sequences. Importantly, existing studies primarily focused on LXRβ or detected binding regardless of the LXR isoforms. Therefore, until now, no published study has uncovered genome–wide LXRα-DNA binding and target gene regulation in human macrophages.

2.7 Aims of this thesis

The purpose of this thesis is to obtain a better understanding of the mechanisms of actions of LXRα in human macrophages during atherosclerosis. Therefore, LXRα binding and gene expression changes will be analysed in THP-1 cell-derived differ-

entiated macrophages and oxLDL-triggered macrophage-derived foam cells under T0901317-induced LXRα activation as compared with untreated macrophages.

Independently, data from chromatin immunoprecipitation experiments coupled with high-throughput sequencing (ChIP-seq) and data from expression microarray experiments tell very different stories. ChIP-seq structurally measures protein-DNA binding that can be used to hypothesize gene regulation by their locations in the genome. Microarray experiments provide a functional view on changes in gene expression regardless of exact regulatory mechanisms. However, the integration of data from both approaches allows the assignment of specific regulatory roles of transcription factors.

Therefore, treatment–specific LXRα cistromes will be determined using genome-wide LXRα occupancy data. Then, cistromes are integrated with genome-wide transcription data to obtain a global view of directly regulated target genes and to construct a network of transcriptional regulators influenced by LXRα activation. Since LXRα is involved in various aspects of metabolism in macrophages, an important question is whether it binds the same genomic regions in different macrophage treatment models. Alternatively, LXRα may bind to treatment specific regions, allowing the regulation of specialized pathways. Another important aspect is the mechanism whereby LXRα selects genomic regions and interacts with the chromatin landscape leading to target gene regulation. It has previously been shown that transcription factor binding correlates with nucleosome-depleted regions of open chromatin that represent active regulatory elements (Gaulton et al. 2010). Therefore, chromatin accessibility that accompanies the binding of LXRα will be investigated using high-throughput sequencing of genomic regions enriched by formaldehyde-assisted isolation of regulatory elements (FAIRE-seq). This analysis also enables investigations regarding the specific co-regulator requirement of functional LXRα binding sites. Collectively, this master's thesis aims to provide an initial framework for understanding and investigating LXRα-dependent gene regulations in human macrophages by the use of integrative analysis strategies.

3 Results

3.1 LXRα is up-regulated in response to the LXR agonist T0901317

Several studies showed that LXRα but not LXRβ transcription is influenced by an auto-up-regulatory loop. Therefore, LXRα occupies the LXR-response element in the *LXR*α gene leading to transcriptional up-regulation upon agonist application. Thus, LXRα activity is influenced not only by specific ligands alone but also by changes in transcription factor expression (Li et al. 2002, Whitney et al. 2001). The auto-regulation of LXRα provides a mechanism for amplifying the effects of endogenous oxLDL in macrophages to promote cholesterol efflux in order to attenuate the transformation of macrophages into foam cells (Whitney et al. 2001). To estimate the amount of ligand specific LXRα up-regulation and to confirm previous findings, expression analysis was performed to estimate LXRα protein levels amongst untreated and T0901317-treated differentiated THP-1 cells and T0901317-treated THP-1-derived foam cells. In accordance with previous results (Laffitte et al. 2001) western blot analysis revealed that LXRα gene expression is induced by T0901317. Coadministration of the natural ligand oxLDL and T0901317 showed an additive effect with strongly up-regulated LXRα protein expression. Contrary, in the absence of ligand LXRα expression was hardly detectable (Figure 1A). Measured mRNA levels support these observations in THP-1 cells (Figure 1B).

3.2 ChIP-seq analysis of LXRα binding

Chromatin-immunoprecipitation and sequencing experiments can quantify the association of a DNA-ineracting protein with every position in the genome. Therefore, proteins are crosslinked with DNA and the isolated chromatin is fragmented before immunoprecipitating the protein-DNA complexes and reversing the crosslinks (Leleu et al. 2010). LXRα ChIP-seq experiments were previously performed in our lab and the obtained data sets were used to identify genomic loci bound by LXRα. The ChIP-derived material was therefore subjected to library preparation followed by next generation Illumina sequencing and the obtained sequence reads were aligned to the genome.

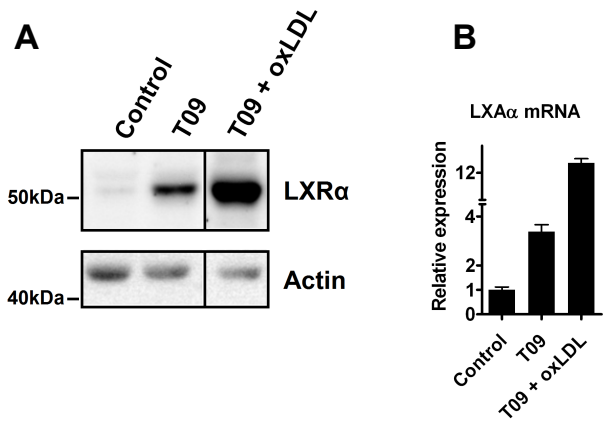

Figure 1: **LXRα is up-regulated in macrophages and foam cells in response to T0901317. (A)** Equal amounts of proteins from nuclear extracts were subjected to western blot analysis using antibodies against LXRα and β-actin (Actin). Differentiated THP-1 cells were treated either with 0.01% DMSO (Control) or 1 μM T0901317 (T09) for 24 hours or with 100 μg/ml oxLDL for 48 hours and 1 μM T0901317 for 48 hours (T09 + oxLDL). **(B)** Microarray measures of LXRα transcript expression levels. Bar graphs indicate relative expression between treated (T09 and T09 + oxLDL) and vehicle-treaded (Control) cells. Data were normalized to the intensity of β-actin as a housekeeping gene. Each point represents the mean of triplicate values ± standard derivation.

3.2.1 ChIP-seq-derived LXRα binding profiles confirm known LXRα target genes

Aligned sequencing reads were processed to generate density profiles, which were examined across loci corresponding to six known LXRα target genes. Profiles from LXRα-induced cells showed LXRα binding with a clear enrichment of tags over a narrow range near loci of *LXRα* itself and the genes such as *ABCA1*, *ACCA*, *FASN*, *SREBF1* and *ABCG1* (Figure 2A). These binding regions were not detected if cells were not treated with LXRα-specific ligands. In order to confirm the robustness of the ChIP-seq data, LXRα ChIP was repeated and the enriched material was assessed using real-time quantitative PCR (qPCR). Visual comparison of the ChIP-seq profiles confirmed high concordance. Binding of LXRα was tested at ten genomic regions in LXRα-induced THP-1-derived macrophages and no binding was observed in the absence of LXRα activation (Figure 2B). In accordance with the ChIP-seq profiles, enhanced signals at binding sites were observed in T0901317-treated foam cells compared to T0901317-treated macrophages.

In addition to binding sites close to the gene transcriptional start sites, LXRα enriched regions were observed in distal putative enhancer regions (*ABCA1*) and in intronic regions of target genes (*ABCG1* and *LXRα*, Figure 2A). Remarkably, alternative promoters of *SREBF1* were individually occupied by LXRα, indicating stringent splice variant regulation. Together, these observations show that LXRα binds to different genomic sites to regulate the same target gene and that binding is not restricted to proximal target promoter regions. Distal binding sites indicate the possibility of remote transcription factor interaction through DNA looping or protein tethering, which also challenges the definition of target genes especially in regions with high gene densities (Nolis et al. 2009, Zhao et al. 2011).

3.2.2 Genome-wide identification of LXRα binding sites

Identification of unknown LXRα target sites and determination of treatment specific changes of LXRα occupancy requires genome-wide determination of LXRα enriched regions. This task is accomplished by using peak calling algorithms that output

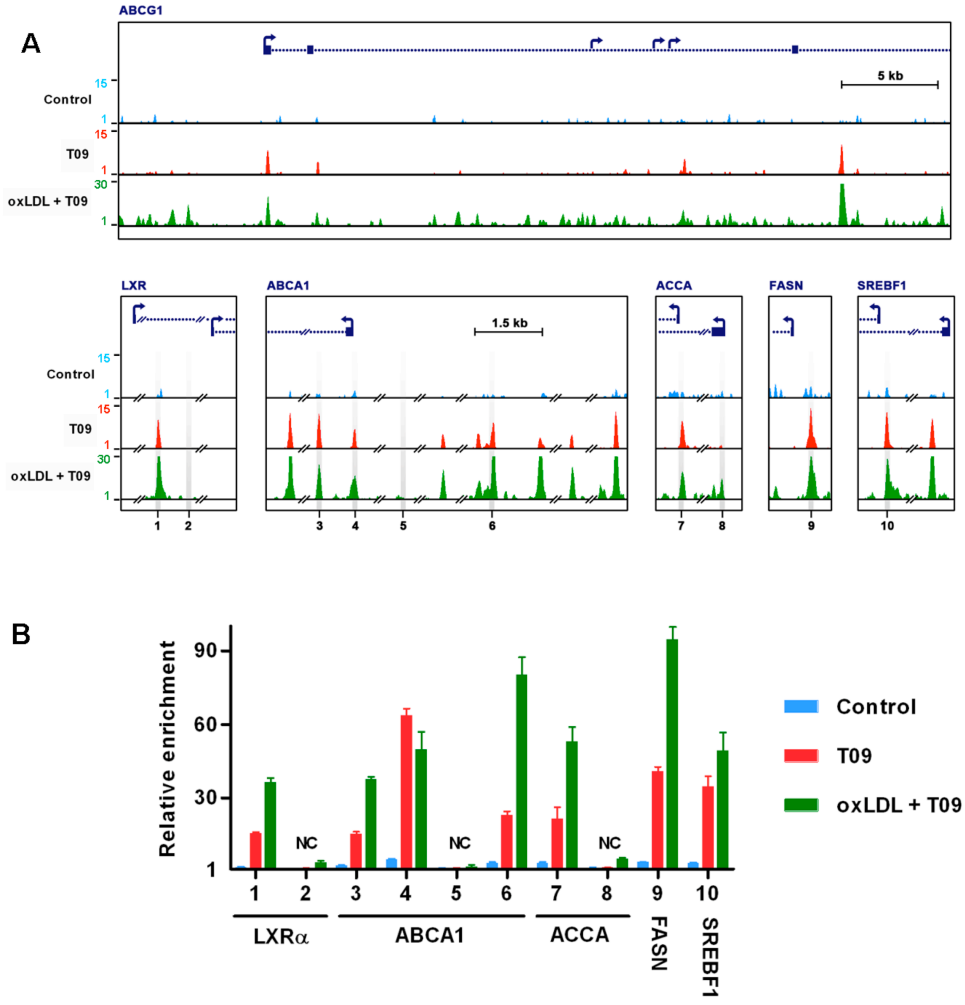

Figure 2: **LXRα occupancy at genomic regulatory elements. (A)** LXRα ChIP-seq profiles of genomic loci for the LXRα target genes *ABCG1*, *LXRα*, *ABCA1*, *ACCA*, *FASN* and *SREBF1*. Clear LXRα enrichments are detected in promoter and enhancer regions of gene loci on T0901317-treated macrophages (T09, red) and foam cells (oxLDL + T09, green), whereas no binding is observed in the absence of ligand (Control, blue) or at negative control regions (2, 5, 8). ChIP-seq data are plotted as the density of 25-bp tags mapping to the region. The y axis represents the estimated number of tags at each position. Gene loci are shown based on the human genome February 2009 assembly (GRCh37/hg19) in the UCSC browser using RefSeq positions. The direction of transcription is shown by the arrow beginning at the TSS. Genomic coordinates of the shown regions: *ABCG1* (chr21:43,608,584-43,654,980), *LXRα* (chr11:47,270,159-47,280,387), *ABCA1* (chr9:107,622,630-107,834,119), *ACCA* (chr17:35,708,974-35,769,074), *FASN* (chr17:80,053,735-80,059,108) and *SREBF1* (chr17:17,725,865-17,742,257). **(B)** ChIP-qPCR validation of LXRα enrichment at sites indicated by numbers below ChIP-seq profiles (A). Data are fold enrichments compared to individual input non-enriched DNA normalized to IgG ChIP DNA. The data are the mean of triplicate values ± standard derivation. Negative control region are indicated (NC).

positions in the genome with more ChIP-seq tags than expected by chance and thus identify genomic intervals of enriched regions as observed at LXRα target gene loci (Figure 3A). Peak intervals were identified genome-wide by the use of the model based-analysis of ChIP-seq (MACS) algorithm (Zhang et al. 2008) with LXRα sequencing data against control IgG ChIP-seq data. Therefore, aligned tags of two biological replicates from T0901317-treated macrophages and untreated macrophages were individually pooled to gain sufficient tag enrichment and to correct for biological variations. The algorithm successfully determined peak intervals at already observed enrichment sites of known LXRα targets. MACS also indicated the absence of LXRα binding in uninduced cells as the derived peak intervals had very low tag enrichments and low peak significances compared to binding sites detected in cells after LXRα activation. Nevertheless, broad fractions of estimated peak intervals of all three data sets showed low significance levels (Figure 3B). Therefore, candidate peaks from data of LXRα-induced cells were filtered by removing those peak intervals that were inconsistent between three individual peak identification runs using data from different IgG-ChIP samples. Those peak intervals were further filtered using k-means clustering (Heintzman et al. 2009) to remove clusters of intervals with low tag enrichments. Filtering defined a high-confidence set of genome-wide LXRα binding sites with 249 and 215 peak intervals of TO901317-stimulated THP-1-derived macrophages and foam cells respectively. Strikingly, only 64 peak intervals are shared in both treatment models upon LXRα activation (Figure 4A).

3.2.3 LXRα binding is induced upon LXRα activation

The observation from sequencing-derived profiles and qPCR validation experiments that show the absence of LXRα binding in untreated THP-1 control cells was also encouraged by the low genome-wide sequencing coverage (Figure 5A). In concert, heat map visualisation of tag densities around LXRα peak intervals from both macrophage treatment models show only marginal tag accumulations in untreated THP-1-derived macrophages (Figure 4B, control). To further investigate these observations, average tag profiles centered at LXRα binding sites were estimated along with sequencing data

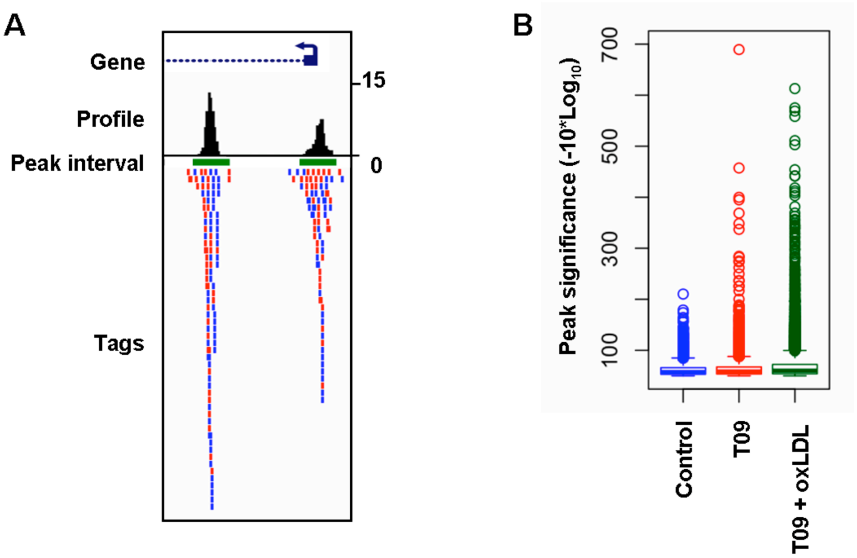

Figure 3: **Peak detection and significance of peaks. (A)** Peak detection and tag density profile generation. Aligned ChIP-seq-derived forward (red) and reverse (blue) tags (Tags) generate a strand-specific pattern that is used for the detection of enriched regions via peak calling algorithms (Peak interval, green). For visualization tag locations are extended by an estimated fragment size in the appropriate orientation and the number of fragments is counted at each position to generate a density profile (Profile, black). Tag density profiles are plotted as the density of 25-bp tags mapping to the region. The y axis of the profile represents the estimated number of tags at each position. Shown is the *ABCA1* promoter region (~2kb). **(B)** Box plot showing the distributions of ChIP-Seq peak interval significances (-10*Log10(p-value)) determined by MACS from vehicle-treated macrophages (Control, blue), T0901317-treated macrophages (T09, red) and T0901317-treated foam cells (oxLDL + T09, green).

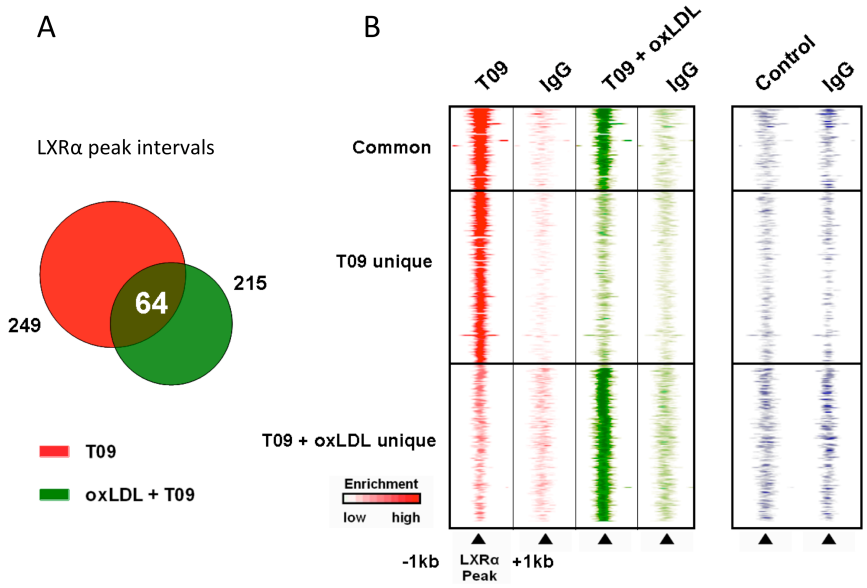

Figure 4: **Ligand-dependent dynamics of LXRα.** (A) Comparison of large-scale ChIP profiling data. Venn diagram of the overlap of LXRα-binding sites of T0901317-treated macrophages (T09, red) and T0901317-treated foam cells (oxLDL + T09, green) as identified by MACS and filtered as described (Methods). 64 of the ChIP-Seq interaction sites are overlapping with at least 1 base pair. **(B)** Heat maps show enrichment over all 400 sorted LXRα binding sites (LXRα Peak), where the shading corresponds to the LXRα ChIP-seq and IgG ChIP-seq read count in the region from vehicle-treated macrophages (Control, blue), T0901317-treated macrophages (T09, red) and T0901317-treated foam cells (oxLDL + T09, green). One-kilobase pairs around the LXRα peaks are displayed.

from input DNA. Sequencing of fragmented chromatin that was de-crosslinked and not subjected to immunoprecipitation generated these input DNA. Input DNA is often used as control in ChIP-Seq experiments as alternative to nonspecific IgG antibodies (Kidder et al. 2011). Remarkably, average tag density profiles at LXRα binding sites of cells that were not exposed to LXRα agonists are similar to tag profiles derived from input DNA samples (Figure 5B). This shows that the minor tag accumulations in untreated cells do not represent indications of LXRα binding and rather reflect inherent sequencing bias, mapping ambiguity or chromatin structure as described previously (Vega et al. 2009).

These findings indicate strictly ligand-induced LXRα binding in differentiated THP-1 cells contrary to the classic model of constitutive LXR binding and replacement of

LXR associated co-repressors with co-activators upon ligand-induced LXR activation (Wagner et al. 2003, Hu et al. 2003). Importantly, even different LXRα activation strategies by T0901317 treatment or combinatorial treatment with T0901317 and oxLDL lead to differential binding patterns as observed from heat map visualisation, LXRα peak interval intersection (Figure 4) and at specific loci (Figure 5C). The conventional mechanism of constitutive LXRα binding was recently challenged by the findings that LXRα/β recruitment was entirely ligand-dependent at the *ABCG1* promoter in HepG2 and THP-1 cells (Jakobsson, 2009). However, absence of basal LXRα binding in untreated cells may be cell line or LXR isoform specific and did not reflect the situation in untreated primary human macrophages where basal LXRα occupancy was detected by ChIP-qPCR (Figure 5D). Additionally, it cannot be ruled out that LXRα binding in untreated THP-1 cells is simply not detectable by ChIP assays due to low levels of LXRα protein in those cells compared to others. Though, LXRα activation by diet-dependent endogenous stimuli is much more likely in primary human cells compared to vehicle-treated macrophages-derived from the THP-1 cell line. However, the global absence of LXRα binding in control cells represents an appropriate macrophage model to study ligand-induced binding upon LXRα activation.

3.2.4 LXRα binds proximal promoter regions and distal regulatory elements

Defined LXRα binding sites were enriched at promoters and coding exons relative to their genomic frequency illustrating that LXRα binds in regions directly associated with transcriptional regulation. The observed preponderance of binding occurred at putative enhancer regions intronic and distal intergenic with nearly unchanged occupancy relative to the genomic frequency (Figure 6A). Precise distance analysis of LXRα peaks relative to genes confirmed these observations and showed accumulation close to promoters with the occurrence of distal binding in T0901317-treated differentiated macrophages and foam cells (Figure 6B). Similar results were obtained by peak distribution analysis relative to gene bodies (not shown). Collectively and in accordance with initial profile inspections, results show that LXRα has widespread distribution patterns similar to other transcription factors (Welboren, 2009) and cannot be categorized to

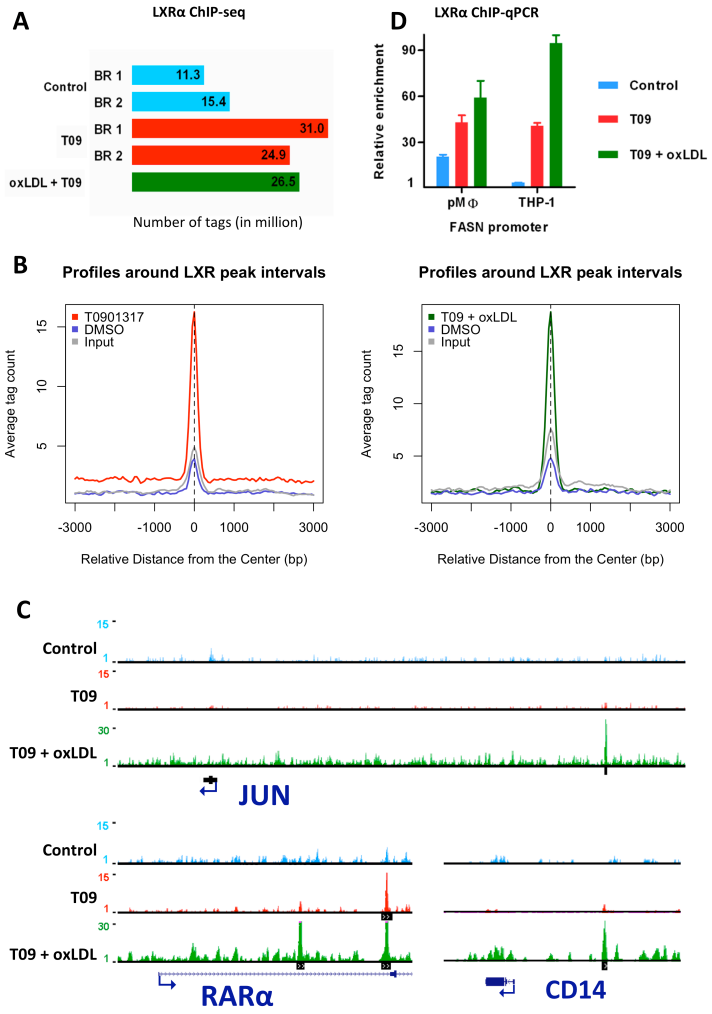

Figure 5: **Influence of ligand application on LXRα DNA binding.** **(A)** LXRα ChIP-seq sequence depth in differently treated macrophages including biological replicates (BR). **(B)** Average LXRα ChIP-seq tag profile at LXRα binding sites of T0901317-treated macrophages (left) and T0901317-treated foam cells (right) show tag enrichment in treated cells (T0901317 and T09 + oxLDL). In vehicle-treated cells (DMSO) tag enrichment is similar to sequenced input DNA (Input). Three-kilobase pairs around the LXRα peaks are displayed. **(C)** Ligand-induced cell model specific LXRα binding sites (peak intervals shown as black bars) at three representative gene loci (*JUN*: chr1:59,226,758-59,353,087, *RARα*: chr17:38,461,237-38,491,262 and *CD14*: chr5:140,007,968-140,023,959). ChIP-seq data are plotted as the density of 25-bp tags mapping to the region. The y axis represents the estimated number of tags at each position. The UCSC Genes track is used to indicate RefSeq validated gene positions. **(D)** ChIP-qPCR of LXRα enrichment at the LXR response element in proximity to the *FASN* promoter in primary human monocyte-derived macrophages and THP-1 cells. Data are fold enrichments compared to individual input non-enriched DNA normalized to IgG ChIP DNA. The data are the mean of triplicate values ± standard derivation.

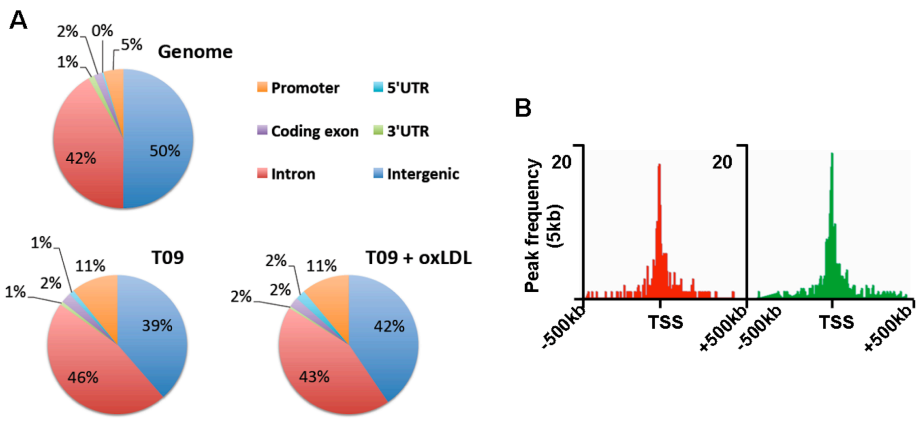

Figure 6: **Genomic distribution of LXRα binding sites. (A)** Distribution of LXRα binding sites over genomic features for T0901317-treated macrophages (T09) and T0901317-treated foam cells (T09 + oxLDL). The percentages of the mappable regions that are located in genomic features (genome background) is shown (Genome). Promoters are defined as TSS ± 3 kb. 'Intergenic' represents the percentage of ChIP regions that do not belong in any of other genomic features. **(B)** LXRα ChIP-seq peak distribution relative to known TSS (RefGene) ± 500 kb (red: T09, green T09 + oxLDL).

either proximal promoter or enhancer binding.

3.2.5 A global inventory of LXRα occupied genes

One of the major challenges in ChIP-seq analysis represents mapping transcription factor binding to the genes they regulate directly, considering the three-dimensional structure of chromatin (Dekker 2008) but also the heterogeneous gene annotation resources (Sherman et al. 2007). A known gene with a proximal transcription factor binding site around its promoter region is usually considered as a direct target gene because proximal transcription factor binding is often manifested by changes in gene expression (Loh et al. 2006). The vast proportion of binding sites located away from transcriptional start sites, challenge the connection of those sites to the corresponding targets. However, to begin to examine the functional significance of LXRα binding on a genome-wide scale, LXRα binding sites were annotated to the nearest gene using gene annotations from the NCBI RNA reference sequences collection (RefSeq). That identified 226 and 197 genes targeted by 249 and 215 LXRα binding events in agonist treated THP-1-derived macrophages and foam cells respectively (Tables 1

and 2). The observed reduction from number of binding sites to number of genes is explained by the fact that LXRα binds at more than one site near or within a gene as previously shown by tag density profile inspection. Regions of multiple binding sites in both treatment groups were exclusively associated with the known LXRα target genes *ABCA1*, *ABCG1*, *SCD*, *APOC1*, *SREBF1* and *RAR*α. Thus, the presence of multiple binding sites in close proximity indicates a mechanism of stringent target gene regulation. Investigation of the functional relationship of LXRα target genes revealed significant associations to lipid, fatty acid and cholesterol metabolic pathways. Furthermore, functional enrichment analysis (Sherman et al. 2007) showed genes that were associated to pathways not directly connected with the common functions of LXRα, suggesting a wider role of LXRα in other biological processes (Table 3).

3.3 LXRα binding triggers differential expression of distinct gene sets

Hypothetically, genes that are stringently modulated by LXRα would contain a LXRα enriched region in their vicinity and show altered regulation of gene expression. To address a broad range of genes that are potentially regulated, genomic binding sites were therefore extensively annotated using different approaches that were combined and finally correlated with treatment-dependent expression changes. Using microarray technology gene expression profiles were generated from isolated RNA of THP-1 cells that were treated in the same manner as cells used for ChIP assays. The comparison of the profiles between untreated THP-1-derived macrophages with both T0901317-treated macrophages and T0901317-treated foam cells revealed that 332 and 942 genes were significantly changed for both treatment conditions respectively.

The performed next gene analysis was restricted to a single gene that is next to a binding site (Table 1 and 2). However, it remains possible that one binding site regulates one or many target genes. The observed ligand-induced co-expression of the neighbouring genes *ACP2* (1.4-fold) and *LXR*α (2.7-fold) that are targeted by only one LXRα binding event support the assumption that an individual binding site may influence a set of surrounding genes. Therefore, the single nearest gene annotation

Group	Chr	Start	End	p-val	Refgene	Symbol	Description	Strand	Distance to TSS
Unique	chr3	43496432	43497090	453.36	NM_018075	ANO10		-	166799
Unique	chr20	30283862	30284550	381.11	NM_138578	BCL2L1	BCL2-like 1	-	26450
Common	chr1	111745502	111746256	332.64	NM_024901	DENND2D	DENN/MADD domain containing 2D	-	-2598
Common	chr3	38125570	38126387	316.56	NM_007337	DLEC1	Deleted in lung and esophageal cancer 1	+	45283
Common	chr17	80245768	80246409	293.5	NM_001893	CSNK1D	Casein kinase 1, delta	-	-14494
Common	chr7	36247507	36248277	281.08	NM_030636	EEPD1		+	55057
Unique	chr15	102050741	102051340	271.57	NM_002570	PCSK6	Proprotein convertase subtilisin/kexin type 6	-	-20853
Common	chr17	38486241	38487120	268.56	NM_001024809	RARA	Retinoic acid receptor, alpha	+	-11590
Common	chr21	43647984	43648615	258.88	NM_207174	ABCG1	ATP-binding cassette, sub-family G (WHITE), member 1	+	8292
Common	chr9	107631068	107631618	250.04	NM_005502	ABCA1	ATP-binding cassette, sub-family A (ABC1), member 1	-	59184
Common	chr6	43931944	43933075	236.01	NM_153246	C6orf223		+	-35827
Common	chr2	113861610	113862257	233.69	NM_173841	IL1RN	Interleukin 1 receptor antagonist	+	-13536
Common	chr6	123111861	123112388	232.29	NM_006714	SMPDL3A	Sphingomyelin phosphodiesterase, acid-like 3A	+	2154
Common	chr10	77189709	77190136	229.48	NR_024422	NCRNA00245		+	26409
Unique	chr4	190756767	190757087	229.42	NM_004477	FRG1	FSHD region gene 1	+	-105046
Unique	chr12	28932992	28933427	221.78	NM_018099	FAR2		+	-443388
Common	chr17	17739387	17739936	211.67	NM_004176	SREBF1	Sterol regulatory element binding transcription factor 1	-	664
Unique	chr1	59347028	59347575	208.35	NR_034014	LOC100131060		+	96479
Unique	chr1	235001946	235002326	197.17	NR_033927	NCRNA00184		+	237080
Common	chr6	90708846	90709269	195.49	NM_032602	GJA10	Gap junction protein, alpha 10, 62kDa	+	104870
Unique	chr10	102100780	102101444	192.13	NM_005063	SCD	Stearoyl-CoA desaturase (delta-9-desaturase)	+	-5659
Common	chr3	49481480	49481741	191.52	NM_032316	NICN1	Nicolin 1	-	-14853
Common	chr6	16131212	16131508	190.51	NM_013262	MYLIP	Myosin regulatory light chain interacting protein	+	2044
Unique	chr20	61200527	61201015	186.71	NR_029676	MIR133A2		+	38653
Common	chr11	47276379	47276973	186.06	NM_001130101	NR1H3	Nuclear receptor subfamily 1, group H, member 3	+	-2820
Unique	chr5	149696514	149697329	182.2	NM_001012301	ARSI	Arylsulfatase family, member I	-	-14396
Common	chr9	107826627	107827263	179.47	NM_005502	ABCA1	ATP-binding cassette, sub-family A (ABC1), member 1	-	-136418
Common	chr1	233248366	233249146	178.72	NM_032324	NTPCR		+	162387
Common	chr13	111188451	111189066	176.61	NM_017817	RAB20	RAB20, member RAS oncogene family	-	25313
Common	chr9	97488821	97489303	171.89	NM_001193331	C9orf3	Chromosome 9 open reading frame 3	+	112
Unique	chr2	15182997	15183691	168.47	NM_145175	FAM84A	Family with sequence similarity 84, member A	+	410535
Common	chr6	53224051	53224774	168.44	NM_021814	ELOVL5	ELOVL family member 5, elongation of long chain fatty acids (FEN1/Elo2, SUR4/Elo3-like, yeast)	-	-10470
Common	chr1	9703679	9704361	167.98	NM_005026	PIK3CD	Phosphoinositide-3-kinase, catalytic, delta polypeptide	+	-7769
Unique	chr17	38478342	38479088	159.7	NM_001145302	RARA	Retinoic acid receptor, alpha	+	4243
Unique	chr2	137003534	137004227	157.19	NM_003467	CXCR4	Chemokine (C-X-C motif) receptor 4	-	-128155
Unique	chr5	146345713	146346215	156.86	NM_001127381	PPP2R2B	Protein phosphatase 2 (formerly 2A), regulatory subunit B, beta isoform	-	-87507
Unique	chr15	74890421	74891313	155.93	NM_003992	CLK3	CDC-like kinase 3	+	-9845
Common	chr1	150849095	150849557	154.02	NM_178427	ARNT	Aryl hydrocarbon receptor nuclear translocator	-	-82
Unique	chr5	139043661	139044289	152.84	NM_016463	CXXC5	CXXC finger 5	+	15675
Common	chr7	153505197	153505553	151.69	NM_001039350	DPP6	Dipeptidyl-peptidase 6	+	-79043
Common	chr17	80056617	80057343	150.22	NM_004104	FASN	Fatty acid synthase	-	-874
Unique	chr4	141172137	141172805	148.89	NM_032547	SCOC	Short coiled-coil protein	+	-5968
Common	chr15	52273689	52274072	145.98	NM_138792	LEO1	Leo1, Paf1/RNA polymerase II complex component, homolog (S. cerevisiae)	-	-9922
Common	chr1	12655854	12656407	144.95	NM_004753	DHRS3	Dehydrogenase/reductase (SDR family) member 3	-	21690
Common	chr13	52123071	52123693	144.69	NM_052950	WDFY2	WD repeat and FYVE domain containing 2	+	-35101
Unique	chr8	134151419	134152090	144.27	NM_001045556	SLA	Src-like-adaptor	-	-36444
Common	chr9	107769294	107769732	141.78	NM_005502	ABCA1	ATP-binding cassette, sub-family A (ABC1), member 1	-	-78986
Common	chr6	47214846	47215207	141.65	NM_014452	TNFRSF21	Tumor necrosis factor receptor superfamily, member 21	-	62654
Unique	chr5	140018630	140018978	140.19	NM_018502	TMCO6	Transmembrane and coiled-coil domains 6	+	-207
Unique	chr15	34942137	34942698	139.65	NR_027410	GOLGA8B		-	-66646

Table 1: Top 50 LXRα binding sites of T0901317-treated macrophages.

Group	Chr	Start	End	p-val	Refgene	Symbol	Description	Strand	Distance to TSS
Common	chr6	53224061	53224870	499.3	NM_021814	ELOVL5	ELOVL family member 5, elongation of long chain fatty acids (FEN1/Elo2, SUR4/Elo3-like, yeast)	-	-10523
Common	chr17	80056520	80057329	466.25	NM_004104	FASN	Fatty acid synthase	-	-818
Common	chr9	107688746	107689237	457.28	NM_005502	ABCA1	ATP-binding cassette, sub-family A (ABC1), member 1	-	1536
Common	chr17	17727084	17727637	426.34	NR_030361	MIR33B		-	-10115
Common	chr17	17739310	17739954	407.63	NM_004176	SREBF1	Sterol regulatory element binding transcription factor 1	-	693
Common	chr6	16131061	16131653	399.82	NM_013262	MYLIP	Myosin regulatory light chain interacting protein	+	2041
Common	chr17	38486274	38487265	354.86	NM_001024809	RARA	Retinoic acid receptor, alpha	+	-11501
Common	chr1	111745502	111746256	332.64	.	DENND2D	DENN/MADD domain containing 2D	.	.
Common	chr10	102132813	102133450	331.09	NR_026762	NCRNA00263		+	-201
Common	chr11	47276327	47276899	326.11	NM_001130101	NR1H3	Nuclear receptor subfamily 1, group H, member 3	+	-2883
Common	chr6	43932313	43933063	323.86	NM_153246	C6orf223		+	-35648
Common	chr21	43654695	43655387	322.72	NM_207174	ABCG1	ATP-binding cassette, sub-family G (WHITE), member 1	+	15034
Common	chr9	107826618	107827216	298.93	NM_005502	ABCA1	ATP-binding cassette, sub-family A (ABC1), member 1	-	-136390
Common	chr6	123111793	123112450	284.75	NM_006714	SMPDL3A	Sphingomyelin phosphodiesterase, acid-like 3A	+	2151
Common	chr7	36247507	36248277	281.08	NM_030636	EEPD1		+	55057
Common	chr13	22583442	22584251	268.68	NM_002010	FGF9	Fibroblast growth factor 9 (glia-activating factor)	+	338632
Common	chr9	107631095	107631708	260.18	NM_005502	ABCA1	ATP-binding cassette, sub-family A (ABC1), member 1	-	59126
Common	chr3	38125459	38126405	255.7	NM_007337	DLEC1	Deleted in lung and esophageal cancer 1	+	45237
Common	chr9	107690166	107690793	249.77	NM_005502	ABCA1	ATP-binding cassette, sub-family A (ABC1), member 1	-	48
Common	chr21	43647988	43648603	249.75	NM_207174	ABCG1	ATP-binding cassette, sub-family G (WHITE), member 1	+	8288
Unique	chr12	7125716	7126466	236.65	NM_005768	LPCAT3		-	-249
Common	chr1	233248404	233249135	234.55	NM_032324	NTPCR		+	162400
Common	chr10	77189564	77190158	226.45	NR_024422	NCRNA00245		+	26348
Common	chr19	45428672	45429065	212.81	NR_028412	APOC1P1		+	-1191
Unique	chr21	43619402	43619982	188.47	NM_207627	ABCG1	ATP-binding cassette, sub-family G (WHITE), member 1	+	-106
Common	chr17	2296041	2296565	186.67	NM_020310	MNT	MAX binding protein	-	7955
Unique	chr21	43640145	43640794	179.1	NM_207174	ABCG1	ATP-binding cassette, sub-family G (WHITE), member 1	+	462
Common	chr13	52123060	52123682	173.81	NM_052950	WDFY2	WD repeat and FYVE domain containing 2	+	-35112
Common	chr3	57102429	57102947	173.48	NM_181727	SPATA12	Spermatogenesis associated 12	+	8220
Common	chr3	13040975	13041529	173.09	NM_014869	IQSEC1	IQ motif and Sec7 domain 1	-	-32292
Common	chrX	152991985	152992646	170.85	NM_000033	ABCD1	ATP-binding cassette, sub-family D (ALD), member 1	+	1993
Common	chr9	107769330	107769678	168.94	NM_005502	ABCA1	ATP-binding cassette, sub-family A (ABC1), member 1	-	-78977
Common	chr17	80245791	80246390	168.49	NM_001893	CSNK1D	Casein kinase 1, delta	-	-14496
Unique	chr21	16594310	16594787	166.01	NM_003489	NRIP1	Nuclear receptor interacting protein 1	-	-157422
Unique	chr18	9849357	9849859	164.86	NM_001098529	TXNDC2	Thioredoxin domain-containing 2 (spermatozoa)	+	-36114
Common	chr9	107755894	107756348	164.17	NM_005502	ABCA1	ATP-binding cassette, sub-family A (ABC1), member 1	-	-65594
Common	chr22	46402054	46402818	163.85	NR_027240	LOC730668		+	-59
Common	chr9	136283070	136283472	163.3	NM_020385	REXO4	REX4, RNA exonuclease 4 homolog (S. cerevisiae)	-	-107
Unique	chr7	17448059	17448566	163.29	NM_001621	AHR	Aryl hydrocarbon receptor	+	110037
Common	chr9	107723479	107723935	158.98	NM_005502	ABCA1	ATP-binding cassette, sub-family A (ABC1), member 1	-	-33180
Common	chr1	9703735	9704355	156.38	NM_005026	PIK3CD	Phosphoinositide-3-kinase, catalytic, delta polypeptide	+	-7744
Common	chr7	153505197	153505553	151.69	NM_001039350	DPP6	Dipeptidyl-peptidase 6	+	-79043
Common	chr6	47214774	47215513	151.16	NM_014452	TNFRSF21	Tumor necrosis factor receptor superfamily, member 21	-	62537
Common	chr1	167569300	167569911	147.14	NM_052862	RCSD1	RCSD domain containing 1	+	-29868
Unique	chr5	17141212	17141722	142.47	NR_027253	LOC285696		-	76064
Common	chr1	150849171	150849520	140.12	NM_178427	ARNT	Aryl hydrocarbon receptor nuclear translocator	-	-101
Common	chr11	86748666	86749297	130.2	NM_001168724	TMEM135	Transmembrane protein 135	+	96
Common	chr1	12655898	12656315	129.99	NM_004753	DHRS3	Dehydrogenase/reductase (SDR family) member 3	-	21714
Common	chr3	49481389	49481767	128.82	NM_032316	NICN1	Nicolin 1	-	-14821
Unique	chr1	94374966	94375517	125.27	NM_002061	GCLM	Glutamate-cysteine ligase, modifier subunit	-	-229

Table 2: Top 50 LXRα binding sites of T0901317-treated foam cells

A

Category	Count	PValue	Genes
Negative regulation of cholesterol storage	4	1.53E-03	ABCA1, ABCG1, NR1H3, APOC1
Regulation of lipid metabolic process	6	5.94E-03	KCNMA1, APOC1, NR3C1, GAL, ABCG1, NR1H3
Phospholipid binding	7	9.73E-03	PFN2, PLA2G15, SNX16, APOC1, SNX4, ABCA1, ABCG1
Lipid and fatty acid transport	6	1.04E-02	ABCD1, APOC1, ABCA1, ABCG1, ABCA13, PLTP
Cell morphogenesis	10	1.12E-02	SLITRK1, NCAM2, SEMA6A, PARD6B, BMP2, BCL11B, TFCP2L1, APBB2, BMPR1B, IFT88

B

Category	Count	PValue	Genes
Negative regulation of cholesterol storage	3	1.07E-03	ABCA1, ABCG1, NR1H3
Fatty acid biosynthetic process	5	4.70E-03	FCER1A, ELOVL5, SCD, FASN, C9ORF3
Response to endogenous stimulus	10	8.05E-03	KCNMA1, DRD5, IL1RN, RARA, IL6R, BCL2L1, EIF2B2, SRF, ABCG1, SRC

Table 3: Functional clustering of nearest gene datasets of T0901317-treated macrophages **(A)** and T0901317-treated foam cells **(B)** by the DAVID gene onthology program.

approach was combined with determination of peak surrounding proximal genes and the association of distal peak intervals with genes in regulatory domains by the use of binomial and hypergeometric tests (McLean et al. 2010). This relaxed annotation strategy considered ~460 putatively LXRα-associated genes in both treatment models.

Comparison of LXRα occupied genes with genes that were significantly differentially expressed upon ligand stimulation, identified an array of 52 genes in both macrophage conditions that are refered to as direct LXRα target genes. Within these sets 20 and 40 genes were classified by LXRα binding and expression changes in T0901317-treated macrophages and foam cells respectively (Table 4 and 5). The majority of the direct LXRα target genes were up-regulated but four genes in T0901317-treated foam cells were down-regulated. These findings confirm that LXRα acts as transcriptional activator as well as repressor (Hu et al. 2003) but also highlights, that direct LXRα target gene regulation preferentially leads to activation of transcription. Only eight up-regulated genes were shared amongst both models, elucidating the distinct role of LXRα in differentiated macrophages and oxLDL-induced foam cells upon LXRα activation.

However, the most obvious conclusion of the performed correlation is that only a very distinct gene set is directly regulated by LXRα. The majority of LXRα bound genes and a large portion of differentially expressed genes is not clearly correlated with direct LXRα regulation. This raises the possibility that LXRα acts through long-range

mechanisms, indirect via other transcription factors, or that many of the LXRα binding events are opportunistic.

3.3.1 Previously unknown LXRα target genes

Gene ontology classification (Sherman et al. 2007) was used to identify biological processes that would be over-represented amongst directly regulated LXRα target genes. Directly regulated target genes fall in the already determined categories, including cholesterol efflux, metabolism of lipids and fatty acid metabolism (Figure 4 and 5). Many of those genes represent known LXRα targets, although direct binding in human macrophages by the use of ChIP assays was only shown for a small minority, such as the LXRα target genes *ABCG1* and *ABCA1* (Jakobsson et al. 2009). However, data mining in biological databases revealed a number of detected genes that are not yet associated with LXRα, such as acid sphingomyelinase-like phosphodiesterase 3A (*SMPDL3*), endonuclease/exonuclease/phosphatase family domain containing 1 (*EEPD1*) and amiloride-sensitive cation channel 3 (*ACCN3*). Interestingly, many of the directly regulated LXRα target genes in T0901317-treated foam cells represent membrane proteins. Categorization of gene sets by gene families additionally revealed the presence of directly regulated transcription factors. Many of those were not yet shown to be direct targets of LXRα.

3.3.2 Correlation of LXRα binding and gene expression changes in different treatment models

To better understand how LXRα binding and gene expression correlate between T0901317-treated macrophages and foam cells, both gene lists were combined and sorted according to common and treatment specific genes. Remarkably, diverse combinatorial clusters were observed, regarding LXRα binding and associated gene expression (Table 6). The comparison indicates, that LXRα binding alone is not sufficient to gain gene expression changes in both treatment models (cluster III and V) and vice versa (cluster IV and II). As expected, combinatorial treatment of T0901317 and oxLDL-derived foam cells induces LXRα binding at almost all gene loci whereas T0901317

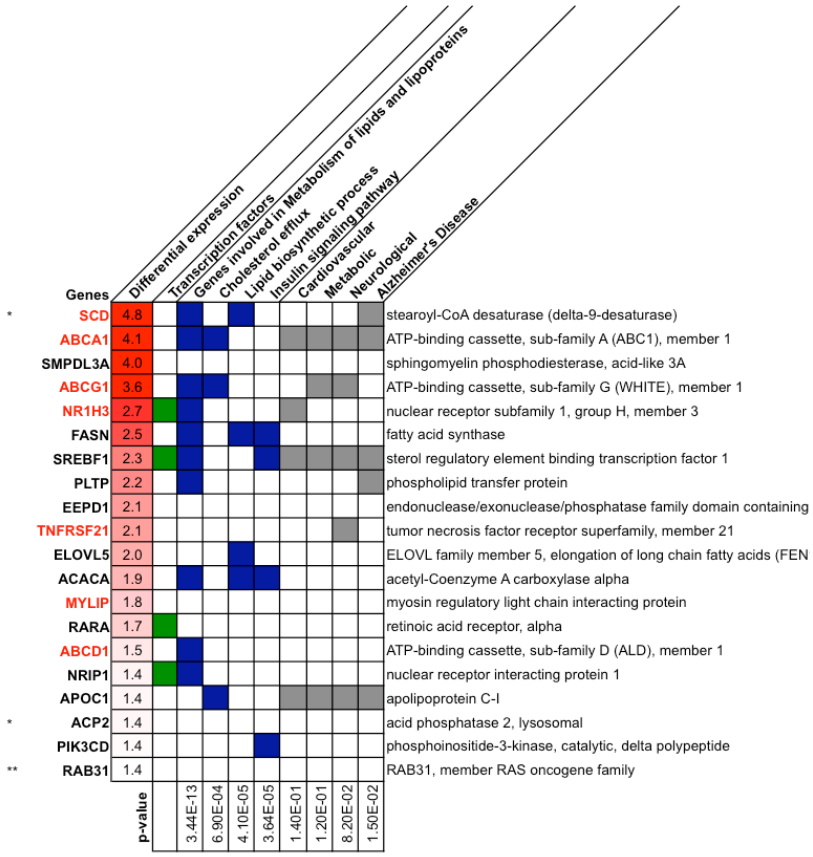

Table 4: **Overview of direct LXRα target genes in T0901317-treated macrophages.** Shown are differentially expressed genes that show LXRα binding within a maximum distance of 200 kb. More than one gene was annotated if the LXRα binding sites was within a maximum distance of 30 kb (*). Additionally, genes were estimated by the use of Genomic Regions Enrichment of Annotations Tool (**) (McLean et al. 2010). Functional annotations and disease associations were derived using DAVID (Huang et al. 2009a) or Gene Set Enrichment Analysis (GSEA) (Subramanian et al. 2005).

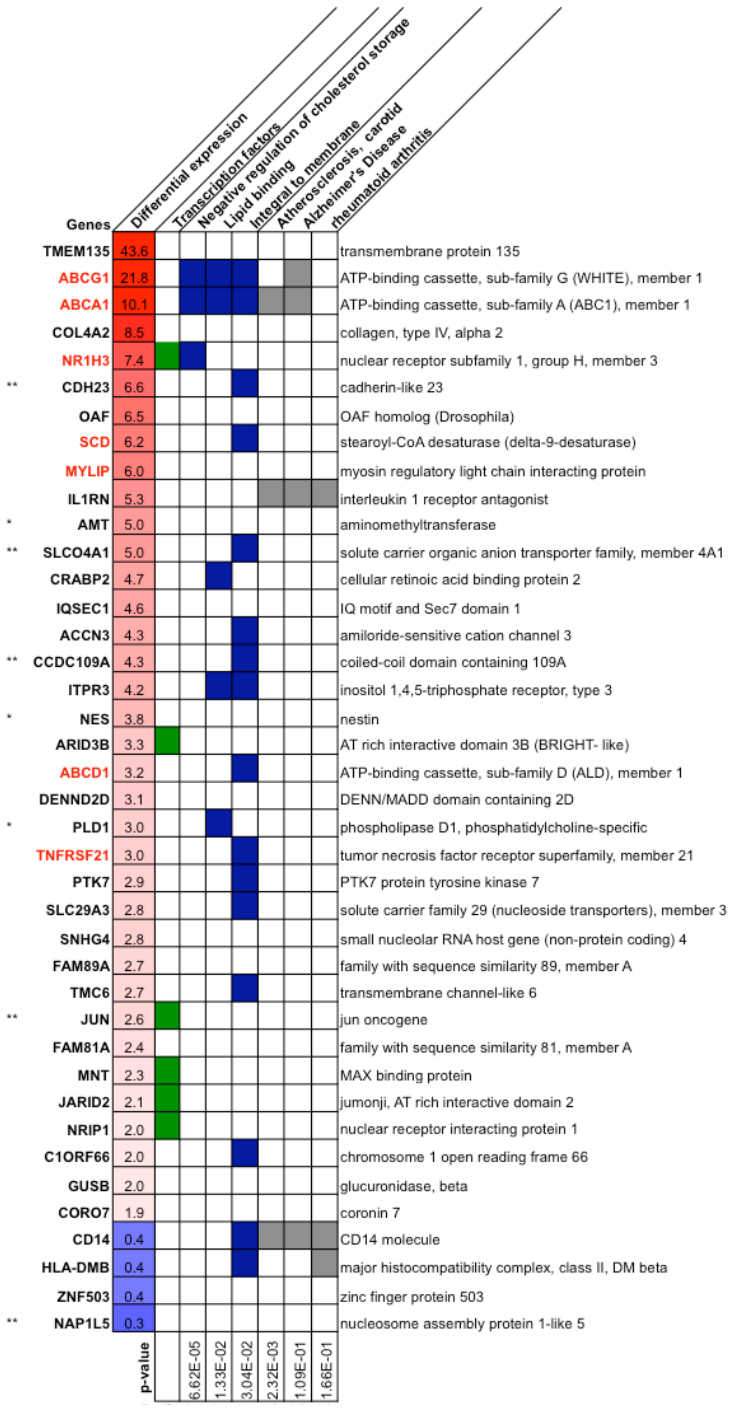

Table 5: **Overview of direct LXRα target genes in T0901317-treated foam cells.** See table 4 for description.

treatment alone induces only a subset of the joined gene loci. Thus, especially genes of cluster VI show highly differential LXRα binding, illustrated at the *JUN* locus (Figure 5C). Interestingly, many membrane-associated proteins fall into this category and show LXRα binding and differential expression only in the foam cell model. The other way around, many genes associated with fatty acid synthesis are only differentially expressed under T0901317 treatment although LXRα binding is also present in foam cells.

Excessive literature mining is necessary to estimate the biological context of these observations in detail and some examples are described below. Together, presence of combinatorial clusters as observed in both treatment models suggests that LXRα-dependent regulation is embedded in a more complex framework that controls regulation of distinct gene sets.

3.4 LXRα directly regulates other transcription factors

Expression microarrays showed that hundreds of genes are differentially expressed upon LXR-specific agonist treatment but only a small number of the genes were directly regulated by LXRα binding. Target gene determination demonstrates that in addition to direct gene regulation, LXRα regulates other transcription factors indicating that LXRα controls a network of responses to activating synthetic and endogenous ligands.

Therefore, to investigate the complexity of LXRα target gene regulation, both direct and putative indirect target genes were considered by the use PMW (position weight matrix) over-representation analysis and publicly available interaction profiles of the THP-1 cell line provided by the FANTOM (Functional Annotation of the Mammalian Genome) consortium (Kawaji et al. 2010). The FANTOM4-EdgeExpress Database (fantom.gsc.riken.jp) is an easily queriable tool to perform network predictions. Network analysis using only direct LXRα target genes revealed interactions of transcription factors including LXRα, retinoic acid receptor alpha (RARα), NRIP1, JUN and MNT but also non-transcription factor targets that generate a rich set for future investigations (Figure 7).

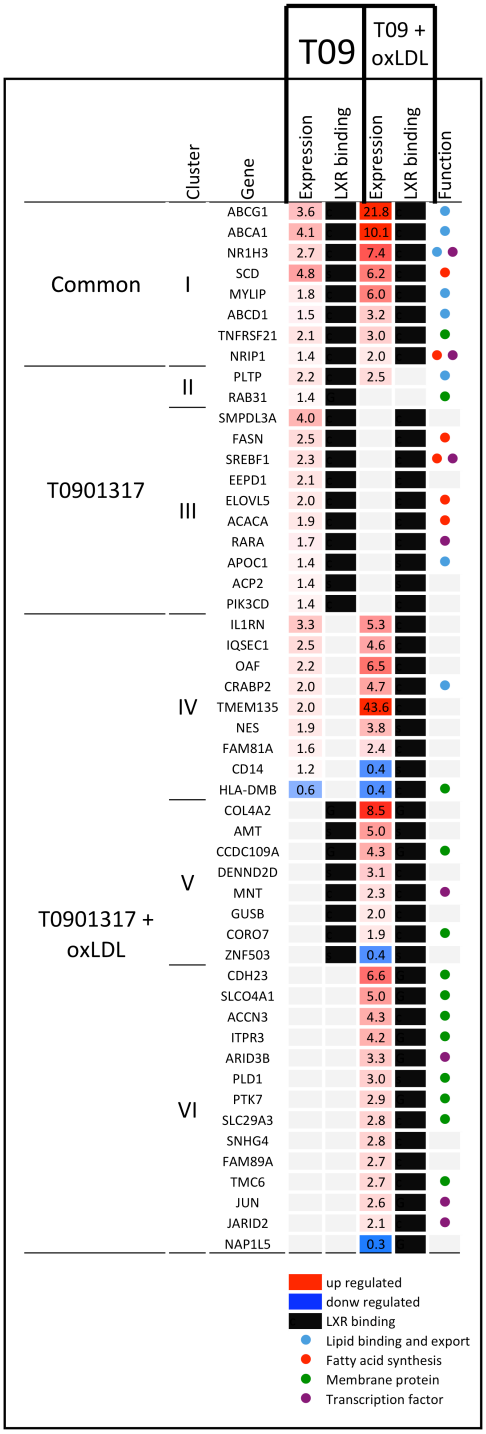

Table 6: **Comparison of LXRα binding and gene expression changes.** LXRα target genes of T0901317-treated macrophages and T0901317-treated foam cells.

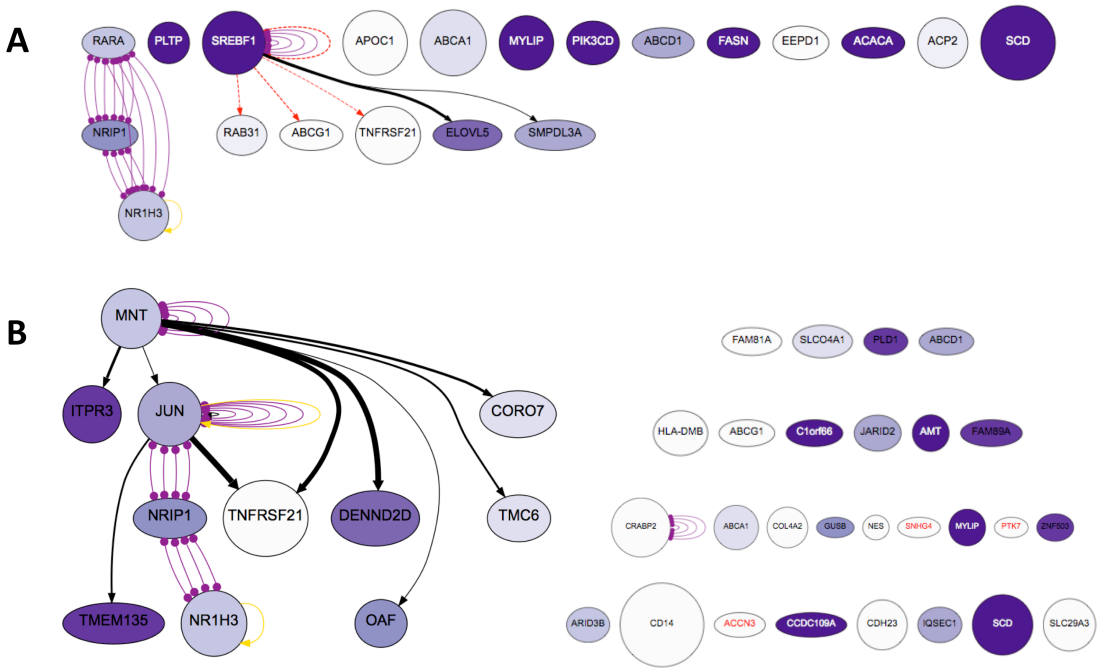

Figure 7: **Interaction network analysis of direct LXRα target genes.** All estimated direct LXRα target genes of T0901317-treated macrophages **(A)** and T0901317-treated foam cells **(B)** are shown. All shown feature properties are estimated by the use of the FANTOM4-EdgeExpress Database. Legend: Edge colours: Black: Transcription factor binding site predictions and miRNA target predictions; Yellow: Published protein-DNA edges; Purple: Protein-protein interactions; Red: siRNA and miRNA perturbation edges. Edge line style: Solid: Direct edges; Dashed: perturbation edges (possibly direct or indirect). Edge terminators: Arrowhead: activating relationships; Round: bidirectional protein-protein relationships. The diameter of each node is scaled to indicate the dynamics of gene expression. Highly dynamic nodes are larger than statically expressed nodes. The color of the node is mapped to a relative scale for each node between white for min(expression) and purple max(expression). If the node has no detectable expression, the name of the node becomes red and the background is white (fantom.gsc.riken.jp).

Category	Count	PValue	Genes
Lipid binding	6	1.49E-03	NISCH, ADAP2, VAV3, CRABP2, RARA, EPN1
Vitamin binding	4	1.92E-03	OGDHL, CRABP2, FASN, ACACA
Response to nutrient levels	4	4.91E-03	SREBF1, CCND1, DUSP1, RARA
Intracellular signaling cascade	7	1.99E-02	CCND1, NISCH, VAV3, DUSP1, NFKBIA, RARA, TUBB3
Glucose metabolic process	3	2.97E-02	NISCH, OGDHL, FBP1
Signal transduction	11	5.76E-02	GPR84, ADAP2, VAV3, DUSP1, CRABP2, RAB3IL1, NFKBIA, RARA, TUBB3, EPN1, CLEC11A

Table 7: Functional clustering of putatively RARα-regulated genes from the PWM network analysis using the DAVID gene onthology program.

3.4.1 RARα putatively contributes to indirect gene regulation by LXRα

To investigate the extent of indirect LXRα targets, ChIP-seq and microarray expression profiling data were combined with a genome-wide search for over-represented motifs of the transcription factors directly targeted by LXRα. Therefore, promoters of differentially expressed genes were scanned using PWMs followed by filtering based on the conservation of the motifs (Qin et al. 2011). PWMs are a collection of motifs that are similar, but not identical to the transcription factor specific consensus sequence and are commonly used to predict transcription factor binding (Klepper et al. 2008). The analysis determined that the direct LXRα target RARα putatively regulates 34 genes, differently expressed in THP-1-derived macrophages exposed to T0901317 (Figure 8). The overlap of RARα motifs in the promoter of those genes was significant (P-value $4.3*10^{-12}$), which indicates that overlapping does not happen randomly. The associated gene set is enriched in diverse metabolic processes and signal transduction pathways (Table 7) and includes five additional transcription factors.

Interestingly, the genes *SREBF1*, *FASN* and *ACCA* were identified as common targets for LXRα and RARα, indicating that both are involved in their regulation. Contrary to the situation in T0901317-treated macrophages; expression of those targets and RARα is not significantly changed in T0901317-treated foam cells but LXRα binding is observed in both conditions. This observation may give some evidence that RARα is required for up-regulation of those common target genes that are implicated in lipid biosynthesis contributing to side effects of LXRα agonists in the liver. However, also other pathways were elucidated that attenuate up-regulation of SREBF1, FASN and ACCA in foam cells (Rowe et al. 2003).

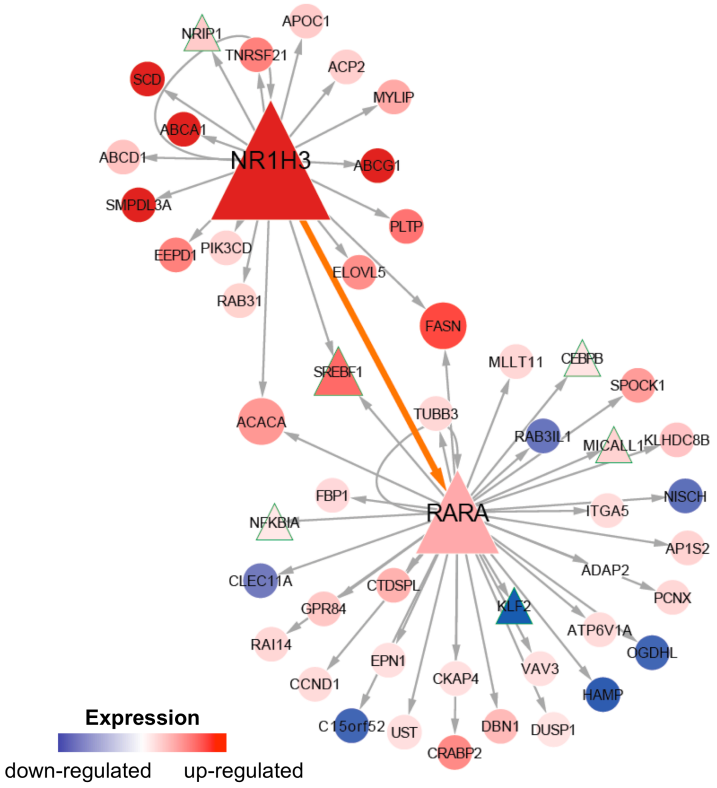

Figure 8: **PWM-based regulatory interactions.** Transcriptional regulatory network showing direct targets of LXRα (NR1H3) including RARα. The regulon of RARα is determined by scanning all promoters of differentially expressed genes with PWM (position weight matrix) of the transcription factors (triangles) from three accessible databases, JASPAR, UniPROBE and UCSC genome browser TFBS track (Qin et al. 2011). Red: up-regulated. Blue: down-regulated. Analysis was performed from data of T0901317-treated macrophages.

The same analysis in T0901317-treated foam cells did not reveal indications for indirect target gene regulation based on PWMs. Thus, the results of the PWM-based analysis in macrophages give some evidence for a possible cross-talk between two nuclear receptors upon T0901317 treatment. However, further functional assays are required to prove this initial observations.

3.4.2 T0901317 and oxLDL-induced differences in gene regulatory networks

To further expand the observations from the PWM-based analysis, interacting genes in both, T0901317-treated macrophages and foam cells were linked to regulatory

networks. Therefore, all genes with a significant change in transcript abundance in treated cells versus untreated cells were selected. Those genes were integrated with known and experimentally validated protein-protein and protein-DNA interactions and results from high throughput siRNA knockdown experiments in THP-1 cells using the FANTOME web resources (Kawaji et al. 2010).

The analysis highlights that a complex network of transcription factors is regulated in T0901317-treated foam cells and macrophages (Figure 9 and 10). Additionally, it shows a stringent but restricted role of LXRα within this network. It must be noted that in total 74 and 37 transcription factors are differentially expressed upon T0901317 treatment in both macrophage models, respectively. Of those factors at least *MNT* and *JUN* in T0901317-treated foam cells and *SREBF1* in T0901317-treated macrophages are characterized as direct LXRα target genes that gather a vast number of putatively regulated genes.

In addition to regulating cholesterol metabolism, LXRs are also negative regulators of macrophage inflammatory gene responses (Shibata and Glass 2009). Interestingly, 36 (p-value 2.8E-8) genes associated with inflammatory responses are repressed in T0901317-treated foam cells, including NFKB1 (0.3-fold) and IL-1β (0.4-fold). Those genes are not directly targeted by LXRα. This suggests the possibility and confirms previous observations that the anti-inflammatory properties of LXRα are generally mediated through indirect LXRα-dependent mechanisms. Similarly, network visualisation elucidated the down-regulation of RXRα indicating that LXRα negatively regulates its own obligate dimerization partner through indirect pathways. Collectively, the motif based and interaction based identification of putative indirect LXRα target genes highlights that a complex network of regulatory responses is triggered by ligand application in both macrophages models.

3.5 Chromatin status and transcription factor binding

To understand the role of chromatin accessibility in regulating LXRα binding and target genes, sites of localized chromatin remodelling were profiled using FAIRE assays. FAIRE is a simple high-throughput method to determine active regulatory

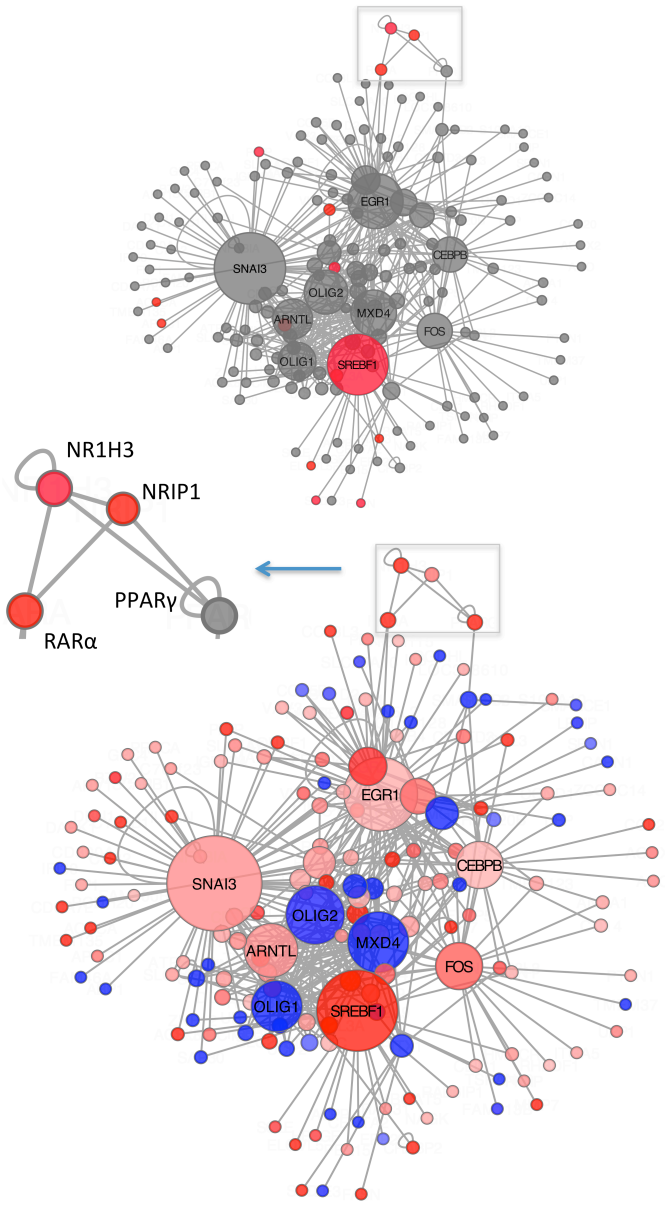

Figure 9: **Network predictions of T0901317-induced response in THP-1 cells (1).** Functional network which connects the identified directly bound LXRα target genes with the global transcriptional T0901317-induced response of macrophages (Figure 9) and foam cells (Figure 10). Basic networks at the top and bottom are equal and show genes that are differentially expressed. Top: Only direct LXRα target genes are colored according to gene expression. Node colors indicate expression levels of genes. The node size is proportional to the relative connectivity to other factors (dominated by transcription factors). Description continued in caption of figure 10.

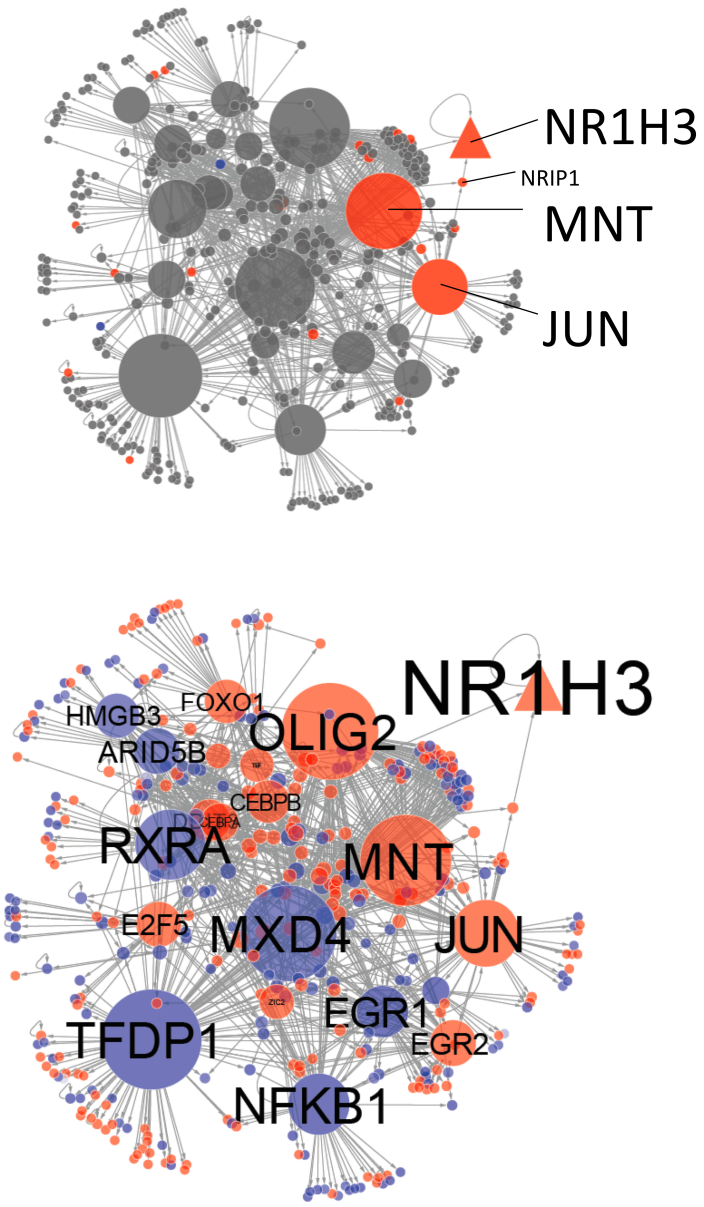

Figure 10: **Network predictions of T0901317-induced response in THP-1 cells (2).** The grey lines (edges) indicate interactions derived from the FANTOM4-EdgeExpress Database. Interactions are assembled from siRNA perturbation and ChIP-seq experiments in THP-1 cells and published data. Additionally, interactions are calculated using expression patterns of mRNAs, microRNAs, and gene promoters in THP-1 cells and publicly available protein-protein and protein-DNA interaction predictions (Kawaji et al. 2010). The size of NR1H3 does not represent its connectivity. Genes without connectivity (singletons) are not shown.

elements based on their decreased nucleosomal content. Nucleosomes are the most abundant and readily crosslinkable component of chromatin and therefore dominate the crosslinking profile compared to other DNA binding proteins (Giresi et al. 2007). FAIRE assays involve crosslinking proteins to DNA using formaldehyde, shearing the chromatin, and performing a phenol–chloroform extraction. The enrichment of protein-free DNA fragments that preferentially segregate into the aqueous phase are then analysed using qPCR or high-throughput sequencing (Giresi and Lieb 2009).

3.5.1 LXRα binding coincides sites of highly accessible chromatin

FAIRE-qPCR signals were initially examined within selected proximal promoter regions and distal putative enhancer elements of validated LXRα regulated genes. As shown in Figure 11, LXRα occupied sites were enriched in FAIRE isolated DNA compared to control regions. FAIRE signals at LXRα binding sites near *FASN*, *SREBF1* and *LXRα* were small but significantly increased in THP-1-derived macrophages upon T0901317-induced LXRα activation. Contrary, an increase in DNA accessibility was not evaluated in T0901317-treated foam cells. When FAIRE-qPCR was employed to compare DNA accessibility at the same regions in primary macrophages, markedly increased FAIRE signals were observed upon ligand treatment. This observation may indicate that primary cells undergo enhanced chromatin remodelling compared to THP-1 cells. Interestingly, FAIRE enrichments in primary macrophage-derived foam cells showed induced open chromatin at LXRα binding sites corresponding to *LXRα* and *ABCA1* but not *FASN*, *SREBF1* and *ACCA*. These results correlate with the altered gene expression of the examined genes. Thus, LXRα binding at sites of induced open chromatin is connected to up-regulation of gene expression of LXRα (7.3-fold) and ABCA1 (10.1-fold). In contrast, LXRα binding to sites of unchanged chromatin accessibility is connected with unchanged transcript abundance for FASN, SREBF1 and ACCA. However, the overall FAIRE-enrichment at functional LXRα binding sites indicates that chromatin accessibility is required for efficient LXRα binding and target gene regulation as described for other transcription factors (Eeckhoute et al. 2009, Lefterova et al. 2010). This suggests that genome-wide identification of FAIRE enriched

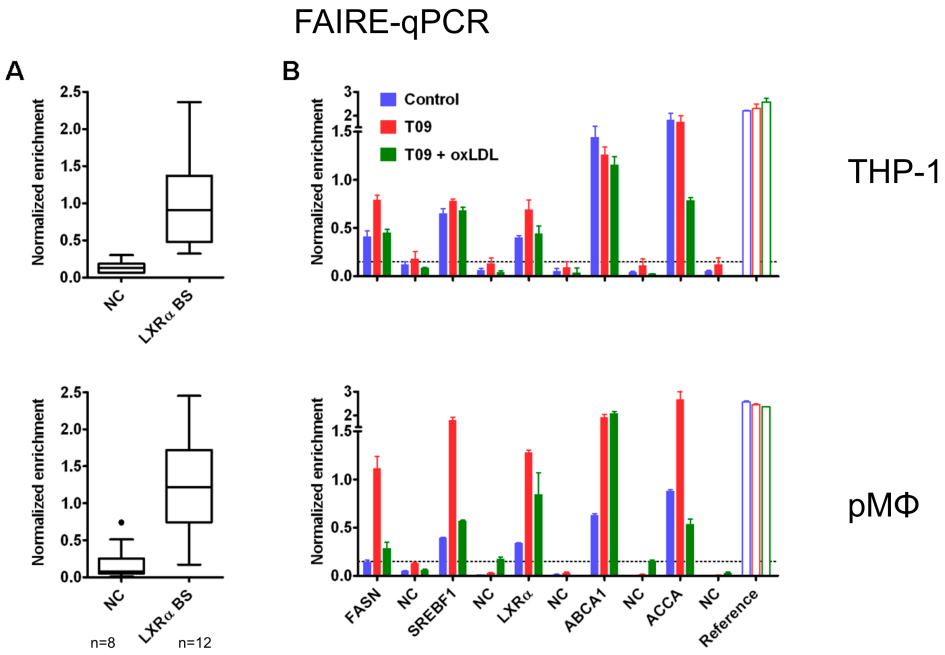

Figure 11: **LXRα binding correlates with DNA accessibility.** FAIRE-qPCR on THP-1 cells and primary human monocyte-derived macrophages (pMΦ) at indicated LXRα binding sites (LXRα BS) of LXRα target genes (*FASN*, *SREBF1*, *LXR*α and *ABCA1*) and negative control regions (NC). FAIRE values were normalized against those measured for three loci at the β-actin promoter (Reference). E rror bars indicate the SE of three samples (THP-1, measured in two to three biological replicates) or the mean of triplicate values ± standard derivation (pMΦ, measured in three technical replicates). **(A)** Box-whisker plots of FAIRE-qPCR including values at binding sites not shown in (B). **(B)** Representative FAIRE-enrichments. Cells were vehicle-treated (Control, blue), treated with T0901317 (T09, red), or T0901317-treated after foam cell induction (T09 + oxLDL).

sites would be an important predictor for functional LXRα-dependent regulation.

3.5.2 Proximal transitions in chromatin structures accompany LXRα binding events

FAIRE was coupled to high-throughput sequencing to gain a global view on accessible regions of chromatin and to classify functional LXRα binding events with high confidence. Following sequencing, 27-31 million uniquely mappable reads were obtained indicating consistent sample purity. Generated FAIRE tag signal profiles, representing nucleosome-depleted chromatin regions, together with LXRα binding profiles are shown

in figure 12 for three representative LXRα target gene loci. The profiles confirm that LXRα binding events co-occur with regions of open chromatin that define active regulatory elements. Additionally, the FAIRE profiles highlight the presence of large numbers of adjacent regulatory elements that are not occupied by LXRα. Interestingly, those sites of open chromatin show strong treatment-dependent changes whereas LXRα binding coincides constitutively open sites at selected target genes (SREBF1 and ABCG1). Similar patterns were recognized at other LXRα target gene loci. These observations may indicate that additional factors act in concert to regulate gene expression at the observed gene loci under different treatment conditions. Thus, in contrast to LXRα, these factors seem highly influenced by local chromatin remodelling events. However, gene loci targeted by multiple LXRα binding events show treatment-dependent chromatin remodelling at LXRα occupied regions with various combinatorial patterns (Figure 12, ABCA1). At the ABCA1 locus, combinatorial patterns of open chromatin may define those LXRα binding sites that contribute to gene regulation. This highlights the possibility that genes targeted by multiple binding events can be regulated in a more complex fashion in response to external stimuli.

3.5.3 Quantitative relationship between LXRα binding and open chromatin

To quantify the relation of LXRα binding and chromatin status, genomic regions with high chromatin accessibility over background were delineated with liberal stringency (Gaulton et al. 2010) and ~176k sites were identified encompassing 2.2% of the genome (~60 Mb). Non-promoter sites of open chromatin (94%) showed dynamic treatment-dependent changes while promoter-associated sites (6%) were relatively constant. Therefore, a small overlap (25%) for all liberal treatment specific open chromatin sites was determined. The overlap was strongly enhanced (62%) if 10.000 rank-ordered peaks from each treatment group were compared, with rank based on the mean signal intensity within each interval of determined open chromatin (Figure 13A). 68% of the LXRα bound regions from both treatments were restricted to those sites and LXRα bound regions exhibit high DNA accessibility compared to randomly selected open chromatin sites (Figure 13B).

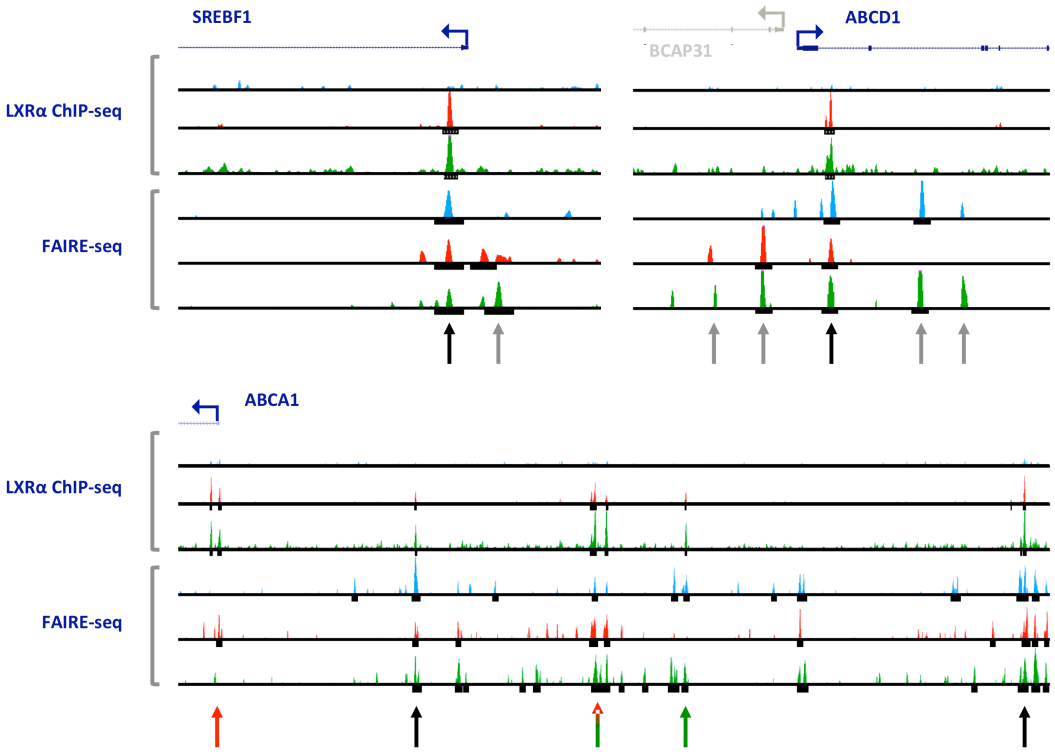

Figure 12: **Mapping of chromatin accessibility using FAIRE-seq.** Gene loci of *SREBF1*, *ABCD1* and *ABCA1* illustrating the correspondence between LXRα occupancy patterns (LXRα ChIP-seq) and FAIRE-enriched accessible regions (FAIRE-seq) in vehicle-treated macrophages (Control, blue), T0901317-treated macrophages (T09, red) and T0901317-treated foam cells (oxLDL + T09, green). Peak intervals of highly accessible sites are indicated as black bars below the density profile. Constitutive sites of accessible chromatin are indicated by black arrows and treatment-specific accessible sites are indicated by red (accessible in T0901317-treated macrophages) and green (accessible in T0901317-treated foam cells) arrows. LXRα unbound sites of open chromatin at the *SREPF1* and *ABCD1* locus are indicated by gray arrows. Scaling of LXRα data as in figure 2 and 5. FAIRE-seq profiles are processed as described and are equally scaled to fit the enriched peak intervals. Genomic locations: *SREBF1*: chr17:17,728,884-17,745,176. *ABCD1*: chrX:152,980,867-153,001,989. *ABCA1*: chr9:107,688,019-107,841,388. UCSC Genes track is used to indicate RefSeq validated gene positions.

Stringent correlation of treatment-dependent LXRα occupancy to FAIRE-seq enriched sites revealed that 43% of T0901317-induced LXRα binding in differentiated THP-1 cells and 76% of LXRα occupied sites in T0901317-treated foam cells are targeted to the 2.2% of the genome defined by regions of open chromatin (Figure 13C). Thus, the increased accessibility at LXRα binding sites in T0901317-treated foam cells correlates with the higher number of direct LXRα target genes, compared to T0901317-treated macrophages. The majority of treatment-dependent LXRα occupancy at open sites (65% and 84%) occurred in constitutively open chromatin whereas 35% and 16% occurred at sites that undergo treatment-induced chromatin remodelling for both cell models respectively. Only a marginal fraction of LXRα sites were located at uniquely pre-treatment open chromatin sites.

The marked differences between both macrophage treatment models regarding their association to accessible chromatin were further investigated by visualizing open chromatin sites at LXRα bound regions. Strikingly, the fraction of LXRα binding sites that are unique to T0901317-treated macrophages are mainly associated with regions of close chromatin whereas LXRα binding sites common to both treatment models or unique to T0901317-treated foam cells showed an equivalently high amount of co-localized open chromatin (Figure 14A). Together, these results indicate that LXRα binding coincides both sites of open chromatin and sites where chromatin exists in a relatively close conformation. Thus, heatmap visualisation indicates that T0901317 induces LXRα binding to inaccessible chromatin in macrophages. Therefore, large fractions of these binding sites may not be functional due to the lack of associated chromatin accessibility that prevents recruitment of co-factors required for transcriptional regulation of target genes.

Previous studies indicate that the level of regulatory factor occupancy on a given genomic region is an important determinant of function (Li et al. 2011). To ask whether LXRα binding to close chromatin reflects a functional mechanism or simply discriminates weak LXRα binding sites, the significance of LXRα peaks was determined relative to the chromatin status (Figure 14B). The analysis revealed that on average LXRα binds with higher affinity to sites of open chromatin compared to its binding affinity to

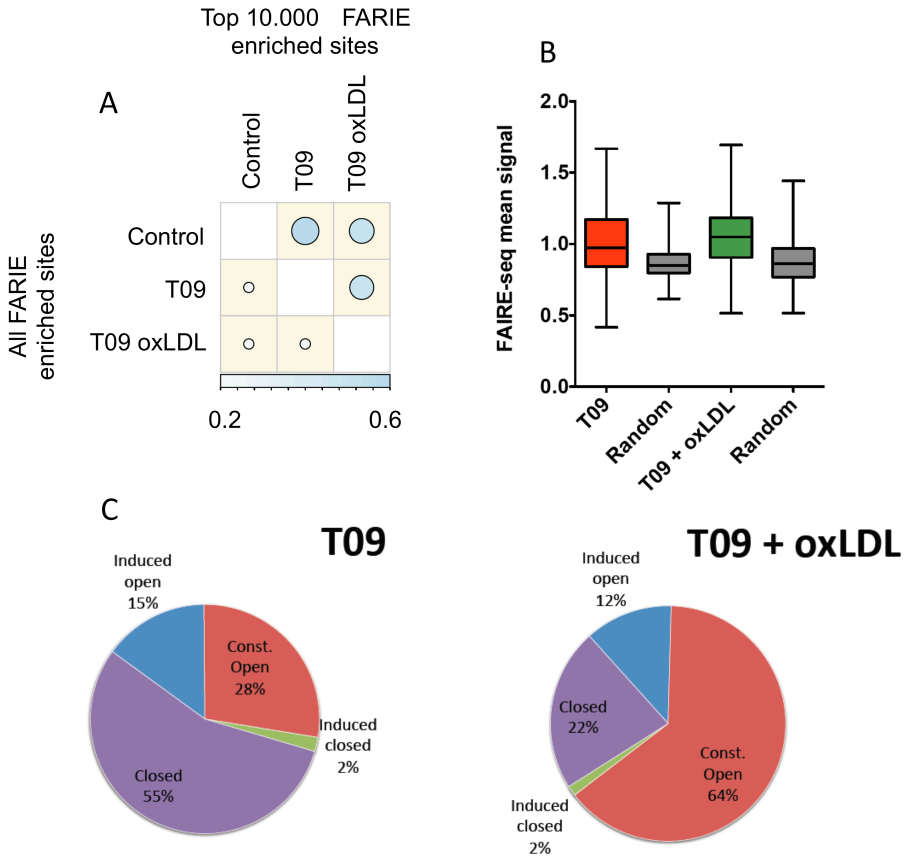

Figure 13: **Global evaluation of chromatin accessibility on LXRα occupancy patterns. (A)** Matrix of Jaccard similarity coefficients between all FAIRE-enriched sites and the top 10k FAIRE-enriched sites. The Jaccard index is estimated as the number of peaks that overlap between two peak files, divided by the union of the two files. The larger the coefficient, the more similar two datasets are in terms of overlapping peaks. Shown values are adjusted to percent overlap. **(B)** Box plot showing FAIRE-seq mean signals at LXRα binding sites of T0901317-treated macrophages (T09, red) and T0901317-treated foam cells (T09 + oxLDL , green) compared to random peak intervals that mimic LXRα peaks (Random). **(C)** LXRα binding and chromatin accessibility in T0901317-treated macrophages (T09), T0901317-treated foam cells (T09 + oxLDL) . Percentage of overlapping LXRα binding sites with determined sites of high accessibility (high FAIRE-enrichment, open) or inaccessible chromatin (low FAIRE enrichment (closed). Legend: Const. (constitutive) open sites are accessible independent of treatment or cell model. Induced open sites are accessible after T0901317 treatment. Induced closed sites are defined as open sites in untreated cells that are inaccessible after T0901317 treatment. Overlapping sites are defined by an intersection of $\geq$ 10 bp.

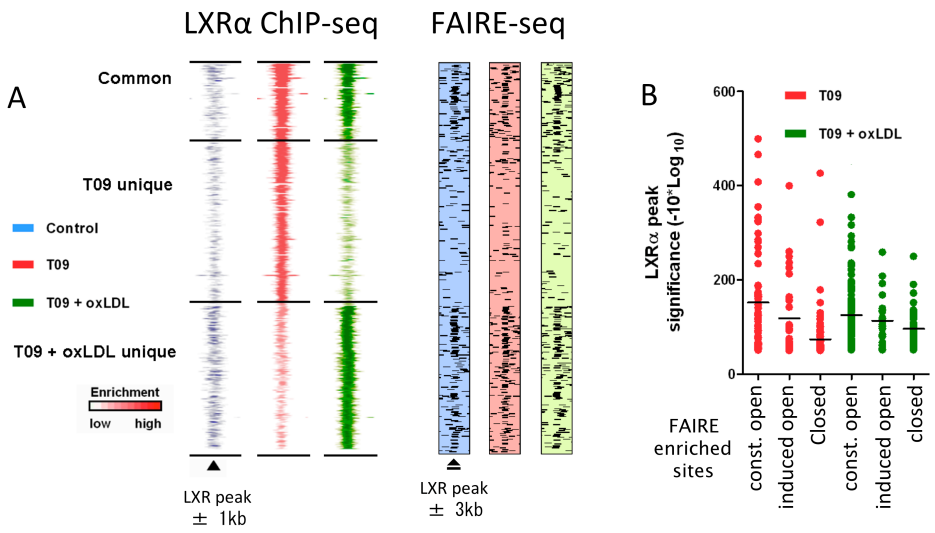

Figure 14: **Global evaluation of chromatin accessibility on LXRα occupancy patterns (2). (A)** Tag enrichments (from figure 4, LXRα ChIP-seq) over all 400 sorted LXRα binding sites (LXR Peak) is shown along with defined sites of open chromatin (FAIRE-seq). **(B)** Aligned dot plot shows LXRα binding sites significance calculated by MACS at defined FAIRE sites (for definitions see figure 13).

close chromatin. Nevertheless, some strong LXRα binding sites mapped also to inaccessible chromatin. Those highly significant binding sites were individually inspected showing that the binding events were almost exclusively annotated to validated LXRα-associated genes that are targeted by multiple LXRα binding events as described for the *ABCA1* gene. In the corresponding loci of positively regulated target genes, at least one LXRα binding interval was situated in open chromatin (Figure 12, ABCA1).

3.5.4 LXRα binding to accessible chromatin positively correlates with differential expression of target genes

To further determine the functional effect of LXRα binding depended on different chromatin states, peak-associated genes (defined by the nearest gene analysis strategy) that are differentially expressed under ligand treatment were grouped according to their chromatin status. Strikingly, genes regulated by LXRα binding are less likely to be differentially expressed if binding is restricted to closed chromatin. The broad majority of differentially expressed genes are targeted by LXRα binding sites in accessible

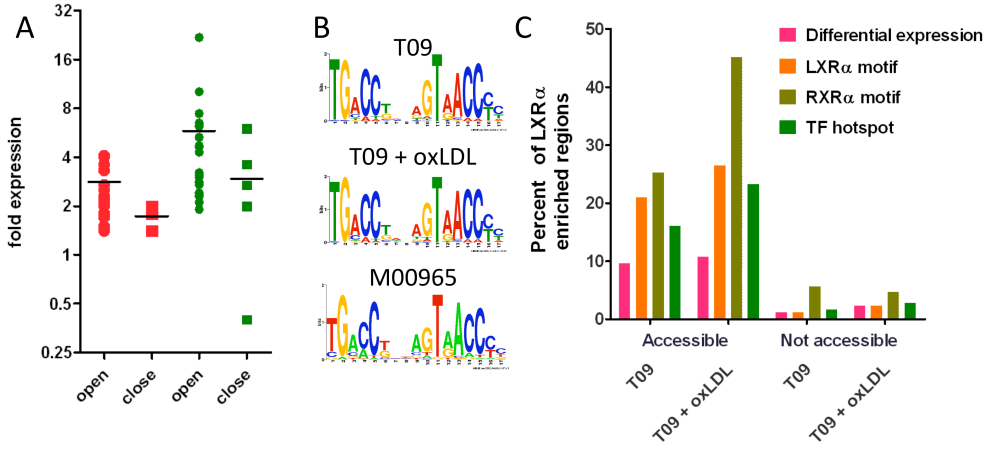

Figure 15: **LXRα binding to accessible sites coincides functionality. (A)** LXRα binding to accessible chromatin positively correlates with enhanced up-regulation of associated LXRα targt genes. The chromatin status at LXRα binding sites is indicated at the *x* axis. Dots indicate fold-expression changes from T0901317-treated macrophages (red) and T0901317-treated foam cells (green). **(B)** Results of *de novo* motif discovery and the reported LXRα motif (M00965). **(C)** Different indicators for functional transcription factor binding sites are over-represented at LXRα binding sites in open chromatin. Transcription factor hotspots (TF hotspot) are defined by $\geq$10 transcription factor binding sites (ENCODE Txn ChIP-seq data, data update: 2011-04-28).

chromatin, indicating that open chromatin is a good predictor of transcription factor binding events that finally lead to gene expression (Figure 15A and C).

3.5.5 Correlation of motif occurrences relative to the chromatin status

The mode of interaction between LXRα to DNA is believed to depend on the sequence context. Therefore recognition-motif occurrence at transcription factor binding regions provides an additional indicator for functional relevance. To investigate whether LXRα binding events at LXRα consensus motifs correlate with accessible chromatin, the occurrence of the motif in open and close chromatin was analysed. Therefore, the motif instances for all defined LXRα binding sites were investigated by *de novo* motif search using the MEME suite (Machanick and Bailey 2011). The analysis revealed that 20% and 26% of the defined LXRα peak intervals stringently contain the sequence motif highly similar to the published LXRα motif (M00965, centipede.uchicago.edu,

Figure 15B) from both treatment groups respectively. Similar to the observations from gene expression, the vast majority of peaks containing the LXRα motif were found in domains of open chromatin and only five motif containing peaks were determined that reside in regions of close chromatin (Figure 15C). Again, this shows that most binding sites with an additional parameter for functional relevance are restricted to regions of accessible chromatin.

An enhanced trend was observed when determining the presence of the RXRα motif in addition with RXRα ChIP-seq enrichments from publicly available data (ENCODE consortium, genome.gov) at LXRα peak intervals (Figure 15C). Because RXRα is an obligatory partner of LXRα this finding also elucidates that the fraction of LXRα motifs found by *de novo* search may be underestimated. *De novo* motif search centred on estimated RXRα binding sites with LXRα peak intervals lacking a detectable LXRα motif did not reveal a specific motif in addition to the RXRα motif. However, this strongly suggests that a fraction of functional LXRα binding events is independent of the known consensus sequence. Unfortunately, the relatively low numbers of binding intervals with these properties challenged the finding of subgroups of variable LXRα motifs. Further investigations by the use of alternative motif determination strategies will be necessary to gain a deeper understanding regarding alternative LXRα consensus sequences.

It was previously shown that only a very small fraction of the genome-wide available transcription factor response element sequences is occupied by direct factor binding (Farnham 2009). Therefore, the genome-wide identification of active regulatory regions by FAIRE remains a promising strategy to specifically investigate motif occurrences at these functional sites.

3.6 LXRα binds to transcription factor hotspots and is associated with a set of pioneer factors

Previous, large-scale profiling of the binding patterns from a set of transcription factors in *Drosophila melanogaster* revealed strongly overlapping localization patterns, indicating the presence of transcription factor hotspots (Moorman et al. 2006, Roy

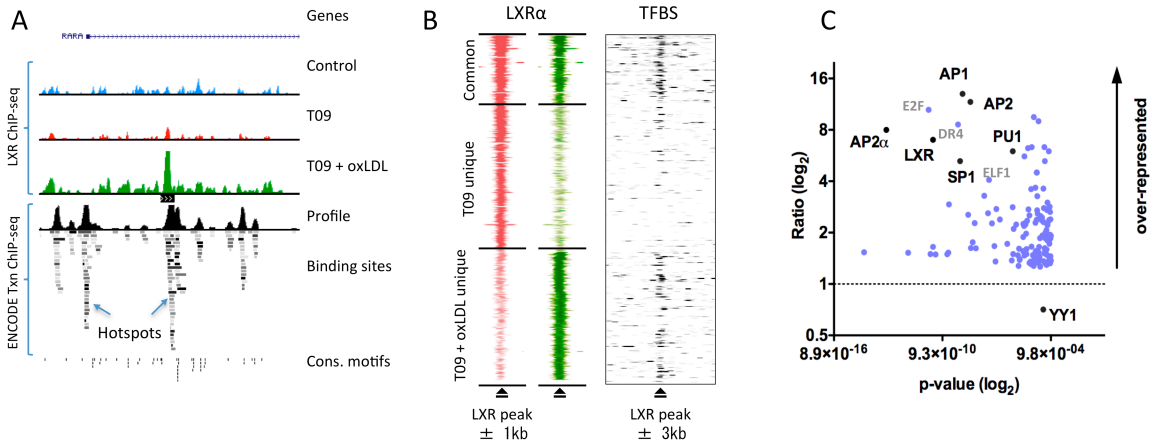

Figure 16: **Co-occurrence of LXRα and other transcription factors.** Transcription factors strongly overlap with each other in the genome and form transcription factor hotspots. **(A)** Representation of LXRα ChIP-seq profiles, profiles of other transcription factors (ENCODE Txn ChIP-seq data, data update: 2011-04-28) and conserved transcription factor binding motifs (Cons. Motifs, UCSC TFBS Conserved Track). **(B)** Tag enrichments (from figure 4, LXRα ChIP-seq) over all 400 sorted LXRα binding sites (LXR Peak) is shown along with transcription factors binding sites ((ENCODE Txn ChIP-seq data). **(C)** Over-represented conserved transcription factor binding sites at sites of LXRα binding to open chromatin.

et al. 2010). Transcription factor hotspots, also termed highly occupied target (HOT) regions, correlate with pattern of open chromatin and also exist in the human genome (Li et al. 2011, Siersbaek et al. 2011). To investigate whether LXRα binding events are located in highly occupied target regions, binding sites of 148 transcription factors from multiple human cell lines released by the ENCODE consortium (genome.gov) were visualized within and around genomic regions of LXRα binding events (Figure 16A and B). Remarkably, this comparison shows that a major fraction of LXRα binding sites are located in transcription factor hotspots. Especially highly significant LXRα binding sites that are common to both macrophage treatment models are associated with regions of broad transcription factor binding site accumulations. Additionally, these results visually confirm the association of hotspots with defined sites of open chromatin. Relating to LXRα, the majority of hotspots with a complexity of ten or more transcription factor binding sites are associated with LXRα occupancy at open chromatin (Figure 15C). Together, these correlations confirm that LXRα is associated with other transcription factors that cluster near each other to cooperatively regulate transcription. The observation that most LXRα binding sites are associated to constitutively accessible regions that are additionally defined by transcription factor hotspots suggests, that hotspots are stable genomic regions kept open via recruitment of specific pioneer factors chromatin remodeling complexes, that facilitate binding of additional transcription factors (Magnani et al. 2011, Voss et al. 2011).

To understand whether LXRα binding is accompanied by the presence of specific transcription factors that may contribute to the definition of functional regulatory elements, transcription factor co-occupancy at LXRα binding sites was further investigated. *De novo* motif search using LXRα peak intervals revealed the presence of the specificity protein 1 (SP1) motif a transcription factor directly associated with accessible and poised chromatin (Biddie et al. 2011). To expand this observation over-representation analysis of numerous conserved transcription factor motif occurrences was performed. Therefor, LXRα binding sites associated with accessible and inaccessible chromatin were used as positive and negative sequence sets, respectively. These sequences were scanned using available PWMs from the Transfac database (Matys

et al. 2003). Afterwards, comparing the positive and negative sequence sets assessed the ratio of enriched transcription factor binding sites along with significance values for each transcription factor. The analysis revealed the expected over-representation of the LXR motif. Additionally, several motifs of pioneer factors were associated with LXRα binding events at open chromatin (Figure 16C). Those include SP1, AP-1, AP-2, AP-2α and PU-1 (SPI1). These findings suggest, that the determined pioneer factors may cross-talk with LXRα. In addition to the known pioneer factors, binding sites of the cell-cycle and apoptosis regulator E2F1 were also significantly overrepresented near LXRα binding sites in open chromatin. Interestingly, the transcriptional repressor protein YY1 was identified as the only factor significantly enriched near LXRα binding sites in close chromatin. Together, these findings revealed novel potential partners of LXRα that influence factor binding and the functional outcome of LXRα activation.

4 Discussion

The abundant expression of the LXRα protein in macrophages present in human atherosclerotic lesions supports the hypothesis that LXRα agonists could have a beneficial effect against development of atherosclerosis (Watanabe et al. 2005, Zhao and Dahlman-Wright 2010). Therefore, the effects of LXR activation have been studied in diverse tissue contexts and cell types, and many LXR target genes were determined using global expression analysis (Joseph et al. 2003). The interpretation of such studies has been hampered because expression analysis alone cannot differentiate between direct and indirect targets and does not provide information on the location of regulatory elements. Therefore, for gaining a general understanding of the mechanisms of LXRα-dependent gene regulation it is essential to monitor the genome-wide location of LXRα to define direct LXRα target genes. To understand the role of LXRα activation in regulating different sets of genes in macrophages attracted to atherosclerotic plaques and already transformed cholesterol accumulating macrophage-derived foam cells, LXRα occupancy and gene expression was determined and correlated in T0901317-treated macrophages or foam cells treated with T0901317 as compared to untreated macrophages.

4.1 Properties of LXRα cistromes

Using ChIP-seq analysis about 249 and 215 LXRα binding sites with a high degree of confidence were identified in T0901317-treated macrophages and foam cells, respectively. LXRα cistromes in these cells are largely distinct, although 16% of the binding locations are shared between the macrophage models. The marked differences of LXRα cistromes are similar to the distinct cell-type specific binding occurrences of other nuclear receptors such as glucocorticoid receptor (GR) and peroxisome proliferator activator receptor gamma (PPARγ) (John et al. 2008, Lefterova et al. 2010). This elucidates that oxLDL stimulation and subsequent foam cell development is sufficient to induce large changes in transcription factor DNA binding locations and thereby targeting different gene sets.

Until recently, the study of LXRα action was limited to promoters of a few well-characterized target genes. However, global analysis revealed that the majority of the identified LXRα binding sites are located in distal intergenic regions or introns whereas fewer sites are localized to proximal promoter regions (11%). The high distribution of binding sites within intergenic and intron regions is consistent with similar reports for other nuclear receptors, including PPARγ (Lefterova et al. 2008), estrogen receptor α (Carroll et al. 2005), androgen receptor (Bolton et al. 2007) and others (Chong et al. 2010, Tang et al. 2011). This finding elucidates that LXRs frequently act as long-range enhancers rather than classic promoter-associated transcription factors.

4.2 Positive regulation of known and novel LXRα target genes

The genomic intervals bound by LXRα in the vicinity of T0901317-responsive genes constitute a rich starting set for the study of LXRα-dependent gene regulation. While LXRα binding to DNA can in principle activate and repress gene expression, combining LXRα occupancy data with measurements of gene expression response showed that LXRα mainly functions as a transcriptional activator. A basic subset of direct LXRα target genes in both macrophage models includes the established LXR target genes *ABCA1*, *ABCG1* and *LXRα*. ABCA1 and ABCG1 are cholesteror transporters and highly induced genes that are central to the antiatherogenic effects of LXR ligands (Wang and Tall 2003). Deficiency of ABCA1 and ABCG1 promotes foam cell accumulation and enhances atherosclerotic lesion development in mice (Yvan-Charvet et al. 2007). Strikingly, these genes are associated with multiple LXRα binding sites, suggesting that these regulatory elements are coevolving to balance target gene expression. Most of the binding sites identified in these classical and well-studied LXR-responsive genes are novel. Beside the proximal LXR response element in the promoter of *ABCA1* (Costet et al. 2000) and two distal LXR occupied enhancers (Shen et al. 2011) five additional sites of LXRα binding were identified. Similarly, two previously unknown LXRα binding sites were identified in the second intron of *ABCG1* that coexist with the previously described promoter proximal LXR response elements (Kennedy et al. 2001, Shen et al. 2011). Previously undetermined LXR binding sites were also identified for

the two known LXR target genes *SCD* and *MYLIP* (Zelcer et al. 2009b). Identification of those novel binding sites will enable further investigations of those important factors.

Correlation of gene expression and LXRα binding also revealed undetermined LXRα target genes commonly regulated in both T0901317-treated macrophage models including *ABCD1*, *NRIP1* and *TNFRSF21*. *ABCD1* encodes a peroxisomal membrane protein which is essential for catabolism of very long chain fatty acids (Weinhofer et al. 2002). Therefore, ABCD1 represents an important novel target to reduce cellular fatty acid levels. The co-repressor NRIP1 is an interaction partner of ligand-activated LXRs (Jakobsson et al. 2007a). NRIP1 and LXR can partner to form distinct activator or repressor complexes to either regulate lipid generation or reduce glucose production (Herzog et al. 2007). TNFRSF21 belongs to the death receptor subfamily of the tumor necrosis factor receptor superfamily (TNFRs) (Pan et al. 1998) and activates a widespread caspase-dependent self-destruction program (Nikolaev et al. 2009). It was observerd that a subset of oxysterols induce apoptosis via unknown acceptor proteins (Shibata and Glass 2009). Expression of TNFRSF21 might therefore represent a possible cellular reaction to oxysterols or LXR ligands in general, which induce apoptosis. Excessive apoptosis is thought to promote atherosclerosis. Paradoxically, mice with deficiency of macrophage specific anti-apoptotic factors are protected from developing atherosclerosis presumably because of increased apoptosis of macrophages during the early stages of plaque development (Im and Osborne 2011).

4.3 Multiple effects of LXR agonists in macrophages and foam cells

Comparison of direct LXRα target genes in T0901317-exposed macrophages and foam cells revealed the effect of hyperstimulation of fatty acid synthesis pathways in macrophages as previously observed (Chisholm et al. 2003). Contrary, in T0901317-treated foam cells these effects were attenuated, presumably by cholesterol-induced suppression of SREBP pathways (Horton et al. 2002). LXRs and SREBPs bind to and activate many of the same genes involved in *de novo* fatty acid biosynthesis (Shibata and Glass 2009). Interestingly, LXRα binding to those genes was maintained in foam cells suggesting that suppression of SREBP pathways would be sufficient to reduce

fatty acid accumulation. This highlights that promising novel LXR agonists should separate beneficial effects from the stimulation of fatty acid synthesis via attenuation of SREBP activation. However, understanding how these opposing functions of LXR activators are regulated is an important area for future investigation. Moreover, further single-gene investigations of LXRα targets that are differentially induced in both macrophage models are required to gain a more comprehensive picture of LXRα actions in different cellular conditions.

4.4 LXRα-dependent repression of pro-inflammatory genes

Although most direct LXRα target genes are transcriptionally activated, four genes were identified that are down-regulated upon LXRα activation. Recent studies have revealed that the activation of LXRs in macrophages inhibits toll like receptor (TLR)-inducible inflammatory genes, such as *IL-1*β and *MCP-1* (Joseph et al. 2003). In accordance inflammatory gene clusters were significantly down-regulated in T0901317-treated foam cells. It was shown that repression of those pro-inflammatory genes is correlated with promoter proximal binding of LXR in mice (Ghisletti et al. 2007, Huang et al. 2009b). Contrary, in human macrophages or foam cells direct LXRα binding was not detected at inflammatory gene loci. One explanation is that LXRα-mediated repression involves long-range cis-interactions or tethering of LXRα to other factors as initially proposed (Li and Glass 2004). However, one might also expect such interactions would become fixed with cross-linking, and would appear as binding sites in ChIP-seq profiles (Reddy et al. 2009).

Interestingly, CD14 is down-regulated and LXRα bound exclusively in foam cells, underscoring that this gene is strictly regulated by LXRα. CD14 acts as a co-receptor along with TLRs and is required for TLR4-dependent activation of inflammatory genes by interfering with nuclear factor-κB (NF-κB) pathways (Triantafilou and Triantafilou 2002, Ghisletti et al. 2007). Together, these observations suggest that suppression of CD14 as an upstream activator of inflammatory genes represents a meaningful explanation of indirect LXRα-dependent anti-inflammatory effects in human macrophages upon oxLDL-induced inflammatory response (Hao et al. 2010).

4.5 Beyond direct target gene regulation

LXRα cistromes in conjunction with transcriptional profiling revealed novel binding regions and identified or substantiated the LXR-responsiveness of a number of genes involved in critical processes. However, beside its direct regulation of target genes LXRα up-regulates a number of distinct transcription factors in T0901317-treated macrophage and foam cells. It was determined that these factors are connected to a vast number of differentially expressed genes. It is therefore interesting to elucidate the functions of these factors to gain insights into the complex regulatory network targeted by LXRα.

Defined LXRα target genes in T0901317-treated macrophages include stringent regulation of the three transcription factors SREBF1, nuclear receptor interacting protein 1 (NRIP1, RIP140) and the nuclear receptor retinoic acid receptor alpha (RARα, NR1B1). As already mentioned, SREBF1 is a well-studied direct LXRα target that plays crucial role in lipid homoeostasis (Repa et al. 2000, Horton et al. 2002). NRIP1 was considered as LXR co-repressor but its direct regulation by LXRα binding remained unexplored (Herzog et al. 2007, Jakobsson et al. 2007b). The nuclear receptor RARα was only recently identified as occupied and regulated by LXRα binding (Rebe et al. 2009). Many differentially expressed genes contain RARα motifs in their promoter regions. Therefore, the cross-talk of LXRα and RARα represents an interesting issue that requires further investigations.

In T0901317-treated foam cells LXRα directly regulates five transcription factors including max-binding protein (MNT) and jun proto-oncogene (JUN) as well as NRIP1 that showed regulation in both cell models. These factors were not yet described as direct LXRα target genes. Widespread interactions were reported for the MNT transcription factor, a player in the MAX-interaction network (Hurlin and Huang 2006). However, its role in macrophages and the development of atherosclerosis is unclear. The JUN gene encodes a protein (c-Jun) that, together with the FBJ murine osteosarcoma viral oncogene homolog (FOS), forms the transcription factor activator protein 1 (AP-1). AP-1 plays a critical role in many signal transduction pathways and was recently implicated in the maintenance of open chromatin to direct glucocorticoid

receptor binding (Biddie et al. 2011). Moreover, the functional connection of AP-1 and LXRs was recently reported (Shen et al. 2011). AP-1 binding sites are also over-represented in regions of open chromatin that are bound by LXRα, indicating that AP-1 is a critical pioneer factor to bookmark functional regulatory elements. Interestingly, LXR agonists induced the binding of AP-1 to its recognition sequences in several gene promoters which contain AP-1 binding sites, indicating that AP-1 might also play an important roles in co-regulating genes such as *ApoE* and *ABCA1* (Huwait et al. 2011, Shen et al. 2011). Moreover, c-Jun is involved in c-Jun N-terminal kinase (JNK) pathways connected to LXR agonists-induced expression of target genes in macrophages albeit the exact mechanism through which LXR agonists activate c-Jun remained unexplored (Huwait et al. 2011). It was suspected that c-Jun-associated pathways are regulated through non-genomic effects (Schmuth et al. 2004). The present study suggests for the fist time that *JUN* is directly LXRα up-regulated by a distal LXR response element. Although additional validation experiments are necessary, this finding possibly explains the molecular mechanism how LXR agonists activate several components of the JNK pathway.

The transcriptional activation of several transcription factors by LXRα illustrates that the action of nuclear receptors in the regulation of gene transcription is complex with control by intracellular signaling pathways of the receptors themselves, co-factors recruited by them or other transcription factors that are required for the maximal expression of downstream genes (Huwait et al. 2011, Burns and Vanden Heuvel 2007). Therefore, directly targeted transcription factors are likely to be critical components of the LXRα transcriptional program, since in principle they can crosstalk with each other and regulate other cascades of genes that finally define the cellular response to T0901317 and oxLDL stimulations in macrophages.

4.6 Agonists influence LXR DNA binding

The influences of agonist binding on DNA occupancy for nuclear receptors *in vivo* in general and for those where endogenous metabolically derived compounds function as agonists in particular is complicated and not clearly understood (Chong et al. 2010).

The differential distribution of LXRα binding events in macrophages and foam cells suggests that agonists influence the specificity of LXRα binding. Remarkably, in contrast to T0901317-treated cells, in untreated THP-1-derived macrophages, LXRα DNA binding was globally undetected. Contrary, the model that LXR is bound to response elements in the absence of a ligand dominates the scientific literature (Li and Glass 2004, Zhu and Li 2009, Zhao and Dahlman-Wright 2010, Viennois et al. 2011). Hu and co-workers using ChIP-PCR initially showed that LXRα bound response elements are constitutively occupied. Ligand activation triggers the release of the co-repressor N-CoR leading to gene expression of occupied promoters (Hu et al. 2003). However according to recent studies, there is evidence for strictly agonist-dependent changes in binding of LXR to DNA in cultured cell models and primary cells determined by ChIP assays. Johansson and co-workers showed promoter specific ligand-dependent LXR recruitment in HepG2 and THP-1 cells (Jakobsson et al. 2009). Several other studies showed ligand-induced binding at a number of LXR responsive genes that are activated or repressed upon LXR ligand treatment (Ghisletti et al. 2007, Kim et al. 2009, Venteclef et al. 2010).

The absence of LXRα binding in uninduced macrophages is in accordance with the low amount of measured LXRα protein levels and thus indicates that the protein level is a critical parameter for subsequent gene regulatory action of LXR. Together, the genome-wide analysis of LXRα cistromes in macrophage suggests that ligand-dependent DNA binding is a general principle to activate gene expression of LXRα and concomitant binding to regulatory regions of LXRα target genes.

4.7 Chromatin accessibility and co-localized transcription factors

Several lines of evidence indicate that sites of open chromatin, defined by FAIRE (Giresi et al. 2007, Giresi and Lieb 2009), reliably identify active regulatory elements because of the following observations that are similar to DNase I hypersensitive sites detection assays (Boyle et al. 2008). It was shown that regions of open chromatin contain widespread and overlapping patterns of determined transcription factor binding sites (Li et al. 2011) and most enriched FAIRE regions were found near known

regulatory active transcription start sites (Gaulton et al. 2010). FAIRE-seq analysis of the chromatin landscape in macrophages at LXRα binding sites confirmed that accessible chromatin is highly correlative with transcriptional regulation of nearby genes. Moreover LXRα occupied regions in open chromatin are accompanied by numerous other factors, which underlines that these regions are functional enhancers (Chen et al. 2008, Roy et al. 2010, Moorman et al. 2006).

Estimation of the genome-wide chromatin accessibility in macrophages is in accordance with previous observations (John et al. 2011, Bernstein et al. 2010, Boyle et al. 2008, Song et al. 2011) and revealed that ~2% of the genome is depleted in nucleosomes and highly accessible. As recognized before (Hurtado et al. 2011), the small overlap of genome-wide treatment specific sites of open chromatin suggests that the vast majority of localized reorganization events are not stable but in fact represent a highly dynamic process. Interestingly, only 43% of LXRα binding sites induced by the synthetic ligand alone are associated to open chromatin whereas 76% of LXRα binding sites of oxLDL-triggered T0901317-treated foam cells matched to those regions. The major fraction of LXRα binding sites at inaccessible chromatin represent binding sites unique for T0901317-treated macrophages. Together with gene expression correlations, this observation indicates that those LXRα binding sites are non-functional and putatively serve as a reservoir to maintain an optimum amount of available transcription factor analogous to other biological buffering systems (MacQuarrie et al. 2011). However, the potential biological role of many of the sites remains largely undetermined (Farnham 2009). Together, this indicates also that artificial activation of LXRα by synthetic ligands is responsible for high amounts of induced non-functional binding. Therefore, the genome-wide analysis of chromatin accessibility is a valuable tool to determine functional LXRα binding events.

Most transcriptional regulators recognize short consensus sequences that occur frequently near most of the genes (Wunderlich and Mirny 2009). The underlying mechanism whereby LXRα selects a limited number of binding sites from a huge number of potential recognition sequences remains elusive. Therefore, the selective binding to a subset of sites in a given cellular environment mediating transcriptional regulation,

begs the question of how binding is orchestrated. Nuclear receptors have been shown to bind preset regions of accessible chromatin (Eeckhoute et al. 2006, Eeckhoute et al. 2009, John et al. 2008, Lefterova et al. 2010). This contradicts the activity of nuclear receptors as pioneer factors and rather suggests that nuclear receptors act cooperatively through cooperation with other factors to mediate transcriptional regulation (Biddie et al. 2010).

Given that LXRα to a large extend occupy pre-existing accessible sites in the genome that are accompanied by other factors, it will be important to understand the role of regulatory factors that initiate and maintain chromatin accessibility. The successful identification of several potentially cooperative transcription factors and pioneer factors at LXRα binding sites in open chromatin therefore represents a meaningful starting set for further investigations. Pioneer factors are defined as a specific class of transcription factors that are required and sufficient to trigger enhancer competency (Magnani et al. 2011). Genome-wide cistromes of LXRβ in human keratinocytes and mouse macrophages already showed co-localization of AP-1 and PU-1 binding respectively (Shen et al. 2011, Heinz et al. 2010). It was shown that PU.1 binding functions as a marker that defines the set of potential cis-regulatory elements through reprogramming the chromatin landscape that will subsequently be bound by LXRβ (Heinz et al. 2010). Similarly, it was shown that the transcription factor AP-1 maintains baseline chromatin accessibility facilitating glucocorticoid receptor (GR) recruitment (Biddie et al. 2011). Thus, this findings suggest that AP-1 is a major partner for productive LXRα-chromatin regulation and LXRα-regulated transcription. Interestingly, LXR binding to close chromatin is accompanied by the presence of the transcriptional repressor protein YY1 ("yin-yang") motif. Understanding the repertoire of LXRα interactions with these factors and cofactors will clearly be important for elucidating novel mechanisms in the pathophysiological processes of LXR action.

4.8 Challenges in genome-wide nuclear receptor research

A major difficulty faced by transcription factor ChIP-seq studies is the technical problem of having to assign binding sites with specific gene promoters (Dietz and

Carroll 2008). Another challenge is to understand gene expression data from cells exposed to specific nuclear receptor agonists. Genome-wide expression profiling shows that T0901317 exposure up-regulates and down-regulates hundreds of genes in macrophages. In contrast, nearest gene analysis revealed a distinct set of only 52 genes in both treatment models that exhibit both, LXRα binding and differential gene expression regulation upon ligand induction. A naïve interpretation of this discrepancy is that the majority of genes associated with LXRα binding regions are apparently T0901317-unresponsive. The observed phenomenon is common to several transcription factor ChIP-seq studies (Bolton et al. 2007, Lefterova et al. 2010, Farnham 2009) and therefore highlights the complexity of transcription factor binding and gene regulation. The importance of indirect LXRα effects through regulation of other transcription factors was already delineated. However, several additional reasons could account for the apparent discrepancy regarding the connection of binding events and gene expression regulation.

It is important to consider the effect of pharmacological LXR activation on gene expression changes. T0901317 is a potent activator of LXRs and LXRα effects are enhanced upon auto-up-regulation. However, this compound is not completely selective for LXR since it is able to activate PXR (Mitro et al. 2007) and FXR (Houck et al. 2004) and inhibits RAR-related orphan receptors alpha (RORα) and RORγ (Kumar et al. 2010). Similarly, the oxLDL-derived oxysterols regulate diverse other nuclear receptors including PPARγ (Shibata and Glass 2009). Therefore, gene expression changes triggered by endogenous or synthetic ligands may exter some aspecific effects. It is therefore crucial for future work to incorporate LXR knock-down expression profiles into correlation analyses.

Another important technical challenge represent the transcription factor binding site annotation. There is no consensus as to how far a transcription factor-binding region should be in order to be considered a putative cis-acting regulatory domain for a given gene (Jariwala et al. 2007). Although binding sites occur in abundance distal to promoters in terms of the linear genomic distance, chromatin is organized into higher-order structures to form chromosomes that are non-randomly positioned in

the three-dimensional nucleus (Takizawa et al. 2008, Biddie et al. 2010). Distal regulatory elements might therefore associate with promoters of responsive genes or enable recruitment of cofactors and the basal transcriptional machinery to transcriptionally active nuclear compartments. For example, in a ligand-dependent manner, LXR facilitates physical interactions between LXR-bound enhancer regions and the promoters of *ABCG1* in Huh7 cells to mediate transcription (Jakobsson et al. 2009). However, genome-wide determination of long-range interactions between regulatory elements using chromatin interaction analysis by paired-end tag sequencing (ChIA-PET) (Li et al. 2010) or Hi-C (van Berkum et al. 2010) approaches are difficult to established. Therefore, it is not yet possible to reliably connect binding events to the array of genes they regulate. Distal LXRα occupied regions may still regulate distant annotated genes on the same or even other chromosomes (Fullwood et al. 2009), or they may regulate nearby unannotated transcripts. Some observations indeed suggest that gene clusters may be regulated by distal LXRα binding events. It was determined that some LXRα binding events are surrounded by widespread clusters of differentially expressed genes that are hundreds of kilobases away and were therefore not annotated to the LXRα binding site. Interestingly, many distal genes and LXRα binding sites were found to be CTCF bound. CTCF has been proposed to partition the genome into functional blocks and mediate long-range interactions (Splinter et al. 2006, Phillips and Corces 2009, Hou et al. 2010). Correlation of publicly available CTCF ChIP-seq data with LXRα binding and gene expression changes indicates the possibility of long-range interaction by DNA looping (Figure 17). However, CTCF binding alone is not able to accurately predict functional long-range interactions as CTCF-bound sites are not exclusively located in the centre of interaction complexes (Handoko et al. 2011, Bau et al. 2011). Clearly, our understanding of the communication between LXRα binding at enhancers and the promoters of target genes requires future work, including the development of comprehensive bioinformatics strategies for binding site annotation.

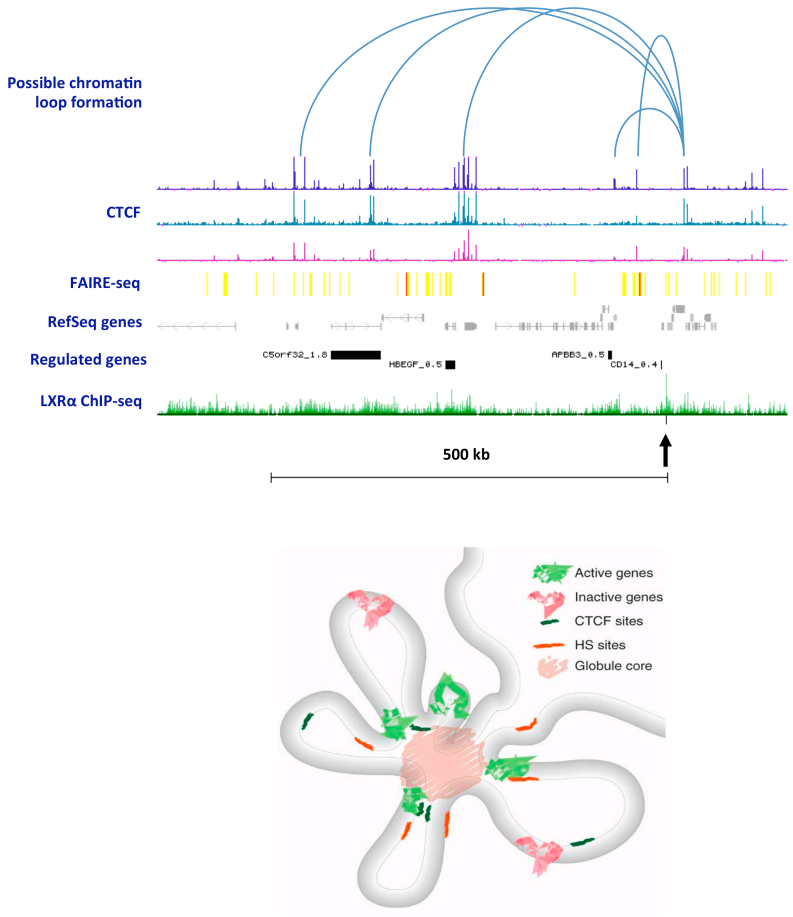

Figure 17: **LXRα binding in a cluster of transcriptionally regulated genes. (Top)** Possible chromatin looping interactions between a differentially expressed gene cluster and a distal regulatory element occupied by LXRα (arrow) in T0901317-treated foam cells. The putative loops (blue) are placed over the one-dimensional representation of a selected genomic region (chr5:139,359,560-140,170,670) and connect intervals occupied by CTCF (ChIP-seq profiles from Broad/MGH ENCODE group in K562 (violet), HeLa-S3 (blue) and HepG2 (magenta) cells). FAIRE-seq heatmap (yellow to red) of T0901317-treated foam cells. The RefSeq genes track is used to indicate gene positions (grey). Regulated genes are shown as black bars and the fold-change is indicated. LXRα ChIP-seq profile of T0901317-treated foam cells (green). **(Bottom)** Model for higher-order chromatin folding of actively transcribed genomic regions. Actively expressed genes (green) dynamically associate with transcription factories or globule cores (light red) whereas inactive genes (red) are located more distal. Many domains that exist as loops are connected by CTCF (dark green) and chromatin at the centre of looping interactions is often highly accessible (orange). Figure from Bau et al. 2011.

4.9 Future perspectives

The combination of LXRα ChIP-seq, FAIRE-seq and global gene expression analysis enabled insights into LXRα-dependent regulation of target genes and molecular mechanisms of LXRα activation. However, integrative analysis revealed that correlation of gene regulation and nuclear receptors DNA binding is highly complex. LXRα does not act individually to regulate particular genes but cooperates with other factors and activates broad regulatory networks via interaction with several transcription factors. Therefore, to understand the effect of LXRα on different metabolic pathways and their complex interactions it is necessary to develop systems biology approaches. Ideally, these approaches must incorporate many associated transcription factors. Secondly, ChIP-seq procedures provides many new hypotheses for follow-up in depth functional studies of distinct genes. The detailed characterization of the T0901317 response in macrophages and macrophage-derived foam cells presented here may help further our understanding of treating atherosclerosis and other diseases by interfering LXRα-regulated key pathways with small molecules.

5 Methods

5.1 Cell culture

Human THP-1 monocytic-like leukemia cells (ATCC) were cultured in RPMI medium supplemented with 10% fetal bovine serum (FBS, Biochrom), at 37°C in a humidified 10% CO_2 atmosphere. The cells were seeded in T-150 flasks at a density of 2100 cells/ml. Cells were split twice times per week and re-seeded in new flasks in order to prevent crowding. The medium was renewed every 3-4 days. Approximately $1.2*10^7$ cells were differentiated into a macrophage-like phenotype by incubation with 0.01 nM phorbol myristate acetate (PMA, Sigmar Aldrich) for 48 hours.

Human primary macrophages were isolated from buffy coats donated by healthy volunteers and kindly provided by the GRC Blood Donor Service East non-profit Ltd. Berlin. Peripheral blood mononuclear cells (PBMC) were isolated by density centrifugation with Ficoll-Paque (GE Healthcare). Monocyte enrichment from PBMC was obtained using MACS Monocyte Isolation Kit II and MACS LS columns (Miltenyi Biotec) yielding >95% purity. For differentiation 5105 cells/ml were plated in RPMI 164 medium supplemented with 10% human AB serum (First Link UK Ltd.) in T-150 flasks and incubated for 7 days at 37°C in a humidified 10% CO_2 atmosphere.

THP-1 cells and primary macrophages were treated either with 0.01% DMSO (vehicle control) or 1 µM T0901317 (Sigma-Aldrich) for 24 hours or with 100 µg/ml oxidized low-density lipoprotein (oxLDL, Autogen Bioclear) for 48 hours to induce foam cell formation and subsequently with 1 µM T0901317 for 48 hours.

5.2 Chromatin Immunoprecipitation (ChIP)

ChIP was carried out using the Transcription Factor ChIP kit (Diagenode, Denville, NJ, kch-redTBP-012).

5.2.1 Cross-linking of chromatin, harvest, and storage

Medium was removed from T-150 flasks and the $1.2*10^7$ cells were washed twice with PBS and incubated with 9.9 ml freshly prepared cross-linking buffer (3 vol. 37%

formaldehyde (Sigma-Aldrich, Steinheim, F8775), 7 vol. Buffer A and 100 vol. PBS) for 10 minutes at room temperature with gentle agitation. To stop cross-linking, 990 µl 1.25 M glycine was added and cells were incubated for 5 minutes with gentle agitation. Subsequently, the liquid was completely aspired from T-150 flasks and cells were washed twice with approximately 5 ml of ice-cold PBS. Then, 1.5 ml ice-cold Buffer B was added. Cells were scraped from the culture flask and transferred to an appropriate tube on ice. After centrifugation (5 minutes at 4°C and 500g) the supernatant was removed and 5 ml ice-cold Buffer C was added to the pellet to lyse the cells. The pellet was resuspended by pipetting up and down several times and incubated for 10 minutes on ice. After incubation the material was spun (5 minutes at 4°C and 500g), the supernatant was discarded and cells were resuspended with 624 µl freshly prepared Buffer D+P.I. (600µl Buffer D and 24 µl 25x Protease Inhibitor Mix) per $1.2*10^7$ cells. Cells were stored at -80°C

5.2.2 Sonication and assessment of chromatin fragmentation

After storage over night at -80°C the lysate was aliquoted to 240 µl into 1.5 ml protein low bind tubes (Protein LoBind, Eppendorf) and sonicated for at least 45 minutes in a 4°C water bath using the Diagenode Bioruptor (UCD-200, Diagenode, Denville, NJ) set to pulse on high for 30 seconds followed by 30 seconds of rest. To clear the lysate of cellular debris samples were spun (10 minutes at 14000g and 4°C) and the supernatant was transferred to new tubes and stored at -80°C. To test shearing efficacy and fragment sizes, 2.5 µl of sonicated material was analysed by agarose gel electrophoresis. Therefore, 7.5 µl Buffer F and 0.2 ml 5 M NaCl was added to the test samples and reverse cross-linking was performed for 16 hours at 65°C using a PCR cycler. DNA was finally purified using the MinElute PCR purification kit (Qiagen, Hilden) and eluted with 16 µl water. Eight µl DNA were mixed with 2µl loading buffer and subsequently analysed on an 1.2% agarose gel (e.g. 0.48mg agarose, 40ml 0.5x TBE and 1µl 20mg/ml EtBr). Chromatin was subjected to chromatin immunoprecipitation after DNA was sheared to an average fragment size of 100 - 600 bp. Further rounds of sonication were performed when needed to ensure that the majority of chromatin

fragments were in the appropriate size range.

5.2.3 Immunoprecipitation

Immunoprecipitation was prepared on ice in 1.5 ml protein low bind tubes using 12 µl 15% BSA, 20 µl P.I, 8 µl antibody (1 µg/µl), 60 µl prepared agarose beads, 60 µl fragmented chromatin (adjusted to 350 ng/µl DNA) and 320 µl water to a final volume of 540 ml. The following antibodies were used: anti-LXRα (1 µg/µl, ab 41902, Abcam) and mouse IgG (kch-819-015, Diagenode) was used as a negative control antibody. The prepared immunoprecipitation mix was incubated on a rotating wheel at 4°C over night. After incubation, beads were spun down (2 minutes at 500g and 4°C) and the supernatants were gently removed. Beads were washed twice with washing Buffer 1, once with washing Buffer 2, once with washing Buffer 3 and twice with washing Buffer 4. For each washing step 700 µl ice-cold wash buffer was added to the beads and incubation was carried out for 5 minutes on a rotating wheel at 8°C. Afterwards, beads were spun down (2 minutes at 500g and 4°C) and the supernatants were gently removed. To elute the DNA, 800 µl room temperature Buffer F was added and the samples were incubated for 20 minutes at room temperature on a rotating wheel. Afterwards, beads were spun down (2 minutes at 500g and room temperature) and supernatants were transferred into 1.5 ml DNA low bind tubes (DNA LoBind, Eppendorf).

5.2.4 Crosslink reversal, DNA purification and quantification

For de-crosslinking 32 µl 5 M NaCl was added to each sample and samples were heated at 65°C and 600 rpm over night using a thermo shaker (TS-100, Biolabo Scientific Instruments). Afterwards, samples were cooled down to room temperature and DNA was purified using the MinElute PCR purification kit (Qiagen, Hilden) and eluted with 30 µl water. DNA fragments were quantified using the PicoGreen assay (Quant-iT PicoGreen dsDNA Kit, Invitrogen) and a NanoDrop 3300 fluorospectrometer (Thermo Scientific). The PicoGreen assay kit uses an ultrasensitive fluorescent nucleic acid stain for quantitating double-stranded DNA in solution. Therefore, 0.5 µl 200x PicoGreen

was dissolved in 95 µl 1x TE buffer and 1.5 µl PicoGreen working solution was added to 1.5 µl precipitated DNA. A standard curve was constructed by a dilution series of standard lambda phage DNA to calculate the double stranded DNA content of immunoprecipitated DNA. During the whole procedure, all samples were protected from light.

5.2.5 ChIP-sequencing

Sample preparation and sequencing was performed by the in house NGS Sequencing Core facility at the Max Planck Institute for Molecular Genetics. Library preparation with 10-15 ng of LXRα-ChIP-DNA and IgG-ChIP-DNA was carried out by the use of the ChIP-Seq Sample Prep Kit (Illumina). Short reads of 36 bp were produced from the Illumina Genome Analyzer IIx.

5.3 ChIP-seq data analysis

5.3.1 Databases

The human genome February 2009 assembly (GRCh37/hg19) was used as reference database. All loci are given as hg19 coordinates.

5.3.2 Mapping of sequence data

Unfiltered 36bp sequence reads were uniquely mapped to the human genome using Bowtie (Langmead et al. 2009) allowing for two mismatches along each tag.

5.3.3 Generation of tag signal profiles

25bp resolution LXRα binding profiles were generated genome-wide using the MACS tool (Zhang et al. 2008) with the option –wig. Resulting wiggle files (.wig) were converted to the bigWig format using the program wigToBigWig (Kent et al. 2010). Normalized signal profiles were generated using makeUCSCfile using the Hypergeometric Optimization of Motif EnRichment (HOMER) software (Heinz et al. 2010). Resulting bedGraph files (.bg) were converted to the bigWig format using the program

bedGraphToBigWig (Kent et al. 2010). BigWig files were uploaded to a webserver and visualized as custome track in the UCSC Genome Browser (Karolchik et al. 2011).

5.3.4 Peak interval determination

Peak identification was performed using the model based-analysis of ChIP-seq algorithm (MACS, Zhang et al. 2008) with aligned sequencing tags in BED format from LXRα-ChIP and IgG-ChIP experiments. The MACS version 1.0.1 was accessed via Galaxy (main.g2.bx.psu.edu). The following peak calling parameters were used: p-value cut-off = 10^{-5}, effective genome size = 2.7^{9}, bandwidth = 300 and mfold = 5. Additionally, three levels (1 kb, 5 kb, 10 kb) of regions around the peak regions were used to calculate the maximum lambda as local lambda. To estimate the false discovery rate (FDR) for each peak interval the traditional default method was used. The method considers the peak location, 1 kb, 5 kb, and 10 kb regions in the control data to calculate local bias.

5.3.5 Assessment of determined peaks

Initially, a total of 3,779 and 16,013 binding regions were identified in ChIP-seq data of TO901317-treated macrophages and foam cells respectively. Contrary to expectations from sequencing depth and visual inspections of ChIP-seq profiles, 6,446 peaks were determined in data from untreated cells (Figure 19A, left). Therefore, MACS-derived peak significances were analysed showing highly significant peaks under treatment and comparably low peak significances in the control set. However, the median significances of all peaks were similar between treatment groups and most peaks had significances close to the defined p-value cut-off (Figure 18A and B). To further understand how the peak interval determinations correspond with actual visible peaks and with likely LXRα binding, genome regions were manually inspected as suggested by Rye and coworkers (Rye et al. 2010). The analysis confirmed previous observations. Determined peaks from untreated cells are not distinct from background (Figure 18C, Control) and some visually observed peaks were not determined due to corresponding enrichments of control data (Figure 18C, +).

By visual determination treatment-derived peaks were likely true positive but co-treatment-derived peaks seem to accumulate in regions with higher background indicating false positive binding regions (Figure 18C, #). Furthermore, sets of both treatments suffered subsequent amounts of weak enrichments that fall into the peak definition (Figure 18C, *). Additionally, defined peaks with strong enrichments and high significances were observed that also showed strong tag accumulation in control date (Figure 18C, right box) and are therefore unlikely to represent true binding sites (Pickrell et al. 2011). Collectively, the determined peak numbers seemed overestimated. The presence of large fractions of false positive peak intervals abolished the possibility of ranking the peaks by decreasing confidence levels either according to coverage by sequencing reads or according to statistical scores provided by MACS as described (Rozowsky et al. 2009). Additionally, any downstream analysis with unfiltered peak interval sets was hugely affected by false positive intervals making feature correlations impossible. These observations make clear that finding the true binding sites in the tag profiles of LXRα data sets is not trivial and different issues must be considered to gain a high-stringency peak set with a maximal amount of true positive peak.

5.3.6 Peak filtering with variable control data

To determine a more stringent peak set the reproducibility of peaks was assessed by peak calling with LXRα data using three biological replicates of IgG control data sets. Therefore, peak calling was carried out individually and overlapping peak intervals were determined that represent a stringent peak set. Estimated peak numbers showed up to 2.4 fold control-dependent variations and an extreme reduction of filtered peak number was observed for both treatment conditions with 260 and 1375 peaks in ChIP-seq data of TO901317-treated macrophages and foam cells respectively (Figure 19A right). The filtered interval sets showed increased significance indicating the successful exclusion of false positive peaks (Figure 19B).

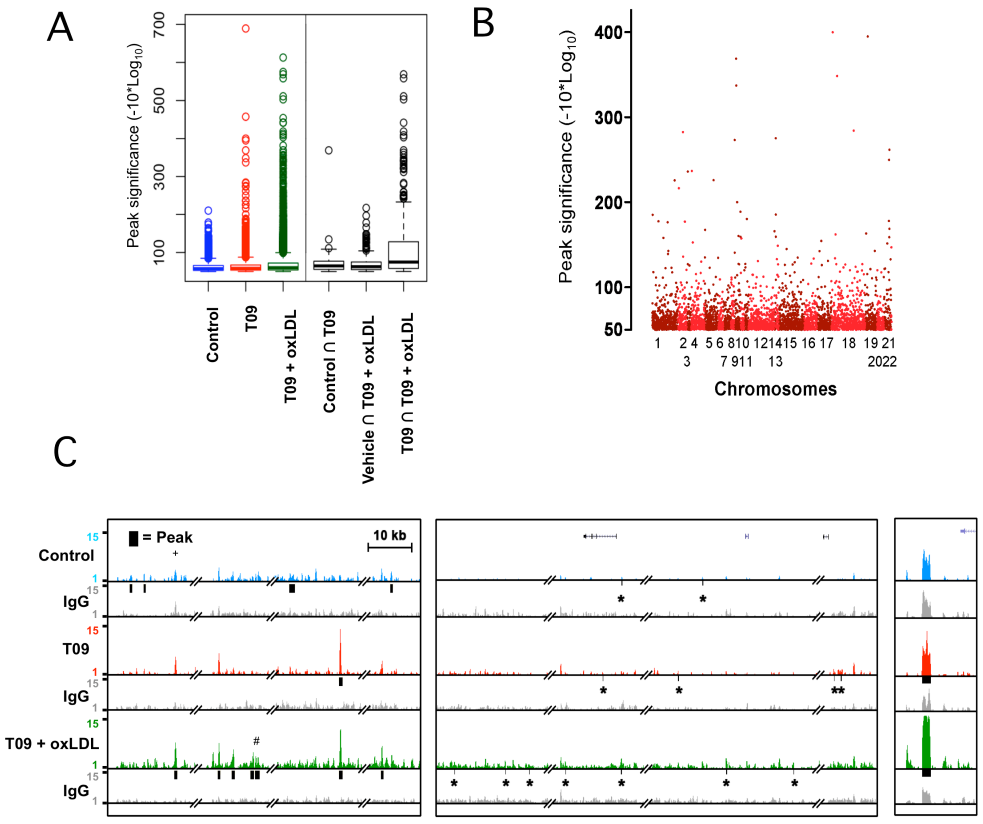

Figure 18: **Inspection of determined LXRα peaks**. **(A)** Box plot showing the distributions of ChIP-Seq peak interval significances (-10*Log10(p-value)) determined by MACS from vehicle-treated macrophages (Control, blue), T0901317-treated macrophages (T09, red) and T0901317-treated foam cells (T09 + oxLDL, green) and significances of peaks that inersect between the data sets. **(B)** Manhattan plot of peak interval significances relative to interval positions over the genome from T0901317-treated macrophages. (C) LXRα ChIP-seq and IgG ChIP-seq profiles and determined peak intervals (black boxes) show peak intervals with low enrichments (# and *), not deterimned peaks due to corresponding enrichments of control data (+) and determined peaks with corresponding enrichments of control data (right).

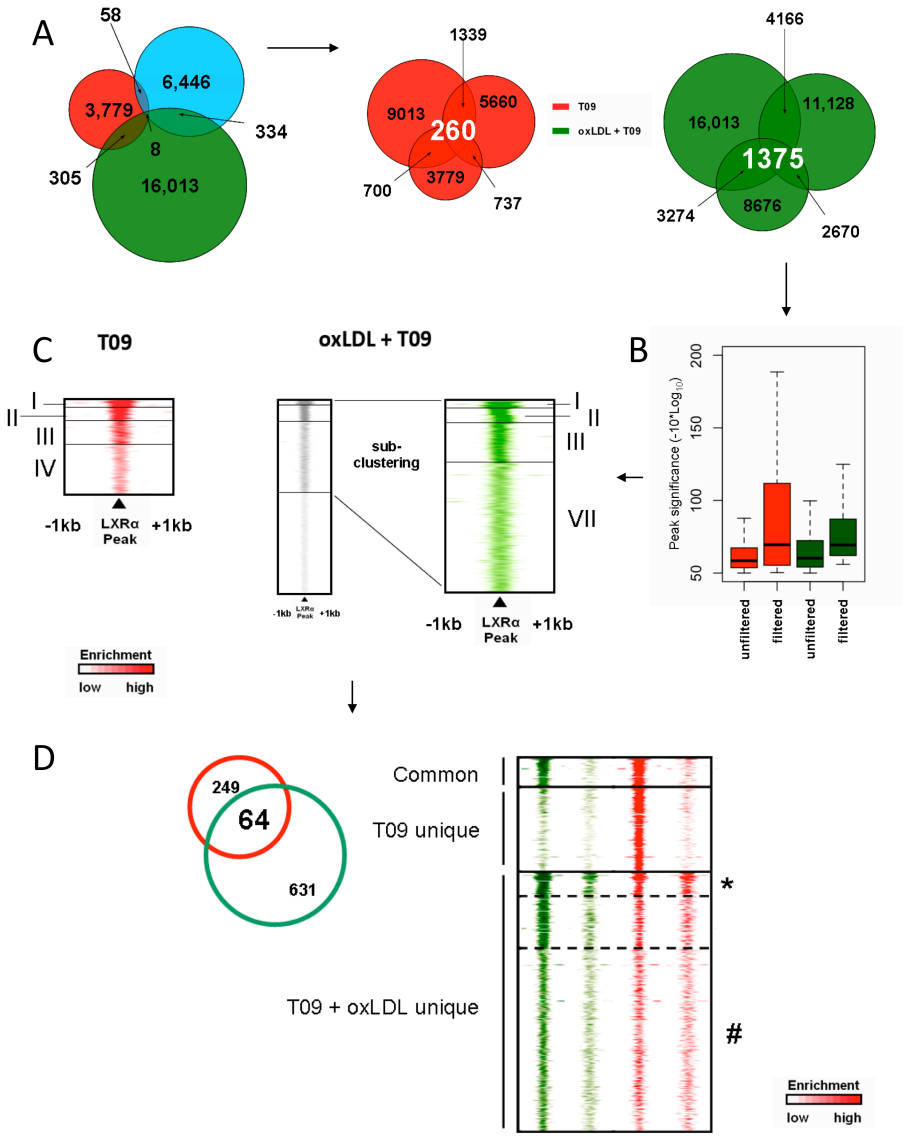

Figure 19: **Peak filtering strategy. (A)** Left: Venn diagrams showing intersection of MACS-determined LXRα peaks from vehicle-treated macrophages (blue), T0901317-treated macrophages (red) and T0901317-treated foam cells (green). Right: MACS-determined peaks using three biological replicates of IgG control data were intersected (filtered). **(B)** Filtered peaks show higher MACS-derived significance compared to unfilterd peaks (unfiltered). **(C)** Heat map visualisation and clustering-assisted sub-filtering of LXRα peak intervals. **(D)** Heat map visualisation of common and unique LXRα binding sites. Profiles of foam cell unique LXRα peaks show strong enrichments of corresponding IgG-derived and T0901317-derived tags over LXRα binding sites (*) and low tag enrichments (#).

5.3.7 Peak filtering by the use of *k*-means clustering

The tag distributions of derived peak sets were individually subjected to k-means clustering (Heintzman et al. 2009) to organize the identified peaks presenting similar read densities within a 2 kb window. Clustering was performed using SeqMINER (Ye et al. 2011). Four clusters were determined to annotate peaks according to enrichment. The observed clusters elucidate different LXRα binding patterns and show sub-groups of sites with different binding affinities (Figure19C, Cluster I-IV and VII). Importantly, clustering allowed exclusion of some peaks with very broad enrichments and sub-clustering of tags from oxLDL-treated cells enabled discrimination of low enriched peak intervals (Figure 19C). Comparison of both peak sets revealed that the majority (93%) of genomic binding sites were unique for each treatment. To test whether tag enrichment corresponds with this observation, LXRα ChIP-seq reads and IgG control reads were visualised around peak intervals. Heatmap visualisation showed first that the oxLDL top clusters have strong enrichments of corresponding IgG-derived and T0901317-derived tags (Figure 19D, *), and second that the bottom cluster showed comparable low tag enrichments in both treatments. To tackle that issue, top cluster peaks were discarded by individual inspection and the bottom cluster peaks were sub-clustered and filtered for the most enriched regions. The applied method does not rule out the possibility that some true binding sites were missed due to the incomplete splitting of large clusters (Duda et al. 2000). However, peak filtering resulted in a total of 249 and 215 peaks for TO901317-treated macrophages and foam cells respectively (Figure 4) Those peak sets were used for down stream analysis.

5.4 Formaldehyde Assisted Isolation of Regulatory Elements (FAIRE)

FAIRE was done essentially as described (Giresi and Lieb 2009) with slide modifications using materials of the Transcription Factor ChIP Kit from Diagenode (Cat. No. kch-red TBP-012). Cells were cross-linked and chromatin was fragmented as described for the ChIP assay. To a 30 µl aliquot of chromatin (adjusted to 350 ng/µl DNA) 170 µl buffer F and 8 µl 5 M NaCl was added. For FAIRE analysis of primary macrophages 15 µl chromatin was used and the volume was adjusted to 30µl with water. An input sample

was prepared as follows. Samples were incubated over night at 65°C and 600rpm using a thermo shaker (TS-100, Biolabo Scientific Instruments) to reverse the chemical cross-linking followed by incubation for 2 hours at 55°C and 500 rpm in the presence of 20 µg Proteinase K (Invitrogen, 25530-049). Input sample and FAIRE sample were diluted with an equal volume of water (200 µl). The FAIRE sample was incubated at 37°C until the solution was cleared from SDS precipitations. Chromatin from Input and FAIRE sample was extracted by adding an equal volume of phenol-chloroform/isoamyl alcohol (25:24:1), mixing, 5 minutes incubating at room temperature and spinning for 5 minutes at 18500g. The aqueous phase was transferred to a new DNA low bind tube (DNA LoBind, Eppendorf) and water was added to gain a volume of 400 ul. A second phenol-chloroform and two subsequent chloroform/isoamyl alcohol extractions were performed to ensure all protein has been removed. The DNA was precipitated by addition of 0.0125 volumes of DNA co-precipitant (Diagenode), 0.1 volumes of DNA precipitant (Diagenode), twice the volume of 100% ice cold ethanol and incubation at -20°C for 2.5 hours. The precipitate was then spun at 20000g for 45 minutes at 4°C. The pellet was washed with 1 ml 70% room temperature ethanol and spun (30 minutes at 18500g at room temperature). Subsequently, all liquid was removed and the pellet was dried for 20 minutes and resuspended in 50 µl water. After addition of 350 µl Buffer F and 16 µl 5 M NaCl samples were incubated over night at 65°C and 600 rpm. Afterwards samples were subjected to RNaseA (10 µg) digest at 37°C and 500 rpm for 30 minutes and subsequent incubation with 40 µg Proteinase K for 2 hours at 55°C and 500 rpm. DNA was finally purified using the MinElute PCR purification kit (Qiagen) and eluted with 30µl water. The DNA concentration was assessed using the NanoDrop spectrophotometer (ND-1000; Nanodrop Technology). DNA fragmentation was tested as described for the ChIP assay. DNA fragments isolated by FAIRE are 100-200 bp in length, with the average length being 135 bp.

5.4.1 FAIRE-sequencing (FAIRE-seq)

FAIRE enriched DNA from T0901317-treated foam cells and three biological replicates of DMSO and T0901317-treated THP-1-derived macrophages was individually pooled,

adjusted to 8 ng/µl DNA and 150 ng DNA was provided for high-throughput sequencing. Sample preparation and sequencing was performed by the in house NGS Sequencing Core facility at the Max Planck Institute for Molecular Genetics. Sample preparation was carried out by the use of the ChIP-Seq Sample Prep Kit (Illumina). Libraries were generated from gel-purified ~200-bp DNA fragments. After adaptor ligation and PCR-based amplification, samples were sequenced on the Illumina Genome Analyzer IIx using standard procedures to produce short reads of 36 bp.

5.5 FAIRE-seq data analysis

5.5.1 Mapping of sequencing data

Mapping was done as described for the ChIP-seq data analysis.

5.5.2 Generation of tag signal profiles

Aligned sequencing tags were converted to a continuous wiggle track with 25 bp resolution using F-Seq that employs Parzen kernel density estimation to create base pair scores (Boyle et al. 2008). The exact command used for this step is:

```
fseq -l 800 -s 25 -v -of wig alignment.bed
```

Where the alignments.bed is a bed file of filtered sequence alignments. The resulting fixed step .wig files per chromosome were concatenated using the Unix command 'cat'. Files were further processed using the Unix command 'sed' to make files compatible for wig-to-bigWig conversion by the use of the program wigToBigWig (Kent et al. 2010). BigWig files were uploaded to a webserver and visualized as custom tracks in the UCSC Genome Browser (Karolchik et al. 2011).

5.5.3 Determination of FAIRE-seq enrichments

Peak intervals that represent sites of FAIRE-seq enrichments were assessed with F-Seq (Boyle et al. 2008). The standard derivations were set for each sample using an empirical estimation of the upper bounds on the number of nucleosome-depleted

regions genome-wide (roughly 200,000) (Gaulton et al. 2010). The exact command used for this step is:

```
fseq -t <s.d.> -l 800 -o alignment.bed
```

Where the alignments.bed is a bed file of filtered sequence alignments and <s.d.> is the standard deviation. For data from vehicle-treated THP-1-derived macrophages, the threshold used was s.d. = 3.75. For data from T0901317-treated THP-1-derived macrophages and foam cells, the threshold used was s.d. = 4. Clusters of determined enrichment intervals were defined by merging the determined enrichment intervals with a maximum distance of 250 bp between intervals into single intervals that span the entire cluster using windowBed (BEDtools) (Quinlan and Hall 2010). The sizes of the intervals were further increased by 250bp using slopBed (BEDtools) (Quinlan and Hall 2010). These intervals represent a liberal set of sites of open chromatin and were used for down-stream correlations.

5.6 Genome-wide gene expression analysis

Genome-wide gene expression analysis was previously done in our lab. Therefore, biotin-labelled cRNA was produced using the Illumina TotalPrep RNA Amplification Kit (Ambion) according to the manufacturers instructions. Cy3-stained cRNA was hybridised on HumanHT-12 v3 Expression BeadChips (Illumina). Scanning was performed using the Illumina BeadStation 50 (Illumina, San Diego, CA, USA) platform and reagents according to the protocols supplied by the manufacturer. Samples were hybridised in biological quadruplicates. Basic expression data analysis was carried out using BeadStudio 3.1 (Illumina Software). Raw data were background-subtracted and normalized using the cubic spline algorithm. Processed data were then filtered for significant detection (P-value < 0.01) and differential expression vs. vehicle treatment according to the Illumina t-test error model and were corrected according to the Benjamini-Hochberg procedure (P-values < 0,05) in the BeadStudio software.

5.7 Quantitative real-time PCR (qPCR)

To assay for the enrichment of ChIP- or FAIRE-derived DNA at regions of interest quantitative PCRs were carried out in triplicates in 384-format PCR plates. Primers are presented in Table 8. A 5-µl reaction mixture contained a minimum of 20 pg DNA for ChIP or 150pg for FAIRE per PCR reaction, 0.5 mM of each primer and 2× SYBR Green PCR Master Mix (Applied Biosystems, 4309155). To normalize for primer efficacy qPCR was carried out for each primer pair using diluted input DNA and IgG-derived DNA (ChIP only). The 7900HT Abi Prism PCR Instrument was applied with the following parameters. The thermal cycle started with an initial denaturation at 95°C for 10 minutes, followed by 45 cycles of denaturation at 95°C for 15 s, annealing and extension at 60°C for 60 s. DNA melting curve analysis was performed for each PCR reaction at temperatures ranging from 60°C to 99°C to assure that a single band was produced. Fluorescence was read in the linear phase and the raw data were expressed as Ct values that had achieved the baseline. The relative enrichment of ChIP-derived DNA was calculated using the following equation:

$$\triangle \triangle Ct = \frac{2^{\left(Ct_{input} - \left(\frac{\log(D)}{\log(2)}\right)\right) - (Ct_{ChIP})} \times 100\%}{2^{\left(Ct_{input} - \left(\frac{\log(D)}{\log(2)}\right)\right) - \left(Ct_{IgG}\right)} \times 100\%}$$

The relative enrichment of FAIRE-derived DNA was calculated using the following equation:

$$\triangle Ct = 2^{-(Ct_{FAIRE}) - \left(Ct_{Input} - \left(\frac{\log(D)}{\log(2)}\right)\right)} \times 100\%$$

Where *D* is the dilution factor of the input DNA.

5.8 Wetern blot analysis

Cells were harvested and nuclear extracts were prepared using NE-PER Nuclear and Cytoplasmic Extraction Kit (Thermo Scientific, Pierce, 78833). Protein contents were determined with the Bradford method using the Bio-Rad Protein Assay Kit (Bio-Rad Laboratories GmbH, 500-0006). Protein concentrations were adjusted to

Name	Forward primer	Reverse primer	Figure 2	Figure 11
hLXRaLXRE1	CATCTGTTTCGGTCTCTTTGG	GCAGATGCTCCAGTCCAGAT	1	5
hLXRaLXRE3	GGATTACAGACCCGCATCAC	CCAGCAATGGTGTGTTGAAA	2	6
ABCA1_1BS	CCCAGCTTCCCCATCTGCGC	CCGGAGGTGGGGTGCCCAAT	3	
hABCALXRE	CTCACTCTCGCTCGCAATTA	ACGTGCTTTCTGCTGAGTGA	4	7
ABCA1_NC	AGAGCGGACCCCAAAGCTGGT	GGCAGTGTGTCCAGGGCTTCC	5	8
ABCA1_2BS	CGGGCTCATGCTCCACTCGG	GCCGATTGCCCCACATCCCT	6	
ACCA1	CGCCCCTGTCTCCCACCTCA	TCGGAGGTGAACGGCCTGGA	7	9
ACCA_promotor1	CGCACTCCGGAGGGGACCAA	TCACTTTGCCCGTGTGGCGC	8	10
FASN	CGGGGTTACTGCCGGTCATCG	GTGGGTGGACGTCCGTCTCG	9	1
SREBP1	CCGCCTTTAACCCGCTCGGTG	CCCTTTAACGAAGGGGGCGGG	10	
FASN_H4K20	CAGGCCAGCCCAAGAGCCAC	GGGGCCACCTTTCCCCCAGA		2
SREBF1_NC	TGTCCATCGACAGGGAATCAGGTGG	GCTTGGTTCCATGTCAACAGCCAG		3
SREBF1_H4K20	AGGAGTGCCAGTGCTTGGTGG	GTAGGGCACAATGGGGGCCC		4
faireACTB1	CCATTGGCAAGAGCCCGGCT	GACACCCCACGCCAGTTCGG		11
faireACTB2	CTCTGCACGGGCGAAGGGG	CACACCCGCCGCCAGGTAAG		
faireACTB3	GCGGCCGCTCGAGCCATAAA	CGAAGCCGGTGAGTGAGCGG		
faireACTB4	GCTTCGCCGCACAGTGCAG	AGGCGGCCAACGCCAAAACT		
faireACTB5	ACCGCGGGACATCCTAGGTGT	GCGTACAGAACCCAGGGCCC		
faireNC1	CACCACCATCTCGGCCCACC	GATGGTGGCTGGCCGCTCC		
faireNC2	AGCACAACTCCCACCACACAGGA	TCGGGGGTGGGTGTCACTGG		
faireNC3	GGCCCCTGAGCCTCTGAGCT	GCTCGGTCAGGTGCAGCGTT		
fairePC1	CCCGCCCCTGGACTGTCGTA	CGCGAGGACCCGAACGTCAA		
NC_h19	CTGGTCTGTGCTGGCCACGG	GCACCTTGGCTGGGGCTCTG		
SCD__intron1	CGTAGGTGCCATGCAGCCCC	CAGCTCGGGCAGATGCCAGG		
SCD_H4K20	AGGGCAGATCACCTGGGGCCTC	AGAGCCAGTCAGCCCCAACAAGA		
c-jun	TTCGGCACTTGGAGGCAGCG	CGAGATGCCCGGCGAGACAC		
ABCG1	CTCTGCAGGCCTGTGGACGC	AGCGCTGTTTTCTCCCGGGC		
ACCA_neg_site	TGCCACTGATCCACGATGTTGCC	AGTGGTCTTGGGAAAGAGCAGGC		
ABCA1_H4K20	TGCACACTTCTGGCCTTGTTCCAC	GCACCTGTGACACCCAACGGA		

Table 8: Primers for ChIP- and FAIRE-qPCR

23 µg per sample and were analysed by western blotting using the NuPage Bis-Tris Electrophoresis System (Invitrogen). SDS-PAGE was carried out using NuPage 15 well Novex 4-12% Bis-Tris gels (1.0 mm) and separated proteins were plotted on nitrocellulose membranes for 75 minutes at 400mA. After blotting membranes were stained with Ponceau S solution (Applichem, A2935,0100) to confirm equal protein loading and de-stained using water. After blocking of membranes (1X TBS, 0.1% Tween-20 with 5% w/v nonfat dry milk), membranes were incubated with 1:1000 LXRa antibody (1 ug/ul, ab 41902, Abcam, mouse) in milk powder solution at 4°C over night. After washing the membranes with TBS-Tween solution, membranes were incubated with 1:2000 goat anti-mouse IgG-HRP andtibody (Santa Cruz Biotechnology, sc-2005) for 1 hour at room temperature. After washing steps luminescence was detected, membranes were striped using Restore Plus Western Blot Stripping Buffer (Thermo Scientific) and incubated with β-Actin (C4) antibody (Santa Cruz Biotechnology sc-47778) for 20 minutes at room temperature. After washing steps the membrane was incubated with 1:2000 goat anti-mouse IgG-HRP andtibody (Santa Cruz Biotechnology, sc-2005) for 20 hour at room temperature.

5.9 Bioinformatics methods

Visualisation MACS-derived peak intervals in the BED format were visualized as a custom tracks in the UCSC genome browser (Karolchik et al. 2011). Box plots were generated using R (RDCT 2011) or Graphpad Prism. Bar plots were generated using Graphpad Prism. Heat maps of tag densities or genomic intervals were generated using SeqMiner (Ye et al. 2011).

Intersection of genomic interval Genomic intervals were intersected using intersectBed from the BEDtools suite (Quinlan and Hall 2010) or via Galaxy (main.g2.bx.psu.edu). The statistical significance of co-occurrence of intervals was calculated using the R package Cooccur (Version 0.54) (Huen and Russell 2010). Therefore, .bed files were converted to .gff files using Galaxy (main.g2.bx.psu.edu).

Generation of average score profiles Average tag counts (Figure5 B) were calculated using the SitePro tool from Galaxy/Cistrome (cistrome.org) and data was visualised using R (RDCT 2011).

Determination of genomic disribution of peak intervals Genomic distributions (Figure 6) were determined using the Cis-regulatory Element Annotation System (CEAS 1.0.2, http://liulab.dfci.harvard.edu/CEAS).

Quantitative determination of enrichments The program bigWigSummary (Kent et al. 2010) was used to retrieve signals from wiggle or bedGraph files based on genomic coordinates of LXRα peak intervals or intervals of open chromatin. The exact command used for this step is:

```
bigWigSummary density.bigwig <chr> <start> <end> 1 type=mean
```

Where the density.bigwig is a bigwig file generated from filtered sequence alignments, <chr> is the chromosome, and <start> and <end> are the starting and ending positions of the interval, respectively.

Annotation of peak intervals to genes As described, three methods were used to annotate LXRα peak intervals to putatively regulated genes. Nearest gene analysis was performed using closetsBed from the BEDtools suite (Quinlan and Hall 2010). Gene definitions were taken from the UCSC Genome Browser's RefGene table (Fujita et al. 2010). Annotation of peak surround genes was done using the Peak Center Annotation script (peak2gene) from the Cistrome Analysis Pipeline (AP) Module (cistrome.org) with a distance of 30 kb from the peak centre. Association of peak intervals with genes in regulatory domains was done using GREAT (McLean et al. 2010). Genes of all three sets were concatenated and filtered for unique entries using the Unix command 'uniq'.

Random intervals Random intervals were generated using shufleBed from the BEDtools suite (Quinlan and Hall 2010).

Jaccard Matrix Similarity coefficient matrix (Figure 13) was generated using the ChIPseeqerComputeJaccardIndex tool from ChIPseeqer (Giannopoulou and Elemento 2011) and R (RDCT 2011) for visualisation.

Gene ontology analysis To classify functions for the genes targeted by LXRα Gene Ontology (GO) enrichment analysis was performed using the Database for Annotation, Visualization, and Integrated Discovery (DAVID) (Huang et al. 2009a). Redundant categories were manually removed and only the top ranked hits from each cluster were presented.

Network analysis PWM based network analysis (Figure 8) was done using the tool ChIP-Array (Qin et al. 2011). Interaction networks (Figue 9 and 10) were derived from the FANTOM4-EdgeExpress Database (Kawaji et al. 2010) as described in the corresponding section. Networks (Figure 8, 9 and 10) were visualised using Cytoscape (Smoot et al. 2011).

Motif analysis *De novo* motif search was done using the MEME suite (Machanick and Bailey 2011).

Over-representation analysis Transcription factor over-representation analysis was done using F-MATCH (http://www.gene-regulation.com).

References

Bau, D., A. Sanyal, B. R. Lajoie, E. Capriotti, M. Byron, J. B. Lawrence, J. Dekker, and M. A. Marti-Renom: 2011, 'The three-dimensional folding of the alpha-globin gene domain reveals formation of chromatin globules'. *Nature Structural & Molecular Biology* **18**(1), 107–114. PMID: 21131981.

Bernstein, B. E., J. A. Stamatoyannopoulos, J. F. Costello, B. Ren, A. Milosavljevic, A. Meissner, M. Kellis, M. A. Marra, A. L. Beaudet, J. R. Ecker, P. J. Farnham, M. Hirst, E. S. Lander, T. S. Mikkelsen, and J. A. Thomson: 2010, 'The NIH Roadmap Epigenomics Mapping Consortium'. *Nature Biotechnology* **28**(10), 1045–1048. PMID: 20944595.

Beyea, M. M., C. L. Heslop, C. G. Sawyez, J. Y. Edwards, J. G. Markle, R. A. Hegele, and M. W. Huff: 2007, 'Selective up-regulation of LXR-regulated genes ABCA1, ABCG1, and APOE in macrophages through increased endogenous synthesis of 24(S),25-epoxycholesterol'. *The Journal of Biological Chemistry* **282**(8), 5207–5216. PMID: 17186944.

Biddie, S. C., S. John, and G. L. Hager: 2010, 'Genome-wide mechanisms of nuclear receptor action'. *Trends in Endocrinology and Metabolism: TEM* **21**(1), 3–9. PMID: 19800253.

Biddie, S. C., S. John, P. J. Sabo, R. E. Thurman, T. A. Johnson, R. L. Schiltz, T. B. Miranda, M. Sung, S. Trump, S. L. Lightman, C. Vinson, J. A. Stamatoyannopoulos, and G. L. Hager: 2011, 'Transcription factor AP1 potentiates chromatin accessibility and glucocorticoid receptor binding'. *Molecular Cell* **43**(1), 145–155. PMID: 21726817.

Bolton, E. C., A. Y. So, C. Chaivorapol, C. M. Haqq, H. Li, and K. R. Yamamoto: 2007, 'Cell- and gene-specific regulation of primary target genes by the androgen receptor'. *Genes & Development* **21**(16), 2005–2017. PMID: 17699749 PMCID: 1948856.

Boyle, A. P., S. Davis, H. P. Shulha, P. Meltzer, E. H. Margulies, Z. Weng, T. S. Furey, and G. E. Crawford: 2008, 'High-resolution mapping and characterization of open chromatin across the genome'. *Cell* **132**(2), 311–322. PMID: 18243105.

Bradley, M. N., C. Hong, M. Chen, S. B. Joseph, D. C. Wilpitz, X. Wang, A. J. Lusis, A. Collins, W. A. Hseuh, J. L. Collins, R. K. Tangirala, and P. Tontonoz: 2007, 'Ligand activation of LXR beta reverses atherosclerosis and cellular cholesterol overload in mice lacking LXR alpha and apoE'. *The Journal of Clinical Investigation* **117**(8), 2337–2346. PMID: 17657314.

Burns, K. A. and J. P. Vanden Heuvel: 2007, 'Modulation of PPAR activity via phosphorylation'. *Biochimica Et Biophysica Acta* **1771**(8), 952–960. PMID: 17560826.

Carroll, J. S., X. S. Liu, A. S. Brodsky, W. Li, C. A. Meyer, A. J. Szary, J. Eeckhoute, W. Shao, E. V. Hestermann, T. R. Geistlinger, E. A. Fox, P. A. Silver, and M. Brown: 2005, 'Chromosome-wide mapping of estrogen receptor binding reveals long-range regulation requiring the forkhead protein FoxA1'. *Cell* **122**(1), 33–43. PMID: 16009131.

Carson, A.: 2010, 'Atherosclerosis - The Future Challenge for Europe's Health Economies'. *European Cardiology* **5**(2), 86–8.

Chen, X., H. Xu, P. Yuan, F. Fang, M. Huss, V. B. Vega, E. Wong, Y. L. Orlov, W. Zhang, J. Jiang, Y. Loh, H. C. Yeo, Z. X. Yeo, V. Narang, K. R. Govindarajan, B. Leong, A. Shahab, Y. Ruan, G. Bourque, W. Sung, N. D. Clarke, C. Wei, and H. Ng: 2008, 'Integration of external signaling pathways with the core transcriptional network in embryonic stem cells'. *Cell* **133**(6), 1106–1117. PMID: 18555785.

Chisholm, J. W., J. Hong, S. A. Mills, and R. M. Lawn: 2003, 'The LXR ligand T0901317 induces severe lipogenesis in the db/db diabetic mouse'. *Journal of Lipid Research* **44**(11), 2039–2048. PMID: 12923232.

Chong, H. K., A. M. Infante, Y. Seo, T. Jeon, Y. Zhang, P. A. Edwards, X. Xie, and T. F. Osborne: 2010, 'Genome-wide interrogation of hepatic FXR reveals an asymmetric IR-1 motif and synergy with LRH-1'. *Nucleic Acids Research* **38**(18), 6007–6017. PMID: 20483916.

Costet, P., Y. Luo, N. Wang, and A. R. Tall: 2000, 'Sterol-dependent transactivation of the ABC1 promoter by the liver X receptor/retinoid X receptor'. *The Journal of Biological Chemistry* **275**(36), 28240–28245. PMID: 10858438.

Dekker, J.: 2008, 'Gene regulation in the third dimension'. *Science (New York, N.Y.)* **319**(5871), 1793–1794. PMID: 18369139.

Dietz, S. C. and J. S. Carroll: 2008, 'Interrogating the genome to understand oestrogen-receptor-mediated transcription'. *Expert Reviews in Molecular Medicine* **10**, e10. PMID: 18377699.

Duda, R. O., P. E. Hart, and D. G. Stork: 2000, *Pattern Classification*. Wiley-Interscience, 2 edition.

Eeckhoute, J., J. S. Carroll, T. R. Geistlinger, M. I. Torres-Arzayus, and M. Brown: 2006, 'A cell-type-specific transcriptional network required for estrogen regulation of cyclin D1 and cell cycle progression in breast cancer'. *Genes & Development* **20**(18), 2513–2526. PMID: 16980581.

Eeckhoute, J., M. Lupien, C. A. Meyer, M. P. Verzi, R. A. Shivdasani, X. S. Liu, and M. Brown: 2009, 'Cell-type selective chromatin remodeling defines the active subset of FOXA1-bound enhancers'. *Genome Research* **19**(3), 372 –380.

Farnham, P. J.: 2009, 'Insights from genomic profiling of transcription factors'. *Nature Reviews. Genetics* **10**(9), 605–616. PMID: 19668247.

Ferre, P. and F. Foufelle: 2007, 'SREBP-1c transcription factor and lipid homeostasis: clinical perspective'. *Hormone Research* **68**(2), 72–82. PMID: 17344645.

Fujita, P. A., B. Rhead, A. S. Zweig, A. S. Hinrichs, D. Karolchik, M. S. Cline, M. Goldman, G. P. Barber, H. Clawson, A. Coelho, M. Diekhans, T. R. Dreszer, B. M. Giardine, R. A. Harte, J. Hillman-Jackson, F. Hsu, V. Kirkup, R. M. Kuhn, K. Learned, C. H. Li, L. R. Meyer, A. Pohl, B. J. Raney, K. R. Rosenbloom, K. E. Smith, D. Haussler, and W. J. Kent: 2010, 'The UCSC Genome Browser database: update 2011'. *Nucleic Acids Research*.

Fullwood, M. J., M. H. Liu, Y. F. Pan, J. Liu, H. Xu, Y. B. Mohamed, Y. L. Orlov, S. Velkov, A. Ho, P. H. Mei, E. G. Y. Chew, P. Y. H. Huang, W. Welboren, Y. Han, H. S. Ooi, P. N. Ariyaratne, V. B. Vega, Y. Luo, P. Y. Tan, P. Y. Choy, K. D. S. A. Wansa, B. Zhao, K. S. Lim, S. C. Leow, J. S. Yow, R. Joseph, H. Li, K. V. Desai, J. S. Thomsen, Y. K. Lee, R. K. M. Karuturi, T. Herve, G. Bourque, H. G. Stunnenberg, X. Ruan, V. Cacheux-Rataboul, W. Sung, E. T. Liu, C. Wei, E. Cheung, and Y. Ruan: 2009, 'An oestrogen-receptor-alpha-bound human chromatin interactome'. *Nature* **462**(7269), 58–64. PMID: 19890323.

Gaulton, K. J., T. Nammo, L. Pasquali, J. M. Simon, P. G. Giresi, M. P. Fogarty, T. M. Panhuis, P. Mieczkowski, A. Secchi, D. Bosco, T. Berney, E. Montanya, K. L. Mohlke, J. D. Lieb, and J. Ferrer: 2010, 'A map of open chromatin in human pancreatic islets'. *Nat Genet* **42**(3), 255–259.

Germain, P., B. Staels, C. Dacquet, M. Spedding, and V. Laudet: 2006, 'Overview of nomenclature of nuclear receptors'. *Pharmacological Reviews* **58**(4), 685–704. PMID: 17132848.

Ghisletti, S., W. Huang, S. Ogawa, G. Pascual, M. Lin, T. M. Willson, M. G. Rosenfeld, and C. K. Glass: 2007, 'Parallel SUMOylation-dependent pathways mediate gene- and signal-specific transrepression by LXRs and PPARgamma'. *Molecular cell* **25**(1), 57–70. PMID: 17218271 PMCID: 1850387.

Giannopoulou, E. G. and O. Elemento: 2011, 'An integrated ChIP-seq analysis platform with customizable workflows'. *BMC Bioinformatics* **12**, 277. PMID: 21736739.

Giresi, P. G., J. Kim, R. M. McDaniell, V. R. Iyer, and J. D. Lieb: 2007, 'FAIRE (Formaldehyde-Assisted Isolation of Regulatory Elements) isolates active regulatory elements from human chromatin'. *Genome Research* **17**(6), 877–885. PMID: 17179217.

Giresi, P. G. and J. D. Lieb: 2009, 'Isolation of active regulatory elements from eukaryotic chromatin using FAIRE (Formaldehyde Assisted Isolation of Regulatory Elements)'. *Methods (San Diego, Calif.)* **48**(3), 233–239. PMID: 19303047.

Glass, C. K. and J. L. Witztum: 2001, 'Atherosclerosis. the road ahead'. *Cell* **104**(4), 503–516. PMID: 11239408.

Handoko, L., H. Xu, G. Li, C. Y. Ngan, E. Chew, M. Schnapp, C. W. H. Lee, C. Ye, J. L. H. Ping, F. Mulawadi, E. Wong, J. Sheng, Y. Zhang, T. Poh, C. S. Chan, G. Kunarso, A. Shahab, G. Bourque, V. Cacheux-Rataboul, W. Sung, Y. Ruan, and C. Wei: 2011, 'CTCF-mediated functional chromatin interactome in pluripotent cells'. *Nat Genet* **43**(7), 630–638.

Hao, M.-x., L.-s. Jiang, N.-y. Fang, J. Pu, L.-h. Hu, L. Shen, W. Song, and B. He: 2010, 'The cannabinoid WIN55,212-2 protects against oxidized LDL-induced inflammatory response in murine macrophages'. *Journal of Lipid Research* **51**(8), 2181–2190. PMID: 20305287.

Heintzman, N. D., G. C. Hon, R. D. Hawkins, P. Kheradpour, A. Stark, L. F. Harp, Z. Ye, L. K. Lee, R. K. Stuart, C. W. Ching, K. A. Ching, J. E. Antosiewicz-Bourget, H. Liu, X. Zhang, R. D. Green, V. V. Lobanenkov, R. Stewart, J. A. Thomson, G. E. Crawford, M. Kellis, and B. Ren: 2009, 'Histone modifications at human enhancers reflect global cell-type-specific gene expression'. *Nature* **459**(7243), 108–112. PMID: 19295514.

Heinz, S., C. Benner, N. Spann, E. Bertolino, Y. C. Lin, P. Laslo, J. X. Cheng, C. Murre, H. Singh, and C. K. Glass: 2010, 'Simple combinations of lineage-determining transcription factors prime cis-regulatory elements required for macrophage and B cell identities'. *Molecular Cell* **38**(4), 576–589. PMID: 20513432.

Herzog, B., M. Hallberg, A. Seth, A. Woods, R. White, and M. G. Parker: 2007, 'The nuclear receptor cofactor, receptor-interacting protein 140, is required for the regulation of hepatic lipid and glucose metabolism by liver X receptor'. *Molecular Endocrinology (Baltimore, Md.)* **21**(11), 2687–2697. PMID: 17684114.

Horton, J. D., J. L. Goldstein, and M. S. Brown: 2002, 'SREBPs: activators of the complete program of cholesterol and fatty acid synthesis in the liver'. *The Journal of Clinical Investigation* **109**(9), 1125–1131. PMID: 11994399.

Hou, C., R. Dale, and A. Dean: 2010, 'Cell type specificity of chromatin organization mediated by CTCF and cohesin'. *Proceedings of the National Academy of Sciences of the United States of America* **107**(8), 3651–3656. PMID: 20133600.

Houck, K. A., K. M. Borchert, C. D. Hepler, J. S. Thomas, K. S. Bramlett, L. F. Michael, and T. P. Burris: 2004, 'T0901317 is a dual LXR/FXR agonist'. *Molecular Genetics and Metabolism* **83**(1-2), 184–187. PMID: 15464433.

Hu, X., S. Li, J. Wu, C. Xia, and D. S. Lala: 2003, 'Liver X receptors interact with corepressors to regulate gene expression'. *Molecular Endocrinology (Baltimore, Md.)* **17**(6), 1019–1026. PMID: 12663743.

Huang, D. W., B. T. Sherman, and R. A. Lempicki: 2009a, 'Systematic and integrative analysis of large gene lists using DAVID bioinformatics resources'. *Nature Protocols* **4**(1), 44–57. PMID: 19131956.

Huang, W., S. Ghisletti, V. Perissi, M. G. Rosenfeld, and C. K. Glass: 2009b, 'Transcriptional integration of TLR2 and TLR4 signaling at the NCoR de-repression checkpoint'. *Molecular cell* **35**(1), 48–57. PMID: 19595715 PMCID: 2759189.

Huen, D. S. and S. Russell: 2010, 'On the use of resampling tests for evaluating statistical significance of binding-site co-occurrence'. *BMC Bioinformatics* **11**, 359. PMID: 20591178.

Hurlin, P. J. and J. Huang: 2006, 'The MAX-interacting transcription factor network'. *Seminars in Cancer Biology* **16**(4), 265–274. PMID: 16908182.

Hurtado, A., K. A. Holmes, C. S. Ross-Innes, D. Schmidt, and J. S. Carroll: 2011, 'FOXA1 is a key determinant of estrogen receptor function and endocrine response'. *Nature Genetics* **43**(1), 27–33. PMID: 21151129.

Huwait, E. A., K. R. Greenow, N. N. Singh, and D. P. Ramji: 2011, 'A novel role for c-Jun N-terminal kinase and phosphoinositide 3-kinase in the liver X receptor-mediated induction of macrophage gene expression'. *Cellular Signalling* **23**, 542–549.

Im, S. and T. F. Osborne: 2011, 'Liver x receptors in atherosclerosis and inflammation'. *Circulation Research* **108**(8), 996–1001. PMID: 21493922.

Jakobsson, T., W. Osman, J.-k. Gustafsson, J. Zilliacus, and A. WÃ€rnmark: 2007a, 'Molecular basis for repression of liver X receptor-mediated gene transcription by receptor-interacting protein 140'. *Biochemical Journal* **405**(Pt 1), 31–39. PMID: 17391100 PMCID: 1925237.

Jakobsson, T., W. Osman, J.-k. Gustafsson, J. Zilliacus, and A. WÃ€rnmark: 2007b, 'Molecular basis for repression of liver X receptor-mediated gene transcription by receptor-interacting protein 140'. *Biochemical Journal* **405**(Pt 1), 31–39. PMID: 17391100 PMCID: 1925237.

Jakobsson, T., N. Venteclef, G. Toresson, A. E. Damdimopoulos, A. Ehrlund, X. Lou, S. Sanyal, K. R. Steffensen, J. Gustafsson, and E. Treuter: 2009, 'GPS2 is required for cholesterol efflux by triggering histone demethylation, LXR recruitment, and coregulator assembly at the ABCG1 locus'. *Molecular Cell* **34**(4), 510–518. PMID: 19481530.

Janowski, B. A., M. J. Grogan, S. A. Jones, G. B. Wisely, S. A. Kliewer, E. J. Corey, and D. J. Mangelsdorf: 1999, 'Structural requirements of ligands for the oxysterol liver X receptors LXRalpha and LXRbeta'. *Proceedings of the National Academy of Sciences* **96**(1), 266 –271.

Jariwala, U., J. Prescott, L. Jia, A. Barski, S. Pregizer, J. P. Cogan, A. Arasheben, W. D. Tilley, H. I. Scher, W. L. Gerald, G. Buchanan, G. A. Coetzee, and B. Frenkel: 2007, 'Identification of novel androgen receptor target genes in prostate cancer'. *Molecular Cancer* **6**, 39. PMID: 17553165.

John, S., P. J. Sabo, T. A. Johnson, M. Sung, S. C. Biddie, S. L. Lightman, T. C. Voss, S. R. Davis, P. S. Meltzer, J. A. Stamatoyannopoulos, and G. L. Hager: 2008, 'Interaction of the glucocorticoid receptor with the chromatin landscape'. *Molecular Cell* **29**(5), 611–624. PMID: 18342607.

John, S., P. J. Sabo, R. E. Thurman, M. Sung, S. C. Biddie, T. A. Johnson, G. L. Hager, and J. A. Stamatoyannopoulos: 2011, 'Chromatin accessibility pre-determines glucocorticoid receptor binding patterns'. *Nature Genetics* **43**(3), 264–268. PMID: 21258342.

Joseph, S. B., A. Castrillo, B. A. Laffitte, D. J. Mangelsdorf, and P. Tontonoz: 2003, 'Reciprocal regulation of inflammation and lipid metabolism by liver X receptors'. *Nature Medicine* **9**(2), 213–219. PMID: 12524534.

Joseph, S. B., E. McKilligin, L. Pei, M. A. Watson, A. R. Collins, B. A. Laffitte, M. Chen, G. Noh, J. Goodman, G. N. Hagger, J. Tran, T. K. Tippin, X. Wang, A. J. Lusis, W. A. Hsueh, R. E. Law, J. L. Collins, T. M. Willson, and P. Tontonoz: 2002, 'Synthetic LXR ligand inhibits the development of atherosclerosis in mice'. *Proceedings of the National Academy of Sciences of the United States of America* **99**(11), 7604–7609. PMID: 12032330.

Karolchik, D., A. S. Hinrichs, and W. J. Kent: 2011, 'The UCSC Genome Browser'. *Current Protocols in Human Genetics / Editorial Board, Jonathan L. Haines ... [et Al.]* **Chapter 18**, Unit18.6. PMID: 21975940.

Kawaji, H., J. Severin, M. Lizio, A. R. R. Forrest, E. van Nimwegen, M. Rehli, K. Schroder, K. Irvine, H. Suzuki, P. Carninci, Y. Hayashizaki, and C. O. Daub: 2010, 'Update of the FANTOM web resource: from mammalian transcriptional landscape to its dynamic regulation'. *Nucleic Acids Research*.

Kennedy, M. A., A. Venkateswaran, P. T. Tarr, I. Xenarios, J. Kudoh, N. Shimizu, and P. A. Edwards: 2001, 'Characterization of the human ABCG1 gene: liver X receptor activates an internal promoter that produces a novel transcript encoding an alternative form of the protein'. *The Journal of Biological Chemistry* **276**(42), 39438–39447. PMID: 11500512.

Kent, W. J., A. S. Zweig, G. Barber, A. S. Hinrichs, and D. Karolchik: 2010, 'BigWig and BigBed: enabling browsing of large distributed datasets'. **26**(17), 2204–2207. PMID: 20639541 PMCID: 2922891.

Kidder, B. L., G. Hu, and K. Zhao: 2011, 'ChIP-Seq: technical considerations for obtaining high-quality data'. *Nature Immunology* **12**(10), 918–922. PMID: 21934668.

Kim, G. H., K. Park, S. Yeom, K. J. Lee, G. Kim, J. Ko, D. Rhee, Y. H. Kim, H. K. Lee, H. W. Kim, G. T. Oh, K. Lee, J. W. Lee, and S. Kim: 2009, 'Characterization of ASC-2 as an Antiatherogenic Transcriptional Coactivator of Liver X Receptors in Macrophages'. *Molecular Endocrinology* **23**(7), 966–974. PMID: 19342446 PMCID: 2703598.

Klepper, K., G. K. Sandve, O. Abul, J. Johansen, and F. Drablos: 2008, 'Assessment of composite motif discovery methods'. *BMC Bioinformatics* **9**, 123. PMID: 18302777.

Kumar, N., L. A. Solt, J. J. Conkright, Y. Wang, M. A. Istrate, S. A. Busby, R. D. Garcia-Ordonez, T. P. Burris, and P. R. Griffin: 2010, 'The benzenesulfoamide T0901317 [N-(2,2,2-trifluoroethyl)-N-[4-[2,2,2-trifluoro-1-hydroxy-1-(trifluoromethyl)ethyl]phenyl]-benzenesulfonamide] is a novel retinoic acid receptor-related orphan receptor-alpha/gamma inverse agonist'. *Molecular Pharmacology* **77**(2), 228–236. PMID: 19887649.

Laffitte, B. A., S. B. Joseph, M. Chen, A. Castrillo, J. Repa, D. Wilpitz, D. Mangelsdorf, and P. Tontonoz: 2003, 'The Phospholipid Transfer Protein Gene Is a Liver X Receptor Target Expressed by Macrophages in Atherosclerotic Lesions'. *Molecular and Cellular Biology* **23**(6), 2182–2191. PMID: 12612088 PMCID: 149472.

Laffitte, B. A., S. B. Joseph, R. Walczak, L. Pei, D. C. Wilpitz, J. L. Collins, and P. Tontonoz: 2001, 'Autoregulation of the human liver X receptor alpha promoter'. *Molecular and Cellular Biology* **21**(22), 7558–7568. PMID: 11604492.

Langmead, B., C. Trapnell, M. Pop, and S. L. Salzberg: 2009, 'Ultrafast and memory-efficient alignment of short DNA sequences to the human genome'. *Genome Biology* **10**(3), R25. PMID: 19261174.

Leal, J., R. Luengo-FernÃ¡ndez, A. Gray, S. Petersen, and M. Rayner: 2006, 'Economic burden of cardiovascular diseases in the enlarged European Union'. *European Heart Journal* **27**(13), 1610 –1619.

Lee, R. T. and P. Libby: 1997, 'The unstable atheroma'. *Arteriosclerosis, Thrombosis, and Vascular Biology* **17**(10), 1859–1867. PMID: 9351346.

Lee, S., J. Lee, S. Lee, and J. W. Lee: 2008, 'Activating Signal Cointegrator-2 Is an Essential Adaptor to Recruit Histone H3 Lysine 4 Methyltransferases MLL3 and MLL4 to the Liver X Receptors'. *Molecular Endocrinology* **22**(6), 1312–1319. PMID: 18372346 PMCID: 2422828.

Lee, T., C. Pan, C. Peng, Y. R. Kou, C. Chen, L. Ching, T. Tsai, S. Chen, P. Lyu, and S. Shyue: 2010, 'Anti-atherogenic effect of berberine on LXRalpha-ABCA1-dependent cholesterol efflux in macrophages'. *Journal of Cellular Biochemistry* **111**(1), 104–110. PMID: 20506155.

Lefterova, M. I., D. J. Steger, D. Zhuo, M. Qatanani, S. E. Mullican, G. Tuteja, E. Manduchi, G. R. Grant, and M. A. Lazar: 2010, 'Cell-Specific Determinants of Peroxisome Proliferator-Activated Receptor gamma Function in Adipocytes and Macrophages'. **30**(9), 2078–2089. PMID: 20176806 PMCID: 2863586.

Lefterova, M. I., Y. Zhang, D. J. Steger, M. Schupp, J. Schug, A. Cristancho, D. Feng, D. Zhuo, J. Stoeckert, Christian J, X. S. Liu, and M. A. Lazar: 2008, 'PPARgamma and C/EBP factors orchestrate adipocyte biology via adjacent binding on a genome-wide scale'. *Genes & Development* **22**(21), 2941–2952. PMID: 18981473.

Leleu, M., G. Lefebvre, and J. Rougemont: 2010, 'Processing and analyzing ChIP-seq data: from short reads to regulatory interactions'. *Briefings in Functional Genomics* **9**(5-6), 466–476. PMID: 20861161.

Levin, N., E. D. Bischoff, C. L. Daige, D. Thomas, C. T. Vu, R. A. Heyman, R. K. Tangirala, and I. G. Schulman: 2005, 'Macrophage liver X receptor is required for antiatherogenic activity of LXR agonists'. *Arteriosclerosis, Thrombosis, and Vascular Biology* **25**(1), 135–142. PMID: 15539622.

Li, A. C. and C. K. Glass: 2002, 'The macrophage foam cell as a target for therapeutic intervention'. *Nat Med* **8**(11), 1235–1242.

Li, A. C. and C. K. Glass: 2004, 'PPAR- and LXR-dependent pathways controlling lipid metabolism and the development of atherosclerosis'. *Journal of Lipid Research* **45**(12), 2161–2173. PMID: 15489539.

Li, G., M. J. Fullwood, H. Xu, F. H. Mulawadi, S. Velkov, V. Vega, P. N. Ariyaratne, Y. B. Mohamed, H. Ooi, C. Tennakoon, C. Wei, Y. Ruan, and W. Sung: 2010, 'ChIA-PET tool for comprehensive chromatin interaction analysis with paired-end tag sequencing'. **11**(2), R22–R22. PMID: 20181287 PMCID: 2872882.

Li, X., S. Thomas, P. J. Sabo, M. B. Eisen, J. A. Stamatoyannopoulos, and M. D. Biggin: 2011, 'The role of chromatin accessibility in directing the widespread, overlapping patterns of Drosophila transcription factor binding'. *Genome Biology* **12**(4), R34. PMID: 21473766.

Li, Y., C. Bolten, B. G. Bhat, J. Woodring-Dietz, S. Li, S. K. Prayaga, C. Xia, and D. S. Lala: 2002, 'Induction of human liver X receptor alpha gene expression via an autoregulatory loop mechanism'. *Molecular Endocrinology (Baltimore, Md.)* **16**(3), 506–514. PMID: 11875109.

Libby, P.: 2002, 'Inflammation in atherosclerosis'. *Nature* **420**(6917), 868–874. PMID: 12490960.

Loh, Y., Q. Wu, J. Chew, V. B. Vega, W. Zhang, X. Chen, G. Bourque, J. George, B. Leong, J. Liu, K. Wong, K. W. Sung, C. W. H. Lee, X. Zhao, K. Chiu, L. Lipovich, V. A. Kuznetsov, P. Robson, L. W. Stanton, C. Wei, Y. Ruan, B. Lim, and H. Ng: 2006, 'The Oct4 and Nanog transcription network regulates pluripotency in mouse embryonic stem cells'. *Nature Genetics* **38**(4), 431–440. PMID: 16518401.

Lu, T. T., J. J. Repa, and D. J. Mangelsdorf: 2001, 'Orphan nuclear receptors as eLiXiRs and FiXeRs of sterol metabolism'. *The Journal of Biological Chemistry* **276**(41), 37735–37738. PMID: 11459853.

Machanick, P. and T. L. Bailey: 2011, 'MEME-ChIP: motif analysis of large DNA datasets'. *Bioinformatics (Oxford, England)* **27**(12), 1696–1697. PMID: 21486936.

MacQuarrie, K. L., A. P. Fong, R. H. Morse, and S. J. Tapscott: 2011, 'Genome-wide transcription factor binding: beyond direct target regulation'. *Trends in Genetics: TIG* **27**(4), 141–148. PMID: 21295369.

Magnani, L., J. Eeckhoute, and M. Lupien: 2011, 'Pioneer factors: directing transcriptional regulators within the chromatin environment'. *Trends in Genetics: TIG*. PMID: 21885149.

Matys, V., E. Fricke, R. Geffers, E. GÃ¶ssling, M. Haubrock, R. Hehl, K. Hornischer, D. Karas, A. E. Kel, O. V. Kel-Margoulis, D. Kloos, S. Land, B. Lewicki-Potapov, H. Michael, R. MÃŒnch, I. Reuter, S. Rotert, H. Saxel, M. Scheer, S. Thiele, and E. Wingender: 2003, 'TRANSFAC: transcriptional regulation, from patterns to profiles'. *Nucleic Acids Research* **31**(1), 374–378. PMID: 12520026.

McLean, C. Y., D. Bristor, M. Hiller, S. L. Clarke, B. T. Schaar, C. B. Lowe, A. M. Wenger, and G. Bejerano: 2010, 'GREAT improves functional interpretation of cis-regulatory regions'. *Nature Biotechnology* **28**(5), 495–501. PMID: 20436461.

Mitro, N., L. Vargas, R. Romeo, A. Koder, and E. Saez: 2007, 'T0901317 is a potent PXR ligand: implications for the biology ascribed to LXR'. *FEBS Letters* **581**(9), 1721–1726. PMID: 17418145.

Moorman, C., L. V. Sun, J. Wang, E. de Wit, W. Talhout, L. D. Ward, F. Greil, X. Lu, K. P. White, H. J. Bussemaker, and B. van Steensel: 2006, 'Hotspots of transcription factor colocalization in the genome of Drosophila melanogaster'. *Proceedings of the National Academy of Sciences* **103**, 12027–12032.

Nikolaev, A., T. McLaughlin, D. D. M. O'Leary, and M. Tessier-Lavigne: 2009, 'APP binds DR6 to trigger axon pruning and neuron death via distinct caspases'. *Nature* **457**(7232), 981–989. PMID: 19225519.

Nolis, I. K., D. J. McKay, E. Mantouvalou, S. Lomvardas, M. Merika, and D. Thanos: 2009, 'Transcription factors mediate long-range enhancer-promoter interactions'. *Proceedings of the National Academy of Sciences* **106**(48), 20222 –20227.

Oram, J. F. and J. W. Heinecke: 2005, 'ATP-binding cassette transporter A1: a cell cholesterol exporter that protects against cardiovascular disease'. *Physiological Reviews* **85**(4), 1343–1372. PMID: 16183915.

Pan, G., J. H. Bauer, V. Haridas, S. Wang, D. Liu, G. Yu, C. Vincenz, B. B. Aggarwal, J. Ni, and V. M. Dixit: 1998, 'Identification and functional characterization of DR6, a novel death domain-containing TNF receptor'. *FEBS Letters* **431**(3), 351–356. PMID: 9714541.

Peet, D. J., S. D. Turley, W. Ma, B. A. Janowski, J. M. Lobaccaro, R. E. Hammer, and D. J. Mangelsdorf: 1998, 'Cholesterol and bile acid metabolism are impaired in mice lacking the nuclear oxysterol receptor LXR alpha'. *Cell* **93**(5), 693–704. PMID: 9630215.

Phillips, J. E. and V. G. Corces: 2009, 'CTCF: master weaver of the genome'. *Cell* **137**(7), 1194–1211. PMID: 19563753.

Pickrell, J. K., D. J. Gaffney, Y. Gilad, and J. K. Pritchard: 2011, 'False positive peaks in ChIP-seq and other sequencing-based functional assays caused by unannotated high copy number regions'. *Bioinformatics*.

Qin, J., M. J. Li, P. Wang, M. Q. Zhang, and J. Wang: 2011, 'ChIP-Array: combinatory analysis of ChIP-seq/chip and microarray gene expression data to discover direct/indirect targets of a transcription factor'. *Nucleic Acids Research* **39**(Web Server issue), W430–436. PMID: 21586587.

Qin, Y., K. T. Dalen, J. Gustafsson, and H. I. Nebb: 2009, 'Regulation of hepatic fatty acid elongase 5 by LXRalpha-SREBP-1c'. *Biochimica Et Biophysica Acta* **1791**(2), 140–147. PMID: 19136075.

Qiu, G. and J. S. Hill: 2008, 'Atorvastatin inhibits ABCA1 expression and cholesterol efflux in THP-1 macrophages by an LXR-dependent pathway'. *Journal of Cardiovascular Pharmacology* **51**(4), 388–395. PMID: 18427282.

Quinlan, A. R. and I. M. Hall: 2010, 'BEDTools: a flexible suite of utilities for comparing genomic features'. **26**(6), 841–842. PMID: 20110278 PMCID: 2832824.

RDCT: 2011, 'R: A Language and Environment for Statistical Computing'. **ISBN 3-900051-07-0**(http://www.R-project.org).

Rebe, C., M. Raveneau, A. Chevriaux, D. Lakomy, A. Sberna, A. Costa, G. BessÃšde, A. Athias, E. Steinmetz, J. M. A. Lobaccaro, G. Alves, A. Menicacci, S. Vachenc, E. Solary, P. Gambert, and D. Masson: 2009, 'Induction of transglutaminase 2 by a liver X receptor/retinoic acid receptor alpha pathway increases the clearance of apoptotic cells by human macrophages'. *Circulation Research* **105**(4), 393–401. PMID: 19628791.

Reddy, T. E., F. Pauli, R. O. Sprouse, N. F. Neff, K. M. Newberry, M. J. Garabedian, and R. M. Myers: 2009, 'Genomic determination of the glucocorticoid response reveals unexpected mechanisms of gene regulation'. *Genome Research* **19**(12), 2163–2171. PMID: 19801529.

Repa, J. J., G. Liang, J. Ou, Y. Bashmakov, J. A. Lobaccaro, I. Shimomura, B. Shan, M. S. Brown, J. L. Goldstein, and D. J. Mangelsdorf: 2000, 'Regulation of mouse sterol regulatory element-binding protein-1c gene (SREBP-1c) by oxysterol receptors, LXRalpha and LXRbeta'. *Genes & Development* **14**(22), 2819 –2830.

Repa, J. J. and D. J. Mangelsdorf: 1999, 'Nuclear receptor regulation of cholesterol and bile acid metabolism'. *Current Opinion in Biotechnology* **10**(6), 557–563. PMID: 10600692.

Ross, R.: 1999, 'Atherosclerosis–an inflammatory disease'. *The New England Journal of Medicine* **340**(2), 115–126. PMID: 9887164.

Rowe, A. H., C. A. Argmann, J. Y. Edwards, C. G. Sawyez, O. H. Morand, R. A. Hegele, and M. W. Huff: 2003, 'Enhanced synthesis of the oxysterol 24(S),25-epoxycholesterol in macrophages by inhibitors of 2,3-oxidosqualene:lanosterol cyclase: a novel mechanism for the attenuation of foam cell formation'. *Circulation Research* **93**(8), 717–725. PMID: 14512442.

Roy, S., J. Ernst, P. V. Kharchenko, P. Kheradpour, N. Negre, M. L. Eaton, J. M. Landolin, C. A. Bristow, L. Ma, M. F. Lin, S. Washietl, B. I. Arshinoff, F. Ay, P. E. Meyer, N. Robine, N. L. Washington, L. Di Stefano, E. Berezikov, C. D. Brown, R. Candeias, J. W. Carlson, A. Carr, I. Jungreis, D. Marbach, R. Sealfon, M. Y. Tolstorukov, S. Will, A. A. Alekseyenko, C. Artieri, B. W. Booth, A. N. Brooks, Q. Dai, C. A. Davis, M. O. Duff, X. Feng, A. A. Gorchakov, T. Gu, J. G. Henikoff, P. Kapranov, R. Li, H. K. MacAlpine, J. Malone, A. Minoda, J. Nordman, K. Okamura, M. Perry, S. K. Powell, N. C. Riddle, A. Sakai, A. Samsonova, J. E. Sandler, Y. B. Schwartz, N. Sher, R. Spokony, D. Sturgill, M. van Baren, K. H. Wan, L. Yang, C. Yu, E. Feingold, P. Good, M. Guyer, R. Lowdon, K. Ahmad, J. Andrews, B. Berger, S. E. Brenner, M. R. Brent, L. Cherbas, S. C. R. Elgin, T. R. Gingeras, R. Grossman, R. A. Hoskins, T. C. Kaufman, W. Kent, M. I. Kuroda, T. Orr-Weaver, N. Perrimon, V. Pirrotta, J. W. Posakony, B. Ren, S. Russell, P. Cherbas, B. R. Graveley, S. Lewis, G. Micklem, B. Oliver, P. J. Park, S. E. Celniker, S. Henikoff, G. H. Karpen, E. C. Lai, D. M. MacAlpine, L. D. Stein, K. P. White, and M. Kellis: 2010, 'Identification of functional elements and regulatory circuits by Drosophila modENCODE'. *Science (New York, N.Y.)* **330**(6012), 1787–1797. PMID: 21177974.

Rozowsky, J., G. Euskirchen, R. K. Auerbach, Z. D. Zhang, T. Gibson, R. Bjornson, N. Carriero, M. Snyder, and M. B. Gerstein: 2009, 'PeakSeq enables systematic scoring of ChIP-seq experiments relative to controls'. *Nat Biotech* **27**(1), 66–75.

Rye, M. B., P. Saetrom, and F. Drablos: 2010, 'A manually curated ChIP-seq benchmark demonstrates room for improvement in current peak-finder programs'. *Nucleic Acids Research* **39**(4), e25–e25.

Schmuth, M., P. M. Elias, K. Hanley, P. Lau, A. Moser, T. M. Willson, D. D. Bikle, and K. R. Feingold: 2004, 'The effect of LXR activators on AP-1 proteins in keratinocytes'. *The Journal of Investigative Dermatology* **123**(1), 41–48. PMID: 15191540.

Schultz, J. R., H. Tu, A. Luk, J. J. Repa, J. C. Medina, L. Li, S. Schwendner, S. Wang, M. Thoolen, D. J. Mangelsdorf, K. D. Lustig, and B. Shan: 2000, 'Role of LXRs in control of lipogenesis'. *Genes & Development* **14**(22), 2831 –2838.

Shen, Q., Y. Bai, K. C. N. Chang, Y. Wang, T. P. Burris, L. P. Freedman, C. C. Thompson, and S. Nagpal: 2011, 'Liver X receptor-retinoid X receptor (LXR-RXR) heterodimer cistrome reveals coordination of LXR and AP1 signaling in keratinocytes'. *The Journal of Biological Chemistry* **286**(16), 14554–14563. PMID: 21349840.

Sherman, B. T., D. W. Huang, Q. Tan, Y. Guo, S. Bour, D. Liu, R. Stephens, M. W. Baseler, H. C. Lane, and R. A. Lempicki: 2007, 'DAVID Knowledgebase: a gene-centered database integrating heterogeneous gene annotation resources to facilitate high-throughput gene functional analysis'. *BMC Bioinformatics* **8**, 426. PMID: 17980028.

Shibata, N. and C. K. Glass: 2009, 'Regulation of macrophage function in inflammation and atherosclerosis'. *Journal of Lipid Research* **50 Suppl**, S277–281. PMID: 18987388.

Shibata, N. and C. K. Glass: 2010, 'Macrophages, oxysterols and atherosclerosis'. *Circulation Journal: Official Journal of the Japanese Circulation Society* **74**(10), 2045–2051. PMID: 20838002.

Siersbaek, R., R. Nielsen, S. John, M. Sung, S. Baek, A. Loft, G. L. Hager, and S. Mandrup: 2011, 'Extensive chromatin remodelling and establishment of transcription factor 'hotspots' during early adipogenesis'. *The EMBO Journal* **30**(8), 1459–1472. PMID: 21427703.

Skalen, K., M. Gustafsson, E. K. Rydberg, L. M. Hulten, O. Wiklund, T. L. Innerarity, and J. Boren: 2002, 'Subendothelial retention of atherogenic lipoproteins in early atherosclerosis'. *Nature* **417**(6890), 750–754.

Smoot, M. E., K. Ono, J. Ruscheinski, P. Wang, and T. Ideker: 2011, 'Cytoscape 2.8: new features for data integration and network visualization'. *Bioinformatics (Oxford, England)* **27**(3), 431–432. PMID: 21149340.

Son, Y. L. and Y. C. Lee: 2010, 'Molecular determinants of the interactions between SRC-1 and LXR/RXR heterodimers'. *FEBS Letters* **584**, 3862–3866.

Song, C., J. M. Kokontis, R. A. Hiipakka, and S. Liao: 1994, 'Ubiquitous receptor: a receptor that modulates gene activation by retinoic acid and thyroid hormone receptors.'. *Proceedings of the National Academy of Sciences of the United States of America* **91**(23), 10809–10813. PMID: 7971966 PMCID: 45115.

Song, L., Z. Zhang, L. L. Grasfeder, A. P. Boyle, P. G. Giresi, B. Lee, N. C. Sheffield, S. GrÃ€f, M. Huss, D. Keefe, Z. Liu, D. London, R. M. McDaniell, Y. Shibata, K. A. Showers, J. M. Simon, T. Vales, T. Wang, D. Winter, Z. Zhang, N. D. Clarke, E. Birney, V. R. Iyer, G. E. Crawford, J. D. Lieb, and T. S. Furey: 2011, 'Open chromatin defined by DNaseI and FAIRE identifies regulatory elements that shape cell-type identity'. *Genome Research* **21**(10), 1757–1767. PMID: 21750106.

Splinter, E., H. Heath, J. Kooren, R. Palstra, P. Klous, F. Grosveld, N. Galjart, and W. de Laat: 2006, 'CTCF mediates long-range chromatin looping and local histone modification in the beta-globin locus'. *Genes & Development* **20**(17), 2349–2354. PMID: 16951251.

Subramanian, A., P. Tamayo, V. K. Mootha, S. Mukherjee, B. L. Ebert, M. A. Gillette, A. Paulovich, S. L. Pomeroy, T. R. Golub, E. S. Lander, and J. P. Mesirov: 2005, 'Gene set enrichment analysis: a knowledge-based approach for interpreting genome-wide expression profiles'. *Proceedings of the National Academy of Sciences of the United States of America* **102**(43), 15545–15550. PMID: 16199517.

Takizawa, T., K. J. Meaburn, and T. Misteli: 2008, 'The meaning of gene positioning'. *Cell* **135**(1), 9–13. PMID: 18854147.

Tang, Q., Y. Chen, C. Meyer, T. Geistlinger, M. Lupien, Q. Wang, T. Liu, Y. Zhang, M. Brown, and X. S. Liu: 2011, 'A Comprehensive View of Nuclear Receptor Cancer Cistromes'. *Cancer Research*. PMID: 21940749.

Tangirala, R. K., E. D. Bischoff, S. B. Joseph, B. L. Wagner, R. Walczak, B. A. Laffitte, C. L. Daige, D. Thomas, R. A. Heyman, D. J. Mangelsdorf, X. Wang, A. J. Lusis, P. Tontonoz, and I. G. Schulman: 2002, 'Identification of macrophage liver X receptors as inhibitors of atherosclerosis'. *Proceedings of the National Academy of Sciences of the United States of America* **99**(18), 11896–11901. PMID: 12193651.

Triantafilou, M. and K. Triantafilou: 2002, 'Lipopolysaccharide recognition: CD14, TLRs and the LPS-activation cluster'. *Trends in Immunology* **23**(6), 301–304. PMID: 12072369.

van Berkum, N. L., E. Lieberman-Aiden, L. Williams, M. Imakaev, A. Gnirke, L. A. Mirny, J. Dekker, and E. S. Lander: 2010, 'Hi-C: a method to study the three-dimensional architecture of genomes'. *Journal of Visualized Experiments: JoVE* (39). PMID: 20461051.

Vega, V. B., E. Cheung, N. Palanisamy, and W. Sung: 2009, 'Inherent signals in sequencing-based Chromatin-ImmunoPrecipitation control libraries'. *PloS One* **4**(4), e5241. PMID: 19367334.

Venteclef, N., T. Jakobsson, A. Ehrlund, A. Damdimopoulos, L. Mikkonen, E. Ellis, L. Nilsson, P. Parini, O. A. JÃ€nne, J.-k. Gustafsson, K. R. Steffensen, and E. Treuter: 2010, 'GPS2-dependent corepressor/SUMO pathways govern anti-inflammatory actions of LRH-1 and LXRbeta in the hepatic acute phase response'. **24**(4), 381–395. PMID: 20159957 PMCID: 2816737.

Viennois, E., K. Mouzat, J. Dufour, L. Morel, J. Lobaccaro, and S. Baron: 2011, 'Selective liver X receptor modulators (SLiMs): What use in human health?'. *Molecular and Cellular Endocrinology*. PMID: 21907760.

Voss, T. C., R. L. Schiltz, M. Sung, P. M. Yen, J. A. Stamatoyannopoulos, S. C. Biddie, T. A. Johnson, T. B. Miranda, S. John, and G. L. Hager: 2011, 'Dynamic exchange at regulatory elements during chromatin remodeling underlies assisted loading mechanism'. *Cell* **146**(4), 544–554. PMID: 21835447.

Wagner, B. L., A. F. Valledor, G. Shao, C. L. Daige, E. D. Bischoff, M. Petrowski, K. Jepsen, S. H. Baek, R. A. Heyman, M. G. Rosenfeld, I. G. Schulman, and C. K. Glass: 2003, 'Promoter-Specific Roles for Liver X Receptor/Corepressor Complexes in the Regulation of ABCA1 and SREBP1 Gene Expression'. *Molecular and Cellular Biology* **23**(16), 5780–5789. PMID: 12897148 PMCID: 166346.

Wang, N. and A. R. Tall: 2003, 'Regulation and mechanisms of ATP-binding cassette transporter A1-mediated cellular cholesterol efflux'. *Arteriosclerosis, Thrombosis, and Vascular Biology* **23**(7), 1178–1184. PMID: 12738681.

Wang, X., H. L. Collins, M. Ranalletta, I. V. Fuki, J. T. Billheimer, G. H. Rothblat, A. R. Tall, and D. J. Rader: 2007, 'Macrophage ABCA1 and ABCG1, but not SR-BI, promote macrophage reverse cholesterol transport in vivo'. *The Journal of Clinical Investigation* **117**(8), 2216–2224. PMID: 17657311.

Wang, Y., B. Kurdi-Haidar, and J. F. Oram: 2004, 'LXR-mediated activation of macrophage stearoyl-CoA desaturase generates unsaturated fatty acids that destabilize ABCA1'. *Journal of Lipid Research* **45**(5), 972 –980.

Watanabe, Y., S. Jiang, W. Takabe, R. Ohashi, T. Tanaka, Y. Uchiyama, K. Katsumi, H. Iwanari, N. Noguchi, M. Naito, T. Hamakubo, and T. Kodama: 2005, 'Expression of the LXRalpha Protein in Human Atherosclerotic Lesions'. *Arteriosclerosis, Thrombosis, and Vascular Biology* **25**(3), 622 –627.

Weinhofer, I., S. Forss-Petter, M. Zigman, and J. Berger: 2002, 'Cholesterol regulates ABCD2 expression: implications for the therapy of X-linked adrenoleukodystrophy'. *Human Molecular Genetics* **11**(22), 2701–2708. PMID: 12374760.

Whitney, K. D., M. A. Watson, B. Goodwin, C. M. Galardi, J. M. Maglich, J. G. Wilson, T. M. Willson, J. L. Collins, and S. A. Kliewer: 2001, 'Liver X receptor (LXR) regulation of the LXRalpha gene in human macrophages'. *The Journal of Biological Chemistry* **276**(47), 43509–43515. PMID: 11546778.

Willy, P. J., K. Umesono, E. S. Ong, R. M. Evans, R. A. Heyman, and D. J. Mangelsdorf: 1995, 'LXR, a nuclear receptor that defines a distinct retinoid response pathway'. *Genes & Development* **9**(9), 1033–1045. PMID: 7744246.

Wu, S., R. Yin, R. Ernest, Y. Li, O. Zhelyabovska, J. Luo, Y. Yang, and Q. Yang: 2009, 'Liver X receptors are negative regulators of cardiac hypertrophy via suppressing NF-kappaB signalling'. *Cardiovascular Research* **84**(1), 119–126. PMID: 19487338.

Wunderlich, Z. and L. A. Mirny: 2009, 'Different gene regulation strategies revealed by analysis of binding motifs'. *Trends in Genetics: TIG* **25**(10), 434–440. PMID: 19815308.

Ye, T., A. R. Krebs, M. Choukrallah, C. Keime, F. Plewniak, I. Davidson, and L. Tora: 2011, 'seqMINER: an integrated ChIP-seq data interpretation platform'. *Nucleic Acids Research* **39**(6), e35. PMID: 21177645.

Yoshikawa, T., H. Shimano, M. Amemiya-Kudo, N. Yahagi, A. H. Hasty, T. Matsuzaka, H. Okazaki, Y. Tamura, Y. Iizuka, K. Ohashi, J. Osuga, K. Harada, T. Gotoda, S. Kimura, S. Ishibashi, and N. Yamada: 2001, 'Identification of liver X receptor-retinoid X receptor as an activator of the sterol regulatory element-binding protein 1c gene promoter'. *Molecular and Cellular Biology* **21**(9), 2991–3000. PMID: 11287605.

Yvan-Charvet, L., M. Ranalletta, N. Wang, S. Han, N. Terasaka, R. Li, C. Welch, and A. R. Tall: 2007, 'Combined deficiency of ABCA1 and ABCG1 promotes foam cell accumulation and accelerates atherosclerosis in mice'. *The Journal of Clinical Investigation* **117**(12), 3900–3908. PMID: 17992262 PMCID: 2066200.

Zelcer, N., C. Hong, R. Boyadjian, and P. Tontonoz: 2009a, 'LXR regulates cholesterol uptake through Idol-dependent ubiquitination of the LDL receptor'. *Science (New York, N.Y.)* **325**(5936), 100–104. PMID: 19520913.

Zelcer, N., C. Hong, R. Boyadjian, and P. Tontonoz: 2009b, 'LXR regulates cholesterol uptake through Idol-dependent ubiquitination of the LDL receptor'. *Science (New York, N.Y.)* **325**(5936), 100–104. PMID: 19520913.

Zelcer, N. and P. Tontonoz: 2006, 'Liver X receptors as integrators of metabolic and inflammatory signaling'. *Journal of Clinical Investigation* **116**(3), 607–614. PMID: 16511593 PMCID: 1386115.

Zhang, Y., T. Liu, C. A. Meyer, J. Eeckhoute, D. S. Johnson, B. E. Bernstein, C. Nusbaum, R. M. Myers, M. Brown, W. Li, and X. S. Liu: 2008, 'Model-based analysis of ChIP-Seq (MACS)'. *Genome Biology* **9**(9), R137. PMID: 18798982.

Zhao, C. and K. Dahlman-Wright: 2010, 'Liver X receptor in cholesterol metabolism'. *The Journal of Endocrinology* **204**(3), 233–240. PMID: 19837721.

Zhao, W., L. Wang, M. Zhang, P. Wang, L. Zhang, C. Yuan, J. Qi, Y. Qiao, P. C. Kuo, and C. Gao: 2011, 'NF-kB- and AP-1-Mediated DNA Looping Regulates Osteopontin Transcription in Endotoxin-Stimulated Murine Macrophages'. *The Journal of Immunology* **186**(5), 3173 –3179.

Zhu, Y. and Y. Li: 2009, 'Liver X receptors as potential therapeutic targets in atherosclerosis'. *Clinical and Investigative Medicine. MÃ©decine Clinique Et Experimentale* **32**(5), E383–394. PMID: 19796580.

Declaration

I herewith declare that I have produced this thesis without the prohibited assistance of third parties and without making use of aids other than those specified.

Cornelius Fischer